CHARACTERISATION OF METAL RODS USING ULTRASONIC NONDESTRUCTIVE METHODS

THESIS
Submitted in partial fulfilment of the
requirements for the degree of
DOCTOR OF PHILOSOPHY

By

YUDHISTHER KUMAR

Under the supervison of
Dr. ASHOK KUMAR

BIRLA INSTITUTE OF TECHNOLOGY AND SCIENCE
PILANI (RAJASTHAN) INDIA

1997

BIRLA INSTITUTE OF TECHNOLOGY AND SCIENCE
PILANI, RAJASTHAN

CERTIFICATE

This is to certify that the thesis entitled CHARACTERISATION OF METAL RODS USING ULTRASONIC NONDESTRUCTIVE METHODS and submitted by YUDHISTHER KUMAR, I.D. No. 92PZYF007 for award of Ph. D. degree of the Institute, embodies original work done by him under my supervison.

Signature in full of supervisor Ashok Kumar

Name Dr. ASHOK KUMAR

Date : May 12, 1997 *Designation* Scientist E - II
Ultrasonics Section
National Physical Laboratory
New Delhi - 110012

ACKNOWLEDGEMENTS

It gives me great pleasure to express my deep sense of gratitude and indebtedness to my revered supervisor, Dr. Ashok Kumar, Scientist - E-II, National Physical Laboratory, New Delhi, for his abiding inspiration and guidance throughout the progress of my work. The invaluable suggestions, close association, contribution through constructive criticism by him have been a source of continuous inspiration. I consider it to be my proud privilege to work under him.

I am greatly indebted to Prof. E.S.R. Gopal, Director, National Physical Laboratory, Prof. S.K. Joshi, Ex-D.G. CSIR and Ex-Director, NPL, Dr. T.K. Saksena, Ex-Scientist F, NPL and Dr. Janardan Singh, Head of Ultrasonics Group, NPL for giving me the permission to register under the BITS-NPL higher degree programme, facility extended to me as an employee and for allowing me to use all the necessary facilities.

My special thanks are due to M/s Jagdish Lal, Basant Kumar, Om Prakash Vaish, A.D. Raheja, Kishan Lal, Ganaur Mehta and Late J.P. Sharma, my close associates at NPL, who were always keen and ready to work with me at any time of the day and for their useful manifold help and wishes during the course of my work.

My deep sense of gratitude is due to Dr. V. N. Bindal Ex-Scientist G, NPL, Dr. S. K. Jain, Dr. Ved Singh, Dr. Harish Bahadur, Mr. Mukesh Chandra, Scientists, NPL for encouragement and kind co-operation. I am also grateful to

Dr. J. N. Som, Mrs. R. Gupta, Mr S. Chandra, Mr.N. N. Swamy, Mr. N.C. Soni, Mr. G.S. Lamba, Mr. V.K. Hans, Mrs. Savita, Mrs. S. Khanna, Scientists and members of Ultrasonics Group, NPL for their manifold help in my work.

It is my great pleasure to acknowledge the help from all the members concerned with NPL-BITS collaborative programme for conducting the course and arranging my registration for Ph. D. Degree. In this regard, I specially remember Prof. L. K. Maheswari, Dean R & C, Dr. G. P. Srivastava, Dr. Raghurama from BITS and Dr. B. K. Das, Scientist F, Mr. F.C. Khullar, Head HRD Group, and Mr. Dharam Vir Saini from NPL. I am extremely grateful to my vulnerable teachers of NPL-BITS, M.S. cum Ph. D. distance learning program.

My heartfelt thanks are due to my friends Mr. K. Chakraborty, Mr. Deepak Varandani, Mr. D. Sarangee, Mr. C. Mukharjee, Mr. Vijay Sharma, Dr. (Mrs) R. Mitra, Dr. (Mrs) K Balakrishna, Mr. P R Bose, Dr. D P Singh for their cooperation, Mr. J S Dhama and Mr. Subhash for Photographs.

I am highly indebted to my parents for their invaluable guidance throughout my life to make me reach at this stage. Here no words could adequately express my feelings of regards to my father who provided the moral support and inspiration upto the final stage of this work. I find it difficult to express in words the thanks due to my wife Santosh for encouragement, son Nitin (13) and daughter Rashmi (10) for their sacrifice and patience during the period.

Kumar 12.5.97

(Yudhisther Kumar)

PREFACE

The need for the characterisation of materials using nondestructive methods has been growing steadily with the advent of newer materials and their applications under stringent conditions. Consequently, continuous efforts for the development of new methods of characterisation becomes an essential requirement. The thesis deals in with the ultrasonic nondestructive methods of material characterisation. In all the methods developed and reported here, the material has been taken in the form of rod. This has not only provided a variation to the existing methods where parallel plates are generally used, but has also resulted into the development of some very accurate, fast and cheaper methods.

The foremost requirement for the characterisation of any material is to ascertain that it is free from any undesirable defect. A C-scan immersion technique has been developed for this work and is reported in Chapter 2 which follows the introductory Chapter 1. The ultrasonic velocity and attenuation data of a material is a very effective tool for the material characterisation. In Chapter 3, a new method for the evaluation of both the longitudinal as well as transverse wave velocity is given. The method uses a single longitudinal wave transducer. A novel method for the determination of the ultrasonic attenuation is described in Chapter 4. Finally, the effect of ultrasound propagation in material rods due to contact with liquid has been given in Chapter 5. The study provides a quick qualitative method for the intercomparison of rods besides having tremendous applications, such as in interface testing, liquid level monitoring etc.

CONTENTS

LIST OF SYMBOLS AND ABBREVIATIONS

α - Ultrasonic attenuation coefficient

α_l, α_t - Ultrasonic attenuation of longitudinal wave and transverse wave respectively

Λ – Cross sectional area of ultrasonic beam

Al - Aluminium alloy

A_1, A_2 - Acoustic pressure of ray immediately after its entrance in rod of diameter d_1 and d_2

B - Bulk modulus

BD - Effective beam width of the transducer in rod

BWE - Back wall echo

CDH - Crved surface drilled hole

d - Diameter of rod or thickness of material

d_1 - Diameter of the rod at one end

d_2 - Diameter of the rod at another end

dB - Decible

D - Diameter of the transducer

DGS - Distance gain size

D_g - Grain diameter

DSO - Digital storage oscilloscope

E - Young's modulus

F - Area of the defect

FBH - Flat bottom hole

FE - Flaw echo

FFT - Fast fourier transform

FSH - Full screen height

G - Shear modulus

γ - Lame constant

h - Height at 80 % of full screen height

K - Constant

Km - Kilometer

λ - Wavelength of sound wave

mm - millimeter

μs - micro second

L - Longitudinal modulus

MHz - Megahertz

MS - Mild steel

NDC - Nondestructive characterisation

NDE - Nondestructive evaluation

NDT - Nondestructive testing

Np - Nepers

p - Pressure of the echo

p_0 - Initial pressure

P, Q - Division on time scale for echoes in air and water respectively

P_{11}, P_{12}, P_{13} - Pressures from echo path T1, T2 and T3 respectively for rod of end diameter d1

P_{21}, P_{22}, P_{23} - Pressures from echo path T1, T2, and T3 respectively for rod of end diameter d2

QE - Water path between transducer and top surface of rod

ρ - Density of the medium

r - Radius of the rod

rf - radio frequency pulse

R - Relative change in envelope area in dB

R_1 - Reflection coefficient for incident longitudinal ray at normal incidence for rod metal-liquid interface

R_2 - Reflection coeffiecient for incident longitudinal ray at an angle 30^0 and reflected longitudinal ray

R_3 - Reflection coefficient for incident longitudinal ray at an angle θ_i and reflected transverse ray at angle θ_t

R_4 - Reflection coefficient for incident transverse ray at angle θ_t and reflected longitudinal ray at angle θ_i

σ - Poission's ratio

SDH - Side drilled hole

SS - Stainless steel

T1 - Back wall echo path into a rod

T2 - Triangular echo path without mode conversion into a rod

T3 - Triangular echo path with mode conversion into a rod

t1 - Time of flight for echo path T1

t2 - Time of flight for echo path T2

t3 - Time of flight for echo path T3

θ_i - Incident angle of longitudinal wave

θ_r - Refracted angle of longitudinal wave

θ_t - Reflected angle of transverse wave for incident longitudinal wave

V_{lr} - Longitudinal wave velocity in rod material

V_{lw} - longitudinal wave velocity in water

V_l - Longitudinal wave velocity

V_t - Transverse wave velocity

w - Width of contact line on curved surface of rod

X, Y - Reduction in gain in dB for air and water respectively

CHAPTER - 1

INTRODUCTION

CHAPTER - 1

INTRODUCTION

In recent years the need has arisen for testing materials, engineering products and components before building them for highly stressed structures such as aeroplane, rockets, etc. Invaluable information is conveyed by the mechanical tests performed on samples representing the batch of material from which a particular material is made. The samples are taken from the actual rod or plate used in making the component and accompany through all the production stages, including heat treatment. A satisfactory set of test figures invites confidence in the quality of the material used in the fabrication of component, but gives no real information about the probable performance of the component itself in service. The component may have hidden defects which no amount of visual inspection can reveal. This makes it essential to detect and gauge these defects to demonstrate integrity and reliability of engineering plant and to avoid risk failure. The characteristics of the material, used to fabricate the component, also need to be ascertained for all the conditions during the end use. The growing requirement in engineering to demonstrate the safety and reliability of components has encouraged the wider use of nondestructive

examination and characterisation of materials. The rods or cylindrical shape materials are no exception.

1.1 CHARACTERISATION OF MATERIALS

Characterisation of materials from the standpoint of their development, manufacture and eventual use is an important subject for modern materials industry. The word characterisation in its simplest form may be said as evaluation of various parameters or features of substance. Broadly speaking characterisation means the evaluation of features of composition of a material, including defects, that are significant for a particular preparation, study of properties or use and suffice for the reproduction of a material [1,2]. The word characterisation may therefore mean different to different people. For example a scientist concerned with single crystals and glasses views defects and structure at the molecular and atomic level, while one involved with polycrystalline and granular materials views them at a macro level. It is therefore not possible to imagine a single, all embracing characterizing technique that would meet all the objectives and even for the evaluation of a single parameter such as the material composition, a number of different methods may be used for the evaluation of materials composition, structure properties etc. and each method is limited by the information it provides besides being either entirely destructive

(wet chemical methods) or partially destructive (dry physical methods).

There are several techniques for the characterisation of materials. The technique adopted depends upon several factors such as parameters to identify, cost, time involved (batch or on line), destructive or nondestructive, accuracy required, accessibility, environment, etc. These techniques may be destructive or nondestructive. The nondestructive testing (NDT) techniques for material evaluation may utilise variety of waves - light, electromagnetic and mechanical as the principal tool for providing useful information.

With advances in techniques, instrumentation and the understanding of various phenomena, the NDT techniques today are capable of giving much more information about the material. Several kinds of defects and number of parameters of the materials can now be evaluated by nondestructive characterisation (NDC). Some of the more popular techniques are as given below in brief [3-5].

i) Radiography : The X-rays produced generally by Co^{60} or C^{14} are incident on the sample. The radiations transmitted through the sample fall either on X-ray films making radiograph or on photosensitive diodes giving real- time radiography on cathode ray tube (CRT). This technique [6] is extremely popular in detection of defects and inhomogenities

in materials, mostly metals.

ii) Magnetic Particle Inspection : When a ferromagnetic material is magnetized by passing through it high DC or HWDC current, there will be magnetic flux concentration around the inhomogenity of lesser permeability. The flux concentration can be seen by spraying fine magnetic particles over the sample surface. This method is widely used for surface cracks detection but can also be used for detection of other inhomogenities [7].

iii) Optical Inspection Method : Optical inspection methods are basically used to characterise the surface of the material for properties such as *inhomogenities*, texture, roughness, geometry, grain size, phase composition etc. Several methods exist today which can be divided in various categories as follows [8] :

(a) Direct visible light viewing such as boroscope, fiberscope, flexible endoscope, optical *profiler*, *video* microscope etc.

(b) Optical microscope such as, stereo microscope, compound microscope, electron microscope etc.

(c) Laser based system such as 2-D scanning, interferometer, holography, vibrometry etc.

(d) *Infra-red imaging*

iv) Liquid penetrant testing : For surface defect detection, different kinds of liquid penetrant are used. These penetrate to the crack present on the surface of the material and make them visible [9].

v) Vibration testing: The material is subjected to small periodic impacts by hammer or electromagnetic vibrator. The vibrations produced in the material are picked up by broad band vibration pickup. The pick up output is subjected to spectrum analysis. This analysis can be used to evaluate various elastic constants and overall soundness of the material [10,11].

vi) X-Ray Diffraction: When the X-rays are incident on a sample at oblique incidence, the beam is diffracted by the atoms inside the sample. The diffracted beam intensity will depend upon the angle of incidence, angle of measurement and the atomic arrangement. Since the atomic arrangement governs several characteristics of the material, the variation of intensity of diffracted beam with angle can be used to characterise a material [12]. It is often limited to laboratory scale being sophisticated, bulky and requiring safety precautions. This technique involves the evaluation of a few parameters such as residual stress, phase, structure, etc.

vii) Eddy Current Method: When a coil, with alternating current passing through it, is brought near to the surface of a conducting material, eddy currents are produced in the material. The eddy currents will be a characteristic of the material just below the surface. The strength of eddy current can be estimated by placing another coil near the generating coil or by the same coil in the pulse mode [13,14]. This technique is used to characterise internal defect, residual stress, composition, conductivity, heat treatment, etc.

viii) Neutron Diffraction Technique : It is similar to X-Ray diffraction but uses thermal (low energy) neutrons in place of X-Rays. Debye temperature, specific heat etc. can be evaluated by this technique [15].

ix) Magnetic Flux Technique : When electric current is passed through a straight conductor, magnetic field is produced around it. It is found that small magnetic particles are attracted to cracks in the metal. If the current is alternating, the change in magnetic flux around the material can be picked up by a current transformer or probe. The voltage output of this probe will be a function of the material properties producing magnetic flux leakage. Residual stress, hysteresis, permeability,

porosity, etc., are the parameters which can be evaluated with this technique [16].

x) Ultrasonic Methods : Ultrasonic nondestructive testing is an important tool for the quality evaluation of materials. Conventionally this technique is used for the detection, location and sizing of the defects in material. With advent of newer material and more stringent conditions and shapes, the emphasis is now being laid on the further evaluation of various elastic parameters of the materials for its characterisation. A high energy pulse of ultrasound is used to detect, locate and evaluate the defects such as cracks [17-20], porosity, deterioration, corrosion, foreign inclusion, etc. Direct contact or immersion testing techniques [21] are generally used with single transducer or some time with dual transducer in through transmission technique for evaluation of defects.

Each of these methods is limited in the information revealed. Among all the known NDT and evaluation techniques, ultrasonic method is capable of revealing more and significant information. Ultrasonic NDT method offers several advantages for characterisation of materials. The most important advantage is its being applicable to virtually any shape or size of the test material. It is usually quick and most effective.

However, there are several variations within the ultrasonic techniques. Choice of proper ultrasonic technique requires some understanding of the link between the ultrasonic parameters and the ultimate parameter being evaluated. Ultrasonic methods of characterisation has been very popular due to the fact that it is capable of evaluating a large number of significant material properties and has several merits over the other methods. This is economical and requires only one side to be accessible, as against radiography which competes well in popularity. Almost all types of materials can be characterized and tested with the ultrasonic methods. The eddy current testing is not possible in case of non-conducting materials and magnetic flux leakage or magnetic particle inspection is suitable only for ferromagnetic materials. The ultrasonic methods are also not limited to the surface and sub-surface characterisation as in case of dye penetrant, magnetic flux leakage, eddy current and visual methods.

The principal advantages of ultrasonic inspection as compared to other methods for nondestructive inspection of metal parts can be listed as follows :

i) Superior penetrating power, which allows the detection of flaw deep in the part. Ultrasonic inspection is done routinely to depths of several feet on many types of parts.

ii) High sensitivity, permitting the detection of extremely small flaws.

iii) Greater accuracy than other nondestructive methods in determining the position of internal flaws, estimating their size and characterizing their orientation, shape and nature.

iv) Only one surface need be accessible.

v) Volumetric scanning ability, enabling inspection of a volume of metal extending from front surface to back surface of a part.

vi) Is not hazardous to operations or to nearby personnel, and has no effect on equipment and materials in the vicinity.

vii) Portability.

The principal disadvantages of the ultrasonic inspection include the following:

i) Manual operation requires careful attention by experienced technicians.

ii) Extensive technical knowledge is required for the development of inspection procedures.

iii) Parts that are rough, irregular in shape, very small or thin, or not homogeneous are difficult to inspect.

iv) Discontinuities that are present in a shallow layer immediately beneath the surface may be difficult to detect.

) Couplants are needed to provide effective transfer

of ultrasonic wave energy between transducers and parts being inspected.

vi) Reference standards are needed for calibrating the equipment and characterizing the flaw.

Use of ultrasound in NDT has been known almost since 1880 discovery of piezoelectricity in quartz and later in tourmaline, KDP, rochelle salt and other minerals. Richardson [22] proposed the ideas of utilizing high frequency sound waves for detection of objects using water or air as the carrier medium of ultrasound. Mulhauser [23] applied ultrasonic waves for detecting flaws in solids. The theory of wave material interaction has been refined further by Vardan [24], Mc Gonnagle [5], Nozdreva [25] and Filipczynski et. al.[26]. It demonstrates the application of ultrasound for the evaluation of materials. All serious investigators of material by ultrasound have stressed the use of ultrasonic method for "more than overt flaw detection" and its use in characterisation of materials by measuring ultrasonic velocity and attenuation at discrete frequencies.

There has been expended interest in the measurement of the elastic properties of solids by using ultrasonic techniques, for they have the very desirable aspect of being in the form of nondestructive test. Further, since these materials are often designed for

exotic applications, it becomes necessary to determine these properties with precision, under unusual environmental conditions. For an isotropic material, by measuring the ultrasound longitudinal and shear velocity various elastic constants can be determined by the following equations [27,28].

Shear modulus (G)	$= \rho V_t^2$	...(1)
Longitudinal modulus (L)	$= \gamma + 2G = \rho V_l^2$	...(2)
Bulk modulus (B)	$= L - 4G/3$	...(3)
Young's modulus (E)	$= G(3L-4G)/(L-G)$	...(4)
Lame constant (γ)	$= L - 2G$	...(5)
Poisson's ratio (σ)	$= (L-2G)/2(L-G)$	...(6)

The various elastic constant can be defined as below :

i) Young's Modulus (E) - When a rod or bar is subjected to a uniaxial stress it is the ratio of applied stress to the change in length per unit length of the rod, some times called elastic modulus.

ii) Poisson's ratio (σ) - It is the ratio of change in dimension in lateral direction to the change in length.

iii) Bulk modulus (B) - For isotropic materials as a result of subjecting it to hydrostatic pressure, bulk modulus is the ratio of applied stress to the change in volume per unit volume.

iv) Shear modulus (G) - Here material is subjected to

pure shear stress and shear modulus is ratio of applied stress to the change in deformation through angle.

v) Longitudinal modulus (L) - It related strain to a longitudinally applied stress.

Ultrasonic wave attenuation is the loss of energy in an ultrasonic wave propagating through a material and can be attributed to scattering and absorption due to heat conduction, viscous friction, and elastic hysteresis [29-31]. The amount of energy scattered depends on the relative magnitude of wavelength and the average grain diameter. Therefore true values of attenuation at a particular frequency are helpful in predicting the grain size of the material. Thus both the velocity and attenuation are used to characterise the material.

1.2 ULTRASONICS AND ITS SCOPE IN NONDESTRUCTIVE CHARACTERISATION (NDC)

Ultrasonics is the branch of acoustics dealing with the frequencies above audible range generally more than 20kHz. The physical principles of classical acoustics however, hold equally good for the audible as well as ultrasonic regime [17,32-36]. Ultrasonics has rapidly advanced and spread into various new areas encompassing almost all aspect of science, industry and medicine. Generally speaking, ultrasonic waves are capable of propagating in all the media with the exception of the

vacuum. This alone describes the scope of ultrasound. Investigation of reflected or transmitted ultrasonic waves from a medium of propagation can provide a valuable information about the medium. Therefore, it is possible to evaluate wide variety of materials and process by ultrasound.

For nondestructive characterisation, besides detection of flaws in metals, ultrasound can reveal information about material properties and microstructure. Similarly, investigation and manipulation of ultrasonic signals from one medium to another can be used to create other applications of interest. A summary of information revealed by ultrasound and its other uses include [27,37-47] :

Elastic constants	Microstructure
Mechanical properties	Density
Thickness gauging	Porosity
Corrosion measurements	Liquid level sensing
Applied stress	Dimensional analysis
In-situ testing	Surface profiling
Surface defects	Object imaging
Internal microscopy	Texture
Internal imaging	Robotics
Object imaging	Artificial intelligence
and more	

The above information is dependent upon the devel-

opment of relationships between the following ultrasonic measurements with the characteristics of wave propagating media :

i. Velocity of longitudinal waves
ii. Velocity of transverse waves
iii. Velocity of surface or Rayleigh waves
iv. Frequency dependence of attenuation of above waves
v. Phase change and phase amplitude of reflected or transmitted waves and
vi. Interference of polarized waves.

Investigation of materials with longitudinal and transverse waves can be used to reveal subsurface and internal defects, thickness or corrosion measurements. Longitudinal and transverse waves can be applied to determine elastic constants, densities and porosity of materials. Surface waves can be used for the detection of surface breaking defects. Investigating of the rest of the above mentioned parameters can be applied to reveal important mechanical properties of materials.

1.3 ULTRASONIC NONDESTRUCTIVE METHODS

For characterisation of materials among the various parameters stated above, detection, location and sizing the defects and velocity and attenuation measurements are being considered most important parameters for the present work. It is important to describe various important technique generally being used by

researchers and users for characterisation of metals. Various techniques used on materials earlier for these parameters with significance of the parameters are given here in brief.

1.3.1 Detection and Location of the Defects

Both direct contact and immersion method are used for detection of defects. In contact testing, the transducer is directly put in contact to the test specimen using a thin layer of couplant. In immersion testing transducer and test specimen both are immersed in liquid and liquid works as the couplant. In immersion technique various transducer movements are possible with protection of wear and tear of the transducer face.

Different techniques used in ultrasonic testing can be classified according to their relative importance and primary physical measuring quantities, like intensity, phase and transit time of the ultrasound [17,48-51]. These may be Direct contact or Immersion type of testing.

1.3.1.1 Intensity Method

Intensity of the ultrasound is measured after it passes through the test piece using two transducers. Voltage produced by a high frequency generator excites the transmitting probe to oscillation which are propagated in coupled test piece. Second probe positioned

coaxially on opposite side receives a portion of the radiated wave and transmits to the input of an amplifier. Amplified voltage is read on indicating instrument. This method can be applied in various different techniques like sound transmission, reflection, conduction and image projection. Image projection can be produced by using a image converter which converts ultrasound intensity into visible light.

1.3.1.2 Acoustic Holography

This is an image projection method [52] using interference effects similar to the optical holography. Ultrasound receiver records the amplitude in respect of magnitude and phase. It can be stated as a two step method :

i) Diffraction pattern of an object irradiated with ultrasonic waves is interfered with mutually coherent reference waves to form and record an acoustic hologram.

ii) An acoustic hologram is illuminated with a beam of light. The resultant diffraction from hologram provides generally reduced object wave, which is used to form a three dimensional visual image of the object.

1.3.1.3 Transit Time or Resonance Methods

These are essentially velocity evaluation methods. A change in velocity gives the required information about the soundness of the sample.

(i) With Continuous Sound Wave

When the thickness of a test specimen is equal to integral number of half wavelength of ultrasound wave, thickness resonance occurs. A transducer is excited by a high frequency generator with variable frequency, usually below its own frequency range, to supply an ultrasound pressure of maximum uniformity over entire frequency range. The test plate draws more energy from transmitter when in resonance. Resonant frequencies are measured for two successive peaks of maximum current observed to evaluate the velocity of the test material

(ii) With Pulsed Sound Wave

(a) Comparative method : In this method unknown transit time is compared with an accurately known but variable transit time for same pulse. Length of the piece and transit time can be measured accurately so velocity can be determined.

(b) Frequency measuring method : This method uses multiple echoes at resonance for measuring transit time, which is the reciprocal of the echo repetition frequency. If returning echo triggers the next excitation pulse and so forth then the pulse repetition frequency (prf)

will be same as echo repetition frequency. Since pulse repetition frequency can be measured with high accuracy by frequency meter, the transit time can be exactly measured. Sing around method works on this principle.

1.3.1.4 Pulse Transit Time or Pulse Echo Methods

In this method, both the transit time and intensity of ultrasound are measured. It can be used with sound transmission and also with reflection method. The sound pulses coming from the transmitter are radiated into the test piece. If it encounters a flaw in its path, the flaw transmits an echo wave - a portion of which, depending on its form and size, reaches the receiver. Receiver and transmitter can be combined in a single probe. The screen is calibrated with a standard reference block. The echo coming from flaw indicates transit time from transmitter to the flaw and to receiver which gives distance of flaw. By scanning the test piece using different normal beam and angle beam probes, the flaw size can be determined. By using ultrasound output from the flaw detector to C-scan or P-scan equipment the cross sectional and three dimensional picture of the sample, including flaw, can be observed.

Some of the more important methods with special reference to the testing of rods are described in Chapter 2.

1.3.2 Size and Shape Estimation of Defects

Determination of the flaw size and shape in the material is important for better estimation of the probability of failure and to reduce number of replacement of costly items. The determination of flaw size and shape is also important in nondestructive characterisation of materials for proper selection of materials and sophisticated design analysis.

In ultrasonic characterisation of materials the estimation of size of defects is based on the energy reflected, diffracted or scattered from flaw back to the probe. Various techniques applied to estimate the size of defects are basically classified in three different possibilities as follows [53-62] :

i) By evaluation of echo amplitude, that is,

(a) 6dB drop from maximum amplitude
(b) 6dB drop from sides
(c) Equal height of echoes from back wall and flaw
(d) Shadow method
(f) Ultrasonic scatter technique
(g) Distance amplitude correction (DAC) curve
(h) Distance gain and size (DGS) diagram

ii) By evaluation of time of flight, that is,

(a) Time of flight diffraction (TOFD)technique
(b) Crack tip reflection technique
(c) Surface wave technique
(d) Surface wave mode conversion technique

iii) By scanning and image reconstruction

(a) Ultrasonic holography
(b) Ultrasonic tomography
(c) Ultrasonic C-scan system
(d) Ultrasonic spectroscopy

The accuracies in this approach is much better if reliance is made on amplitude alone and some acceptance criteria is set. Nevertheless, accuracies better than ±3 mm or ± 20% would be rare. The techniques is also confined to defects of size greater than the probe beam diameter. The DGS diagram developed are the good attempts to standardise the echo in predicting the equivalent flaw size either bigger or smaller than the ultrasonic beam. The flaw sizing based on echo amplitude is strongly influenced by flaw orientation and flaw type than flaw size and in some cases can either under size or oversize then the actual size.

Other advanced techniques which may appear a little more difficult to apply than the conventional techniques may be very useful where size is to be measured more accurately. Ultrasonic C-scan is the system used for present study for detection, location and measurement of the size of the defect present in the rods. The C-scan technique is described in detail in a latter chapter.

1.3.3 Ultrasonic Velocity Measurement

Ultrasonic velocity has become an important tool for the study of the physical properties of the matter. Ultrasonic velocity measurement offers a rapid and nondestructive method for the characterisation of materials. Various elastic parameters and estimation of

grain size has been going on for the past several years. Some of the methods for the measurements of ultrasonic velocity are given below in brief [63-72].

1.3.3.1 Diffraction Method

It is the direct method for measuring the ultrasonic velocity in transparent samples, liquid or solid. This method makes use of diffraction pattern in the optical Fresnel zone, the region along the optical axis immediately behind the ultrasonic wave. Collimated light is incident on to a standing ultrasonic wave. The resulting Fresnel diffraction pattern which is a series of real images of the ultrasonic wave fronts is examined by a microscope. Since images of wave fronts are $\lambda/2$ apart, one can evaluate the velocity.

1.3.3.2 Basic Pulse-echo Method

A pulsed rf signal of given frequency is converted by means of a transducer into a pulsed ultrasonic wave of the same frequency. The ultrasonic pulse travels through the sample and is reflected between the sample boundaries until it decays away. The velocity is determined by measuring the transit time between the reflected pulse and the corresponding pulse propagation distance in the sample.

1.3.3.3 Sing Around Method

In this method a second transducer is used as

receiver and placed at the end of the sample opposite the transmitting transducer. The received signal is used to trigger the pulse generator thereby generating a continuous succession of pulses. Since repetition rate of this pulse sequence depends on the travel time in the sample, the ultrasonic velocity may be determined by measuring repetition rate.

1.3.3.4 Pulse Echo Superposition Method

A series of rf pulses from a pulse generator is introduced into the sample. The repetition rate of these pulses, controlled by frequency of continuous wave oscillator, is adjusted to correlate approximately to some multiple of an acoustic round trip transit time in the sample. Acoustically measured time delay between superimposed 'in phase' pulses is the reciprocal of the continuous wave oscillator frequency.

1.3.3.5 Pulse Echo Overlap Method

As with the above method a series of rf pulse introduced into the sample. Pulse repetition rate is controlled by continuous wave oscillator. During the acoustic time measurement oscilloscope is switched to an X-Y mode in which the continuous wave oscillator provides the sweep. CRT intensity is reduced and two intensified echo of interest are visible. The echo can be made to overlap cycle for cycle.

Besides there are several other methods such as interferometer method, long pulse buffer rod for small samples etc.

1.3.4 Ultrasonic Attenuation Measurement

Ultrasonic attenuation is a combined effect of absorption and scattering. A number of sources of error need to be considered if one is measuring attenuation. Among the errors are those arising from :

i) velocity dispersion
ii) transducer coupling
iii) phase cancellation - resulting from lack of parallelism of the sample
iv) material inhomogeniety
v) diffraction

Acoustic waves emitted by a transducer into a sample spread out into a diffraction field. Diffraction error is related to ratio of source dimension to acoustic wavelength and thus is especially large for low frequencies, small transducers and high velocity materials. The error due to the diffraction can be of the order of magnitude as that of the measured value some time.

Some of the methods for the measurement of ultrasonic attenuation are given below in brief. Systems of measurements studied earlier [63,73-85] can be divided

in three fundamental classes of techniques based on optical, pulsed wave and continuous wave methods.

1.3.4.1 Optical Systems

Light diffraction offers a technique for measuring ultrasonic wave attenuation . The method depends on satisfying the conditions for linearity between ultrasonic wave intensity and light intensity in the first diffraction order. Length of ultrasonic beam is then scanned and attenuation measured. Method is useful at high frequencies or for materials having high attenuation coefficient.

1.3.4.2 Pulse Echo Method

In the basic pulse echo method for measuring attenuation a pulsed rf signal of given frequency is converted by means of a transducer into a pulsed ultrasonic wave of the same frequency. Ultrasonic pulse travels through the sample and is reflected between the sample boundaries until it decays away. Ultrasonic attenuation is obtained from amount of electrical attenuation introduced into the circuit to maintain a constant amplitude of a selected echo into the receiver [23]. It can also be evaluated from the exponential decay using well known expression for the attenuation.

Pulse spectrum analysis technique uses pulsed wave from the highly damped transducers and spectrum

analyser for measuring the attenuation as a function of frequency. A technique based on long pulse buffer method for attenuation measurement in thin, highly attenuating material is also used. It is a two transducer arrangement for a solid sample.

1.3.4.3 Continuous Wave Systems

(i) Transmission technique : This technique is used for acoustic transmission measurements through flat and parallel homogeneous samples. A stable oscillator is tuned to a mechanical resonance peak, determined by peaking the signal observed on the oscilloscope. The frequency separation between corresponding resonances is measured. The full frequency width of each resonance at 50% power is used to determine the sample attenuation.

(ii) Sampled continuous wave technique : In situations in which electromagnetic cross talk is a problem, one can measure attenuation by a sampled continuous wave (SCW) spectrometer, which eliminates electromagnetic cross talk and provides for both time domain and frequency domain measurements. The time domain decay information is useful for determining attenuation.

(iii)Transmission oscillator ultrasonic spectrometer (TOUS): This instrument does not use an external

oscillator and is an acoustic analog of the marginal oscillator used in nuclear magnetic resonance technique. Also called marginal oscillator ultrasonic spectrometer (MOUS),

A different resonance technique makes use of a sealed cylindrical resonator consisting two transducers, a thin spacer with O-ring and a housing to hold the components and provide electrical coupling.

1.4 PROBLEMS FACED FOR NDC OF ROD MATERIALS

Unlike other products having plane surface, the evaluation of defects in rolled, cylindrical or circular rod products is a bit difficult. The scanning from the end of the rod of course can find transverse defects if the diameter of the rod is comparatively bigger like for rolls, heavy axles and rotor forgings. The possibilities of ghosts caused by mode conversion at shoulders and section changes may exist and all such indications may be well checked. Small diameters bars can have small defects, and to find these by scanning from the end is not likely to be successful because of small area presented by the flaw to the probe and the masking by energy traveling either side of the defect. Rods should, therefore, be also scanned along their whole length besides the testing from the end. When a plane wave strikes the curved surface of the rod, it gives rise to a number of triangular reflections of longitudinal

waves, mode converted transverse waves, creeping waves radiations, surface waves etc. [86]. This causes problem in interpretation of the results. In contact testing the virtual line contact doesn't damp out the ringing of the transmitter in the same way as a flat surface does. Consequently, if the transducer is also a receiver, persistent ringing when flaw echoes arrive might mask them.

When curved surface of the rod is to be inspected by ultrasound, commonly a widening or divergence of the ultrasonic beam is encountered due to reflection, refraction and reduced effective source dimension where the probe contacts and only a part of the transducer plane is utilised. The fact results in reduced testing sensitivity compared with the case of a flat surface.

The amount of divergence, in contact testing, depends on the ultrasound velocities of couplant and rod material. For inspection of the rods therefore adaptor blocks (shoe) are used to obtain full contacting area between probe and curved surface of rod. By suitable choice of adaptor material, it is theoretically possible to achieve a focussing, but the reflection losses due to the great difference of sound impedances of adaptor block and couplant generally are higher than the gain obtained by the focussing. An echo, sequences of course, generated at the coupling area which can disturb the

interpretation of the indication on the CRT screen. Therefore design of an adaptor need most care and should be as short as possible or should be so long that multiple echoes don't occur in the test range.

1.5 SCOPE OF THE PRESENT WORK

Present work deals in with the characterisation of material in the form of rods by ultrasonics. The work may contribute significantly towards the solution for several problems faced in the characterisation of rod shaped materials.

A new idea for the detection and location of defects present in the rod shaped materials by ultrasonic C-scan system has been developed. It is found to be superior than the known methods in several aspects and is described in Chapter 2.

For the measurement of ultrasonic velocity in rod materials, a new method has been developed which gives both the longitudinal wave and the transverse wave velocities. Results have been presented for ultrasonic velocity in various rods of varying diameter with the new technique and compared with the velocity obtained from the bulk material. This method is described in Chapter 3.

The ultrasonic attenuation measurement in rod material is given in Chapter 4. A new technique is used

which doesn't require the beam diffraction correction and uses a single rod and single transducer for the measurement of ultrasonic attenuation of both the longitudinal and transverse wave.

The effect of water loading on the ultrasound propagation in the rods has also been studied. The results show a dependence of ultrasonic wave propagation on the characteristics of the material and thus offers a novel technique for the characterisation of material in the shape of rod. This study has been presented in Chapter 5.

Finally a summary of the work done and its importance in the characterization of rod material has been given in Chapter 6.

1.6 REFERENCES

1. Bhardwaj, M.C., Fundamental developments in ultrasonics for advanced NDC, Proc. NDT of High Performance Ceramics, Boston, Aug. 25-27 (1987) 472-527

2. National Research Council, Characterisation of Materials, National Bureau of Standards, U.S. Deptt of Commerce, Pub. No. MAB-228-M (1967)

3. McMaster, R.C., Non-destructive Testing Handbook, Vol.1 and 2, The Ronald press Co., New York (1963)

4. Hinsley, J.F., Nondestructive Testing, Macdonald & Evans Ltd., London (1959)

5. McGonnagle W. J., Nondestructive Testing, Mc Graw-Hill Book Co., Inc. N.Y. (1961)

6. Halmshaw, R., Development of industrial radiography technique over the last fifty years, INSIGHT, 37 (1995) 684-687

7. Lovejoy, D.J., A practical approach to probability of detection with magnetic particle inspection, INSIGHT 37 (1995) 974-977

8. Fletcher, M.J., Optical examination - a review of optical examination, INSIGHT, 38 (1996) 270-275

9. Prokhorenko, P.P., Migoun, N.P., Hydrodynamic principles and physical aspects of liquid penetrant testing, Proc. 14WCNDT (1996) 1235-38

10. Shiloh, K, Ellingson, W.A., Sharma, M., Nondestructive evaluation of Nicalon/SiC composite by vibration analysis, Proc. 14WCNDT (1996) 1163-69

11. Bindal, V.N., Ashok Kumar, Som, J., Yudhisther Kumar, Lal J., Nondestructive evaluation of graphite electrode, Proc. ICU-90 (1990) D18-23

12. Klug, H.P. and Alexander, L.E., X-Ray Diffraction Procedures, John Willey & Sons, New York (1954)

13. Sasada, I., Watanade, N., Eddy current testing probe for NDT, IEEE, Trans. Magnetics, 31 (1995) 3149-3151

14. Yamada, S., Katou, M., Twahara, M., Dawson, Eddy current testing probe composed of planar coils, IEEE Trans. Magnetics 31 (1995) 3185-3187

15. Balasko, M., Progress and status of neutron radiography and gauging in Europe, Proc. 14WCNDT (1996) 1465-68

16. Sekine, K., Lizukka, A., An improved method of magnetic flux leakage inspection for farside corrosion type defects of ferromagnetic specimens, Proc. 14WCNDT (1996) 1627-30

17. Krautkramer, J. and Krautkramer, H., Ultrasonic Testing of Materials, Third edition, Springer Berlin, Bonn (1983)

18. Highmore, P.J. and Rogerson, A., Advances in ultrasonic flaw characterization, in Nondestructive Testing (Ed. JM Farley and RW Nichols), 3 (1987) 1553-1563

19. IS 6394 (1986), Code of practice for ultrasonic testing of seamless metallic tubular products by contact and immersion methods, Bureau of Indian Standards.

20. ASTM E-1001 (1984), Standard practice for detection and evaluation of discontinuities by the immersed pulse echo ultrasonic method using longitudinal waves, American Society of Testing Materials.

21. IS 3664 (1981), Code of practice for ultrasonic pulse echo testing by contact and immersion testing, Bureau of Indian Standards.

22. Richardson, L.F., Apparatus for warning a ship at sea of its nearness to large objects wholly or partially in water, British Patent Specification, 11,125, March 27 (1913)

23. Mulhauser, O., Varfahren zur Zustandbestimung von Werkstoffen, Besonders zur ermittlung con fehlren darin, German Patent Specification 569,598 Jan. 10 (1931)

24. Vardan, V., Ma, Y. and Vardan, V., A multiple scattering theory for elastic wave propagation in discrete random media, J. Acous. Soc. Am. 77 (1985) 375-85

25. Nozdreva, V.F., Soviet progress in applied ultrasonics, Vol. 1, Ultrasound in industrial processsing and control, English translation, Consultant Bureau, N.Y. (1964)

26. Filipczynski, L., Pawlowski, Z., and Wehr, J., Ultrasonic Methods of Testing Materials, English translation by Schlachter, K.R. and Blitz, J., Buttersworth, London (1966)

27. Schreiber, E., Anderson, O.L. and Soga, N., Elastic Constants and Their Measurement , McGraw Hill Book Co., N.Y. (1973)

28. Blitz, J., Fundamentals of Ultrasonics, Plenum press, NY (1967)

29. Herzfeld, K.F., and Litovitz, T.A., Absorption and Dispersion of Ultrasonic Waves, Academic Press, NY & London (1959)

30. Bergman, L., Ultrasonics, John Wiley & sons, Inc., NY (1938)

31. McSkimin, H.J., in 'Physical Acoustics' (W.P. Mason, ed.), Academic Press New York, IA (1964) 271-417.

32. Kinsler, L.E. and Fray, A.R., Fundamentals of Acoustics, Wiley Eastern Ltd., (1990)

33. IS 2417 (1978), Glossary of terms relating to ultrasonic testing, Bureau of Indian Standards.

34. ASTM E 500 (1989), Terminology relating to ultrasonic examination, American Society for Testing Materials

35. Babikov, O.I., Ultrasonics and Its Industrial applications, Consultant Bureau, NY (1960)

36. Fitting , D.W. and Adler, L., Ultrasonic Spectral Analysis for Nondestructive Evaluation, Plenum Press, NY & London (1981)

37. Nadal, M., Cyril, H., Gondard, C. and Luc, P., Determination of elastic constant in material submitted to high temperature by ultrasonic methods, Proc. 14WCNDT (1996) 2259-62

38. Kino, G.S., Peterson, D.K. and Bennett, S.D., Acoustic imaging, in New procedures in Nondestructive Testing by P. Holler, Springer Verlag Berlin (1983) 113-125

39. Silk, M.G., Sizings crack like-defects by ultrasonic means, Research Techniques in Nondestructive Testing 3(1977)51-99

40. Berner, K., Stilke, H., Bach, G. and Horst, B., Fully automatic ultraasonic testing of heavy plate including inspection for surface defects in tail regions, Proc. 14WCNDT (1996) 569-572

41. Ghost, J.K., Murlidhar, S. et.al., Development of an ultrasonic GIG for monitoring a buried pipe line, Proc. 14WCNDT (1996)613-616

42. Zebo, S., Wang, X. and Song, S., Ultrasonic inspection of the impact damage to CFRP laminated plate, Proc. 14WCNDT (1996) 691-694

43. Ogi, H., Hirao, M., Fukuoka, H., Ultrasonic measurement of bending stress in electric resistance welded pipe by electromagnetic acoustic resonance, Proc. 14WCNDT (1996)875-858

44. Narayan, K., Derrick, D.H. and Rose, J.L., Ultrasonic NDE of stressed metal parts, Proc. 14WCNDT (1996) 549-552

45. More, J.R., Patanakar, V., Joshi, V., Gopalkrishna, K., Advanced ultrasonic imaging system for NDT/NDE, Proc. 14WCNDT (1996) 2071-74

46. Mak, D. K., Ultrasonic imaging analysis using multitransducer technique, Ultrasonics 29 (1991) 308-311

47. Workman, G.L. and Walker, J., Update on the development of a Robotic acoustic ultrasonic system, Proc. 14WCNDT (1996) 2067-2070

48. Rose, J.L., Nestleroth, J. and Balasubramaniam, K., Utility of feature mapping in ultrasonic nondestructive evaluation, Ultrasonics 26 (1988) 124-131

49. Drury, J.C., Ultrasonic flaw detection for technicians, Unit Inspection Co. Ltd (1983) 163-195

50. Silvus, H.S.Jr., Advanced ultrasonic testing system - A state of the art survey, NDT Information Analysis Center (1976) 10-15

51. ASTM E-127 (1989), Standard practice for fabricating and checking aluminium alloy ultrasonic standard reference blocks, American Society for Testing Materials.

52. Kock, W.E., Acoustic holography, in Physical Acoustics By Mason W.P. and Thurston R.N. Vol. 10, Academic Press, N.Y. (1973) 297-381

53. Georgiou, G.A. and Hayward, K.S., Ultrasonic techniques for sizing flaw lengths , British J. NDT 11 (1991) 545-548

54. Silk, M.G., Defect sizing using ultrasonic diffraction, British J. NDT, 21 (1979) 12-1531.

55. Kino, G.S., Corl, D.,Bennett, S.D. and Peterson, D.K., Real time synthetic aperture imaging system, Proc. IEEE Ultrasonics Symp. (1980)

56. Whaley, H.L. and Adler, L., Flaw characterization by ultrasonic frequency analysis, Mat. Eval. 29 (1971) 182-188

57. Silk, M.G., Developments in Ultrasonics for sizing and flaw characterization, in Development of Pressure Vessel Technology - 2 by Nichols, R.W., (1979) 101 - 139

58. Mak, D.K., Accuracy in locating a point scatterer in ultrasonic testing, using the TOFD technique, British J. NDT 31 (1989) 481-484

59. Jansen, D., Hutchins, D.A, Young, R.P., Ultrasonic tomography using scanned contact transducers, J. Acoust. Soc. Am. 93 (1993) 3242

60. Gordan, G.A., Canumalla, S. and Tittman, B.R., Ultrasonic C-scan imaging for material characterization, Ultrasonics 31 (1993) 373-380

61. Wustenberg, H., Erhard, A., Montag, H.J. and Schenk, G., Measurement of crack depth with ultrasonic methods-through transmission and reflection modes, in New Procedures in Nondestructive Testing, by P. Holler, Springer Verlag NY (1983) 213-228

62. Krautkramer, J. Thirteen years of DGS diagrams in ultrasonic NDT, Proc. Ultrason. Conf., London (1971) 39-41.

63. Breazeale, M.A., Cantrell, J.H. Jr. and Heyman, J.S., Ultrasonic velocity and attenuation measurements, in Methods of Experimental Physics by L. Marton and C Marton, Edited by P. Edmonds, Academic Press, N.Y. (1981)67

64. Panakkal, J., Longitudinal ultrasonic velocity as a predictor of material properties of porous materials, Proc. 14WCNDT (1996) 2279-82

65. Mayer, W.G. and Hiedemann, E.A., Corrected values of elastic module of sapphire, J. Acoust. Soc. Am 32 (1960) 1699-700

66. Huntington, H.B., Phys. Rev. 72 (1947) 321

67. McSkimin, H.J., Variation of the ultrasonic pulse superposition method for increasing the sensitivity of delay time measurement, J. Acoust. Soc. Am. 37 (1965) 864-871

68. Papadakis, E.P., Ultrasonic attenuation and velocity in three transformation products in steel, J. Appl. Phys. 35 (1964) 1474

69. Williamson, R.C., and Eden, D., Coherent detection of technique for variable path length measurements of ultrasonic pulses, J. Acoust. Soc. Am. 47 (1970) 1278-81

70. Teodoru, G. and Herf, J., Engineering society cologne presents itself (NDT methods), Proc. 14WCNDT (1996) 934-44

71. Venkadesan S., Palanichamy, P., Vasudevan, M. and Baldev Raj, Ultrasonic velocity measurement - A potential sensor for intelligent processing of austenitic stainless steel, Proc. 14WCNDT (1996) 557-560

72. Ashok Kumar, Yudhisther Kumar and Basant Kumar, On the measurement of longitudinal and shear ultrasonic velocities, Nondestr. Test. Eval. 13 (1996) 121-126

73. Jeon, H., Determining the constituent volume fraction of metal matrix composite by a multiple NDT technique, Proc. 14WCNDT (1996) 695-702

74. Mak, D.K., Comparison of various methods for the measurement of reflection and ultrasonic attenuation, British J. NDT,33 (1991) 441-449

75. Papadakis, E.P., Fowler K.A., and Lynnworth, L.C., Ultrasonic attenuation by spectrum analysis of pulses in buffer rods., J. Acoust. Soc. Am. 53 (1973) 1336-1343

76. Simpson, W.A., Time frequency domain formulation of ultrasonic frequency analysis, J. Acoust. Soc. Am. 56 (1974) 1776

77. Papadakis, E.P., Measurement of small changes in ultrasonic velocity and attenuation, Critical Review in Solid State Sciences, 3 (1973) 373-418

78. Papadakis, E.P., Ultrasonic spectroscopy applied to double refraction in worked metals, J. Acoust. Soc. Am. 55 (1974)783-784.

79. Adler, L. and Lewis, D.K., Scattering of a broadband ultrasonic pulse by discontinuities, IEEE Trans. Son. Ultrason. SU-23 (1976) 351-356

80. Yudhisther Kumar, Ultrasonic attenuation measurement in aluminium alloy, BITS ZG628T, Dissertation M.S.(PSC), 30th Nov. (1993)

81. Basant Kumar and Ashok Kumar, Direct evaluation of ultrasonic attenuation, Ultrasonics 34 (1996) 847-53

82. Seki, H., Granto, A. and Truell, R., Diffraction in the ultrasonic field of a piston source and their importance in accurate measurement of attenuation, J. Acoust. Soc. Am. 28, (1956) 230-238

83. Adler L, Rose J.H. and Mobley C., Ultrasonic method to determine gas porosity in aluminium alloy castings : theory and experiment, J. Appl. Phys. 59, (1986) 336-347

84. Papadakis E.P., Ultrasonic attenuation and velocity in three transformation products of steel, J. Appl. Phys., 35, (1964) 1474-1482

85. Pandey, J.C., Jha, R., Singh, M.P. and Mohanty, O., Ultrasonic attenuation technique and quality of steel products, Proc. 14WCNDT (1996) 2247-52

86. Neubauer, W.G., Observation of acoustic radiation from plane and curved surfaces, in Physical Acoustics By Mason W.P. and Thurston R.N. Vol. 10, Academic Press, N.Y. (1973) 61-125

CHAPTER - 2

CHARACTERISATION OF ROD BY DETECTION OF DEFECTS

CHAPTER - 2

CHARACTERISATION OF ROD BY DETECTION OF DEFECTS

2.1 INTRODUCTION

Rods and rod shaped components are widely used in engineering plants, building of highly stressed structures, various types of components like pin, axle, shaft, penetrator (bullets), frame structure, etc. Structural components may be subjected to heavy stress and fatigue during their subsequent use in individual system. This may mean failure of the system if the rod has been found defective or undergone some hidden defects during use. Moreover the rods are also being used in the form of cladded rod as acoustic wave guide [1-3] and characterisation provides better estimation of performance for use in a particular application.

For better interpretation of results in nondestructive evaluation, a knowledge of the type of possible defects in material is very helpful. Manufacturing defects occurring in semi-finished products of round bar or rod shaped material can either be internal or surface defects [4-6]. Internal defects originate either from ingot defects elongated during drawing, namely shrinkage

cavities and inclusions, mainly in the core (Fig.1). Other defects due to rolling and drawing include piping and cracks in the core which in cross-section appear flat or star shaped. Surface defects usually result from drawing may be such as radial incipient cracks or spills which penetrate to the surface at a flat angle. Most of these flaws extend in longitudinal direction which requires that axis of sound beam lies in a cross sectional plane either normal or oblique to the surface so that the flaw is always normal to the beam axis.

Casting may also give defects [7,8] which may be stated as follows :

i) Gas defects : These are generally caused due to low gas passing tendency of mold. Gas defects can be of various types such as blow holes and open holes, air inclusion and pin holes etc.

ii) Shrinkage Defects : These are caused by liquid shrinkage occurring during the solidification of the casting. It can be shrinkage cavities or pipe.

iii) Molding material defects : These defects are caused due to the characteristic of molding materials and are cuts and washes, metal penetration, fusion, runout, swell, drops etc.

iv) Pouring metal defects : These defects are caused due to the impurities in starting metal and speed of pouring it into the mold. It can be mis run and

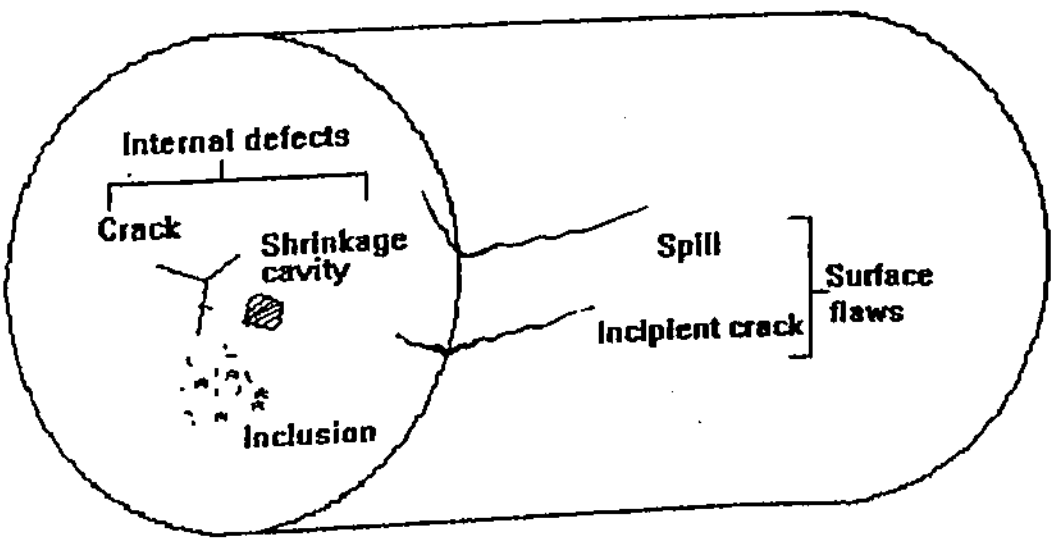

Fig. 1. Types of defects in rod and round stock

cold shut, nonmetallic / slag inclusion

v) Metallurgical defects : These defects are caused due to unwanted cooling stress or by chilling of casting like hot tears, hot spots.

vi) Deformation of geometrical form : These are caused due to improper assembly of mold. The geometrical shape of casting is not obtained as per design and dimensions.

vii) Cracks : Defects grouped in this category are hot crack and cold cracks

The forging defects may be like clinks, forging lap, forging bursts or cracks, pipe, inclusions, hair-line cracks etc.

To demonstrate the integrity and reliability of the system and to avoid risk failure, it is essential to detect and size these defects. The growing requirement to demonstrate the safety and reliability of plants has encouraged the wider use of nondestructive examination. Ultrasonics is a valuable technique because of its convenience, sensitivity and quantitative results. Amongst all the NDE techniques, ultrasonic method is capable of revealing more or significant information. Ultrasonic NDT methods offer several advantages for characterization of materials [4,9-15]. The technique is commonly used for flaw evaluation and thickness gauging

of metallic and non-metallic materials. A high energy pulse ultrasound is used to detect, locate and evaluate the defects such as cracks, porosity, deterioration, corrosion, foreign inclusion, etc. [16-19]. Direct contact or immersion testing techniques [20-22] are generally used with single transducer or some time with dual transducer in through transmission technique for evaluation of defects.

Considerable difficulties are encountered in the testing of round bars or rods for internal defects. Any type of irregularity in material cross section may effect the sound path. However it is not easy to identify the defect from the sound image, and to correlate the interference echoes to particular defect. Nevertheless a knowledge of these correlation is very important for an NDT expert to give a way to wide application of ultrasonics in NDE.

As against the advantages described for ultrasonic NDT, there is a serious draw back. Although it is quite easy to find even small defects, it is very difficult to determine somewhat accurately the size of the defect. The attempt here actually is to find ways which enables one to make an exact statement about the size and nature of the defect in rod of various materials. The defect evaluation in rods of small diameters i.e. below 40 mm is more difficult and determinations of flaw below 30 mm is very difficult. Earlier studies [23-28] have shown

maximum clarity of defects in rods of diameter 50 to 60mm.

Attempts have been made in past to determine size of defects with sufficient accuracy. At first it was believed that the problem could be solved with the rules of geometric optics [23-24]. It was also tried to calculate the defect size by the ratio of flaw echo to back wall echo when defect surface is at right angle to the direction of ultrasound beam by the following formula.

$$FE/BE = F/A$$

where FE = flaw echo amplitude

BE = back wall echo amplitude

F = area of defect

A = cross sectional area of sound beam

However, the beam divergence effect could not be taken into account in the above equation. Due to this, for the constant work piece length, a defect of given size will give a higher defect echo if it is nearer to the sound irradiation. At the same time the back wall echo decreases. Applicability of this equation is therefore limited due to the fact that it does not consider the distances between transducer-defect, transducer-back wall and defect-backwall. In usual probes or narrow beam probes, the sound pressure varies with increasing distance from irradiation point. It declines in the far

field region and the curve proceeds discontinuously for distances in near field region. Therefore the measurement of echo ratio in the short range field does not allow one to infer the size of the defect. It is sufficient if only one of two echoes is situated in the near field range. Therefore, while using echo ratio, size measurements of defect must be carried out in the long range field. The near field is smaller for low frequency transducer but they show a dispersed input pulse in the luminous screen image, the so called dead zone, and defect echo cannot be recognized. One is often thus forced to make some compromise. However it has been proved that variation of pulse width or receiver sensitivity does not markedly effect the echo ratio, till the two echo ratios lie in linear region of instrument amplifier. In order to radiate a continuous sound wave at maximally possible sound pressure and a given frequency it is logical to excite a plate at natural frequency and keep its damping minimum. But in case of nondestructive examination, even if continuous sound wave is used it will usually be necessary to sweep the frequency to avoid the creation of standing waves in test piece. In the shifting of frequency, if we desire, amplitude should remain constant as possible which, however, a narrow resonance curve does not permit. Therefore to broaden the resonance curve a suitable damping is introduced, resulting in the band decreasing to about 70% of the maximum value at this limit.

In echo method length of the pulse may prevent the detection of defects near the surface. The pulses of minimum duration is therefore desirable and it is necessary to generate and transmit pulses at frequencies which are not excessively high and with a minimum number of oscillation i.e. shock pulses or transients. Keeping this as criteria the problem stated above that the defect can be sized only in far field is removed and it will be far better to size a defect in near field which even does not require the correction of beam divergence effect.

For a plane wave probe emitting uniform beam width in test sample in near field (NF), the echo heights from equal size defect A and B will be the same except the attenuation in material (Fig.2 a). This will happen for broad band transducer. However, in narrow band transducers, the acoustic pressure varies significantly with distance in the near field. In such a case echo heights from A and B can be of any value. If shadow is considered in this case, BWE height due to A and B will be same for broad band transducer and narrow band transducer both.

In far field or diverging beam field (Fig.2b), echo height from A and B will vary depending upon attenuation and diffraction effects. Echo height of B will be always less than that of A. If shadow is considered in

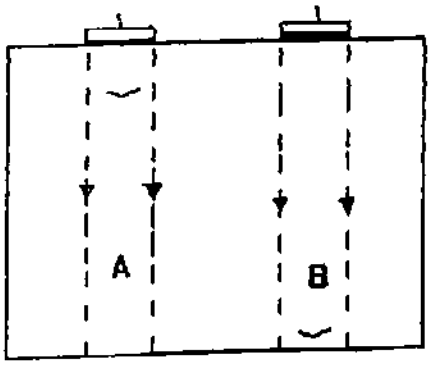

(a) in near field

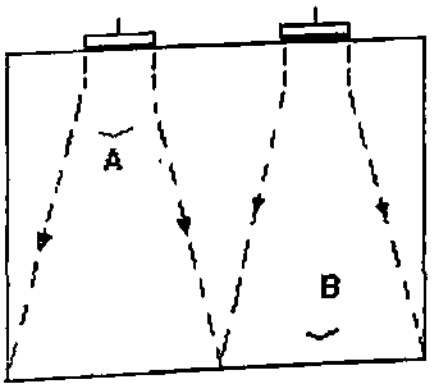

(b) in far field

Fig. 2. Effect of echo height on two same size defects from broad band and narrow band transducers in near field and far field

this case BWE height will vary. The defect A will caste wider shadow than B and hence BWE height due to A will be less than due to B.

To detect internal or surface defects on a rod both types of methods, that is, direct contact and immersion are used. Some of the techniques used earlier for defect detection in rods are described below in brief [4,5,23-34]

To find defects in core, the stationary rod is coated with viscous oil and scanned continuously with the protected normal longitudinal probe along a few longitudinal tracks, at least on two tracks being transposed 90° in order to obtain an echo with sufficient probability. Usually frequencies are of 2 to 6 MHz, the higher frequencies and a small probe diameter being used on thin material in view of the better close range resolution. The width of flaw can be estimated roughly from the ratio between flaw echo and bottom echo. But for sizing the flaw, the depth of flaw, diameter of rod and diameter of probe and frequency used should be taken into consideration. The care should be taken to avoid mistaking triangle echoes for flaw echoes.

Thin bright rods down to approximately 5 mm diameter are preferably tested by TR probe. Two probes may be placed on the circumference displaced 90° from each other and mounted in a continuously moving specimen. A

flow of water may be used as coupling. Device for guiding the probes greatly facilitates these tests. The V-shaped shoe of angle 120° are also used for guiding the probes to contact the rod along the diameter and movement along the surface.

Surface defects are found with oblique transverse waves or with surface waves, the later, however, can be used only on very smooth surface, making furthermore quantitative difference between deeper and shallower cracks impossible. If an angle probe with 45 or 60° is suitably ground, the broad beam after a few reflections fills a zone under the surface fairly completely upto a depth of approximately 1/5 of the diameter (Fig.3a) and covers internal defects in addition to surface defects. These surface defects can only be distinguished by finger tips

Thin bright round stock, down to a diameter 1 mm can be checked for longitudinal surface defects by dry contact with plane normal probes of frequency 4 to 6 MHz protected by a plastic shoe against wear. Cracks with a minimum depth of 0.1 mm are detectable provided that extend in longitudinal direction at least 10 to 20 mm. However the method has not been applied to any appreciable extent because of tiresome and time consuming visual inspection.

Since sensitivity of oblique transverse wave drops

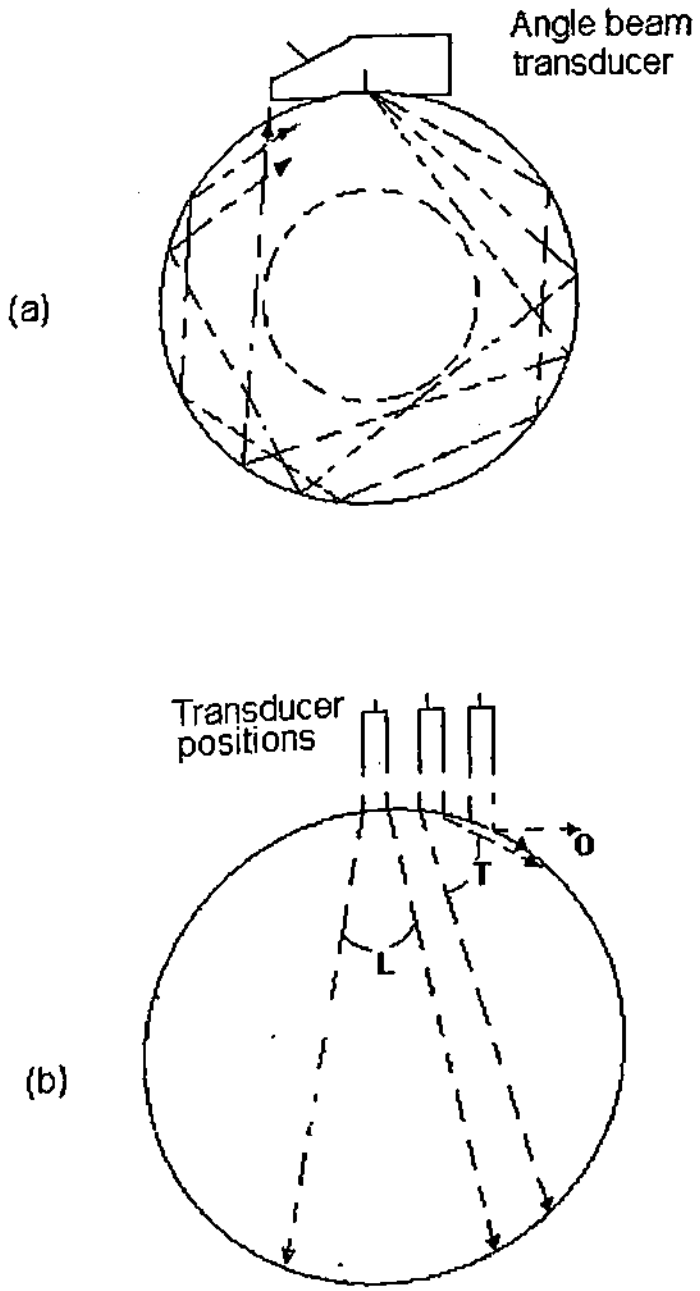

Fig. 3. Some of the technique used for testing of rod material

after several reflections, the flaw as far as possible should be encountered in the first third to one half of the circumference. Thus in case of stationary rods, test may be carried out along 2 to 3 longitudinal tracks and the probe should be advanced along a zigzag path on the circumference. Flaw echoes than travel back and forth on the CR screen and can be detected easily.

Immersion technique provides testing flexibility since the transducer can be moved underwater to introduce a sound wave at any desired angle. It is suitable for high speed and scanning system because the transducer does not contact the test object and therefore is not subjected to wear. Also all types of waves and testing directions can be obtained by using a movable probe, including a surface wave (Fig.3b). Further to evaluate defects in material, its surface should be uniform and smooth for contact testing. Immersion testing is useful for examining irregularly shaped objects when submerged in a liquid. The continuous testing for defects evaluation in rod, tube or bar is performed using immersion testing. In regular test objects having uniform and plane surface, ultrasound beam scanning is not so difficult for 100% inspection of test object. In rod shaped materials, it is a bit complex, for the surface of the rod being curved changes the beam shape drastically. The change in shape depends upon the relative ultrasonic velocities in water and in rod material. For exam-

ple, in steel rods where velocity is about 4 times of that in water, the beam diverges on entering into the rod. The beam divergence increases with smaller diameter rods as the radius of curvature decreases and the incident angles gets larger. The beam divergence exacerbates the difficulty in testing the rods, already present due to change in transmittivity of ultrasonic waves. The transmission coefficient is different at different angles and the ultrasonic beam are incident on the rod at different angles at different points on surface. This changes the variation in pressure in the beam and is difficult to account for.

Imperfections which are radial in nature and oriented predominantly longitudinally to the major axis of the rod are detected by this technique. The rod is rotated transversally and also advanced longitudinally through some glanded test tank. The ultrasonic beam describe the helical scan path of required pitch and overlap on the surface for 100% inspection of the test object. The scan is known as Helical scanning. A holder mounting the probes for detecting the longitudinal surface and core defects, rides on the rod. Probes are submerged, the water level kept constant to compensate for the losses at the entrance and exit openings. Probes can be adjusted in the holder for correct positioning for any diameter. The method is extensively used and commercial on-line testing system have been

available for past several years.

After reflection from the inner wall a diverging beam of shear waves inside a rod converges to form a caustic. This surface of high sound intensity forms a well defined structure within the sample under test which can be used as a probe for internal defects. The returned pulse echo data can be utilized to determine the size, shape and position of the defects. Width of energy concentration at the caustic has been measured and used to calculate the resolution of such a testing system [35-36].

If the surface is not perfectly smooth, trouble-some interfering echoes in zone behind the entrance echo some times may be observed in immersion testing using broad sound beam. These in case of thinner rods may mask the echoes of core defects completely. There-fore narrow or focussed sound beams are used or masks with a round opening or a slot can be inserted in the sound path. The relative positions of probe, mask and round stock is kept fixed. This can be done by simply using a probe holder, mask which may be rotatable, mounted in front of probe and contains two eccentric openings (Fig.4a). Two transverse waves circulating in opposite directions can determine shallow defect or two longitudinal beams through the core of the rod. Rod with mill rough, slightly oxidized surface down to 12 mm diameter can be tested using probe of frequency 4 to 6

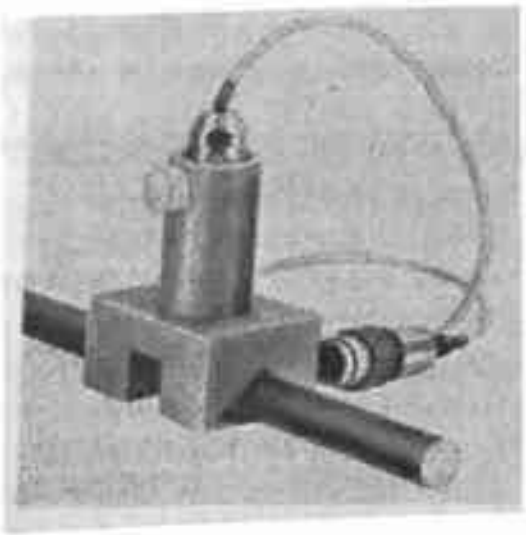

(a)

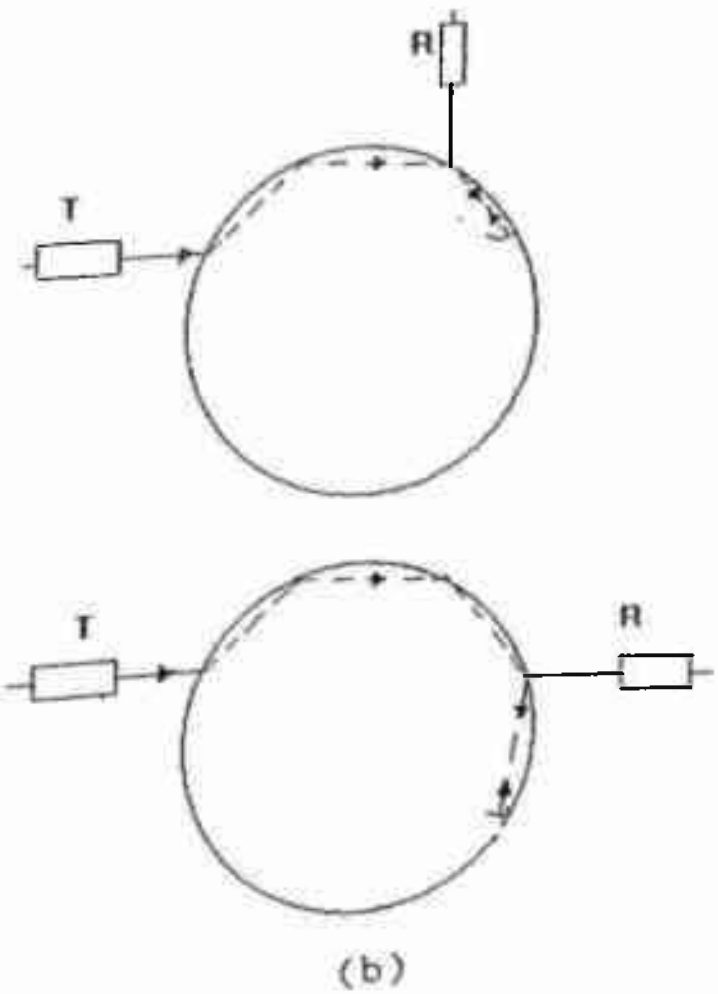

(b)

Fig. 4. (a) Probe holder for testing the rod
(b) Arrangement for detection of longitudinal defects

MHz.

With focussed probe the decrease in sensitivity due to the strong refraction in rod can be compensated. TR probes also have a pronounced sensitivity maximum at a definite depth.

Longitudinal defects close to the surface of rod can be tested by two probes as transmitter and receiver and arranging in a immersion tank at 180° or 90° (Fig.4b). Transmitted sound beam travel along a polygon and may be reflected by the longitudinal defect if present and can be received by receiving probe. When the rod is rotated defect echo is observed as traveling echoes. To detect spills in two possible directions of inclination, the test is usually carried out simultaneously in two parallel testing planes and sound circling in opposite directions.

Magnetostrictive method [4] has also been tried for detecting longitudinal surface defects (possible only in steel and nickel). An array of several coils is mounted in a way that the excited ultrasonic pulse spirals around the rod at a steep pitch (Fig.5a). Receiving coil is orientated so that it can receive part of the sound beam reflected by a longitudinal defect and thus produce defect echo. Other receiving coil can receive the spiraling wave directly, the sound transmission indication obtained in this way can reveal, by its

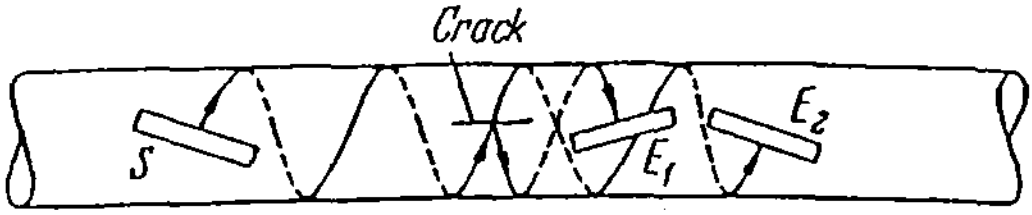

Fig . 5. (a) Rod testing by magnetostrictive excitation.
E - Receiver, S - transmitter

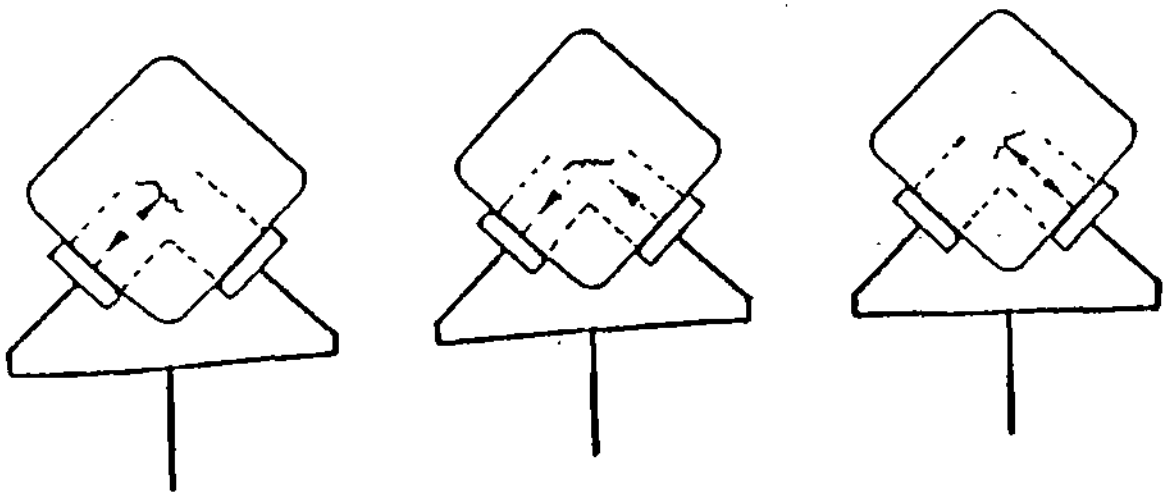

Fig . 5. (b) Testing billets with two probes

disappearance, the presence of large defects. The instruments are capable of testing 2 to 14 mm diameter rods. In case of bright stock, longitudinal defects at least 0.05 mm deep can be detected in this way.

Core defects in rolled, round billets with diameters 50 mm and more are detected by transporting these without rotating on conventional rollers. This is carried out with two probes from two sides to cover wider angular range of flaw orientations (Fig.5b). Longitudinal defects in round billets can be detected by means of angle probes or pipe probes in the same way as for the drawn rods. Owing to the rough and not very uniform surface of the round billets, the coupling conditions are less favourable. Testing by hand can therefore be considered where the requirement of flaw detectability is not too high. For continuous testing the specimen should be fed in a spiral motion, which in round billets usually meets with difficulties because they are not sufficiently straight.

In the case of drawn steel rods, testing of internal defects on material thicker than 30 mm is one of the oldest application of pulse echo method. Perhaps the characterisation of defects depends on beam width, frequency, transducer, diameter of rod, rod material velocity and water path (in immersion testing). Optimization of these factors may give improved results.

In the present chapter theoretical expression and results have been evaluated for optimal selection of the frequency, transducer diameter, rod diameter, rod material velocity and water path for better evaluation of a defect in various rods. Beam width is the important parameter to evaluate or resolve the smallest defects. The variation of beam width with respect to rod diameter and transducer diameter are evaluated and plotted. The theoretically obtained results have been compared by performing the experiments on various samples of rods with simulated defects using various transducers in varying frequency and diameters. Thus limit to detect and size the smallest possible defect in varying size rods has been estimated.

In the present studies rods of diameter ranging from 5 to 55 mm with simulated defects are taken. A new technique is developed using immersion testing C-scan system [37,38] to scan the rod circumferentially through the diameter using normal beam longitudinal transducer. An add-on arrangement has been developed for the existing facilities of C-scan system. This allows the scan of rod circumferentially as well as longitudinally.

2.2 C-SCAN TESTING OF RODS - A NEW METHOD

In immersion testing, the test object is placed in the tank filled with water and transducer is set to transmit ultrasonic waves normal to the surface of

object, if the test object has a smooth and plane surface. In ultrasonic C-scan systems, there is no arrangements for evaluation of defects in rod shape materials.

The ultrasonic C-scan technique [38-41] is an important tool for the NDE. It allows high resolution imaging of subsurface regions, which is inaccessible with the conventional techniques of optical or scanning electron microscopy. The fundamental measures of performance of a C-scan system are resolution and penetration. To determine these measures quantitatively, attention must be paid to the type of probe and the technique employed.

A broadband probe is excited by a spike. The emitted ultrasonic energy is coupled from probe to the sample by water filled in the tank. Data in the form of return signal amplitude is collected along a two dimensional grid as the probe is raster scanned over the specimen. Electronic gate is set to extract the selected echo from the entire return signal and these data are then used to vary the intensity on a monitor or are printed to paper. Magnification or reduction can be achieved by scaling the scanning grid. System can be configured in a variety of modes, such as pulse echo, through transmission, double through transmission and angle beam using plane or focussed wave transducers.

In the present system, in addition to the water tank for C-scan system, an arrangement to push the rod to be tested is made in such a way that the rod both revolves and advances uniformly with respect to the transducer (Fig.6a, b, c). A leveling plate is placed inside the tank. Rod to be inspected is kept on the plate. A U-shaped frame (Fig. 7a, b,c) is fixed on the rod carrying the Y-movement of transducer. This frame is used to push (advance) the rod. The pushing force and the gravitational force and frictional force combined rotates the rod while it is advancing on the leveling plate. The frame is also attached with a braking mechanism that does not allow the rod to move forward more than the movement given by the frame. Leveling plate is so adjusted that its face is parallel to the plane of the transducer. It ensures that the transducer plane is always parallel to the plane on which rod is revolving. The transducer and the specimen rod are set in such a way that the axis of rod is perpendicular to the axis of sound beam as shown at position 2 in Fig.8 throughout the scanning. This ensures that the distance between transducer and the rod interface and rod axis remains constant throughout the scanning. Once this condition is achieved, the time of travel and echo amplitude from water rod interface would be equal at both ends of rod.

During the scanning of the rod, following points are always kept in mind.

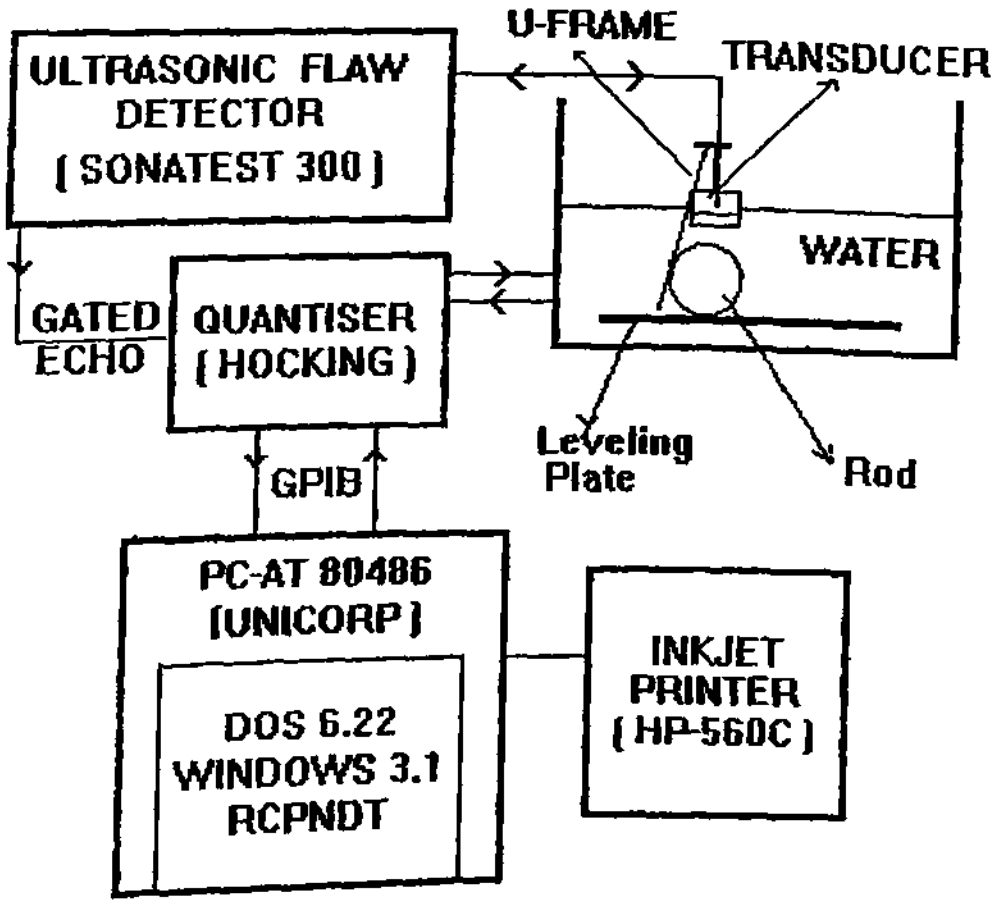

Fig. 6(a). Block diagram of experimental setup

Fig. 6(b) Photograph of the experimental system

6(c) Photograph of the image analysing system

7 (a)

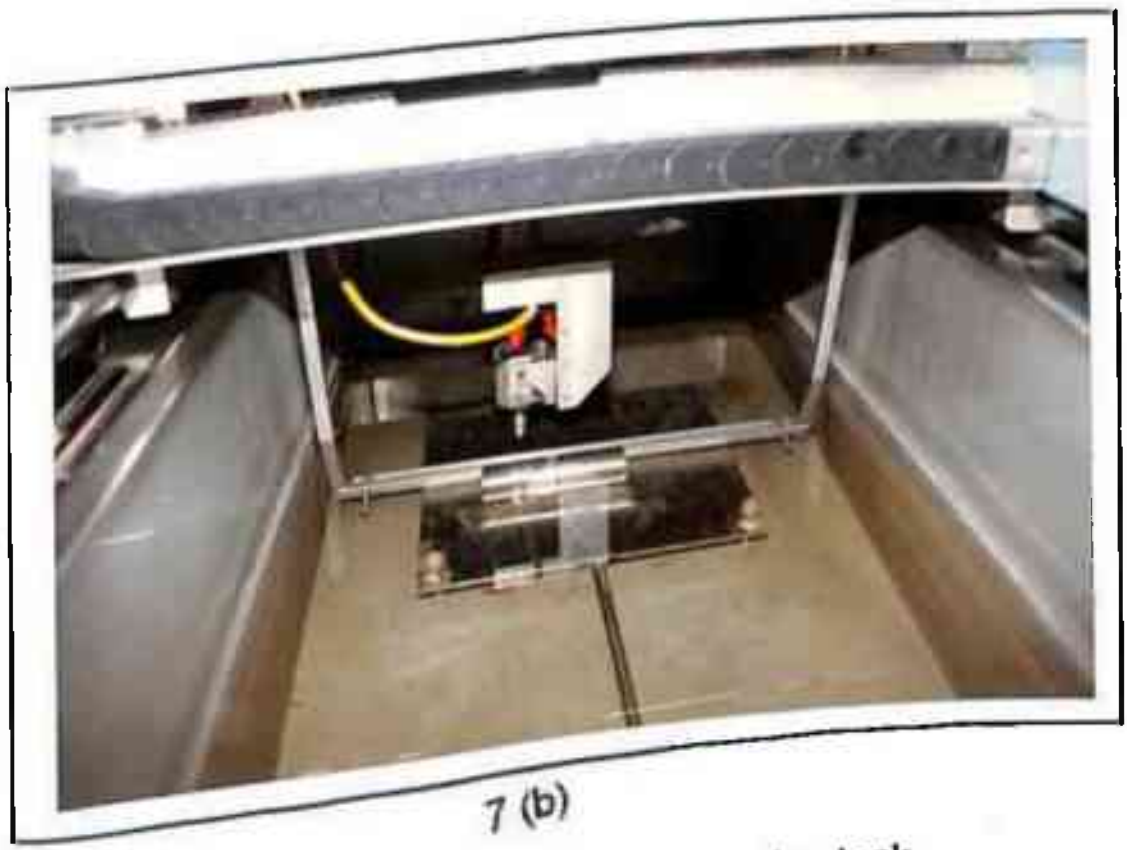

7 (b)

Fig. 7. Photograph of the scanning tank

(i) Axis of the rod and beam axis should be in the same plane and perpendicular to each other. This will make the beam axis of the transducer along the diameter of the rod.

(ii) The rod diameter should be uniform all over.

(iii)The rod surface facing the transducer should be free from any defect, otherwise variation in echo height will be observed.

(iv) The rod axis should be in a plane parallel to the plane in which the transducer face moves for the scanning. This can be achieved if the plane of the leveling plate is parallel to the scanning plane of the transducer.

Ultrasonic signal from the rod may be received back after reflection, refraction, multiple reflections etc. The earliest echo signal, after the water rod interface echo, will result either from the back wall of the rod or the defect present in between the interface and back wall within a particular beam width. The back wall echo has to be identified and selected using the suitable electronic gate width and position available in the flaw detector system. The overall effect of flaw present in the rod will have its contribution seen in the received signal from the back wall.

2.2.1 Positioning of time gate

The C-scan image can be formed by fixing the time gate at different positions in the following ways.

(i) Gating the interface echo : The echo will be affected by surface defects, varying smoothness, but will not effect due to the internal defects of the rod.

(ii) Gating between interface and back wall : This will obscure the echo from the smaller defect if a larger defect is present in the same line, for the gate captures only the highest signal available. Also, the echo height will depend upon the depth of the defect due to attenuation. This will overestimate the size of the nearby defect and underestimate the size of the far of defect.

(iii) Gating the back wall echo only : The back wall echo gating will give better results as compared to the above gate positions. The obstruction by the defect will reduce the reflected signal from back wall. If the beam width remains uniform throughout the thickness of the material, the reduction in back wall echo will be same irrespective of depth of defect. The height of the back wall echo will not depend on the attenuation or any such parameter. This will always give the correct size of the defect whatever be the position of the defect.

2.3 EFFECT OF BEAM WIDTH ON ROD TESTING

The ultrasonic reflection from curved surface in rod is complex and some defects could be missed depending upon frequency, rod diameter, surface roughness etc.[42,43]. Yet it is desired that continuous testing of rod is performed using ultrasonic immersion testing.

For evaluation of shape and size of defects it is better to minimize the beam width into the material such that the reflected or received signal from the defect is comparable to the back wall echo and hence sufficient to analyse. The beam in contact with the surface of the rod is supposed to have an effective width for which ultrasonic energy is received after reflection from the defect or ground boundary of rod (back wall). Keeping this point in view, the beam width has to be evaluated for optimal selection of the frequency, transducer diameter and water path for particular rod diameter.

To find the effective beam width for a given water path, rod diameter and transducer diameter, let us refer to Fig.8.

Let BD = effective beam width of the transducer

QE = water path between transducer and top surface of the rod

r = radius of rod

D = diameter of transducer

θ_i, θ_r = angle of incidence and refraction respectively

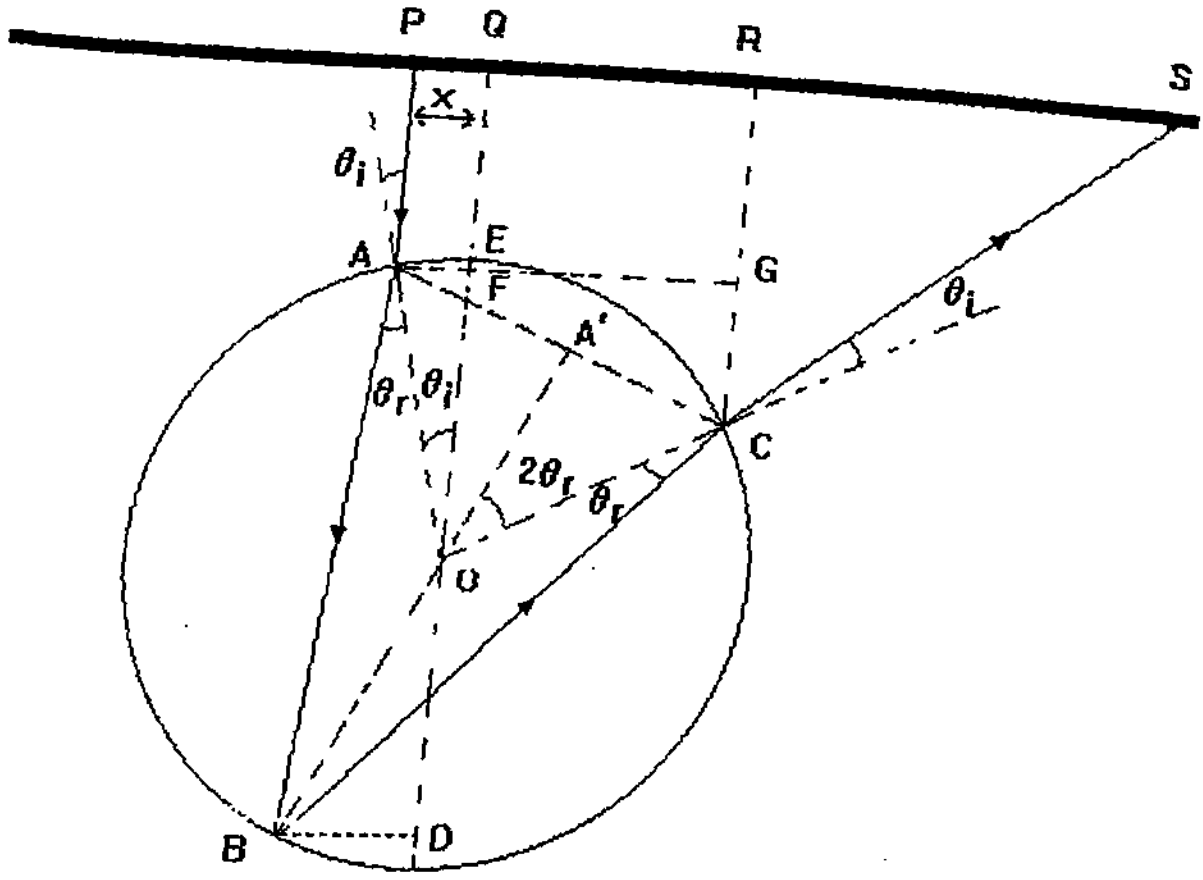

Fig. 9. Evaluation of effective beam width when a plane wave strike curved surface of the rod

Then in triangle OBD, $\angle$ BOD = $\angle$FOA' = $(2\theta_r - \theta_i)$

Therefore BD = $r \sin(2\theta_r - \theta_i)$ ...(1)

Here θ_r can be expressed in terms of θ_i as

$$\frac{\sin \theta_r}{\sin \theta_i} = \frac{V_{lr}}{V_{lw}} \quad \ldots(2)$$

where V_{lr} = velocity of longitudinal wave in rod

V_{lw} = velocity of longitudinal wave in water

The problem now is to find out θ_i in such a way that the ray CS strikes the transducer at S where

QS = D/2

For this we find θ_i in terms of QS.

$$QS = QR + RS \quad \ldots(3)$$

$$QR = FG = AG - AF$$

From triangle AGC, $AG = AC \cos(2\theta_r - \theta_i)$

$$AC = 2\,AA' = 2r \sin 2\theta_r$$

or $AG = 2r \sin 2\theta_r \cos(2\theta_r - \theta_i)$

$$AF = r \sin \theta_i$$

or $QR = 2r \sin 2\theta_r \cos(2\theta_r - \theta_i) - r \sin\theta_i \quad \ldots(4)$

$$RS = RC \tan(RCS) = RC \tan(4\theta_r - 2\theta_i)$$

$$RC = RG + GC$$

$$RG = QE + EF = QE + (r - r\cos\theta_i)$$

From triangle AGC,

$$GC = AC \sin(2\theta_r - \theta_i) = 2r \sin 2\theta_r \sin(2\theta_r - \theta_i)$$

$$RS = [QE + r - r\cos\theta_i + 2r \sin 2\theta_r . \sin(2\theta_r - \theta_i)] \tan(4\theta_r - 2\theta_i) \quad \ldots(5)$$

Substituting the values of QR from equations (4)

and RS from (5), we can get QS in terms of r, θ_i, QE which is equal to D/2, that is,

$$D/2 = QR + RS \qquad \ldots(8)$$

For a particular rod, transducer and water path, we can find out the value of θ_i which satisfies equation (8). This value of θ_i is then used to evaluate the value of BD from equation (1)

The beam width is determined theoretically using the above expression and with the help of a BASIC program for 5 mm and 50 mm diameter rods and transducer of frequency 5 MHz and diameters 12.5 and 25 mm at varying water path (Fig.10). Theoretical values for beam width were evaluated for varying water path for 3, 5, 10, 25 and 50 mm rod diameters with a transducer diameter of 19 mm (Fig.11).

It is found that the beam width decreases

i) with decrease in transducer diameter

ii) with increase in water path. However, after the near field, the increase in water path does not change the beam width appreciably.

iii) with decrease in rod diameter.

Clearly, for thicker rods, one shall have to use smaller diameter transducer for lesser beam width.

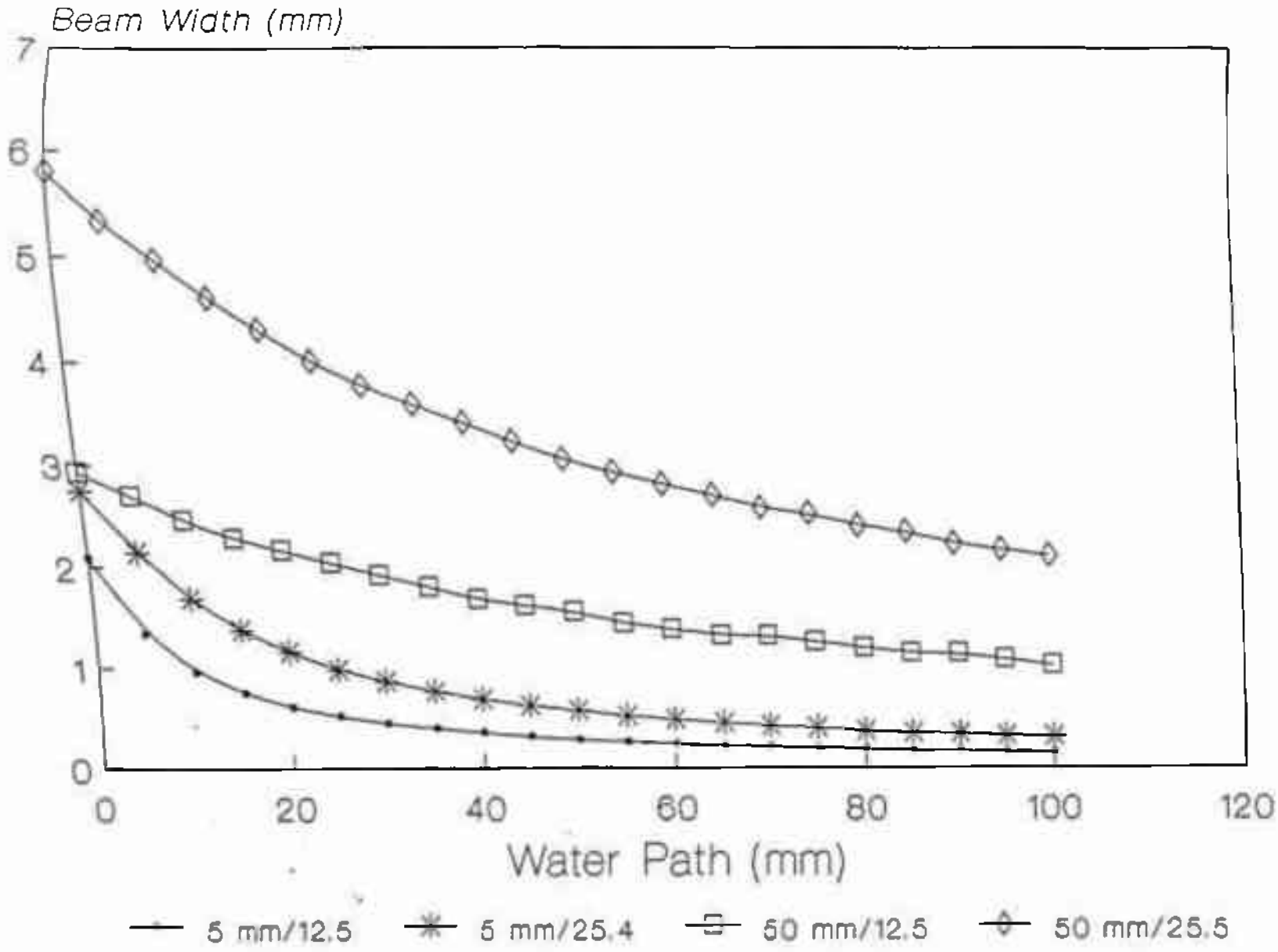

FIG.10. Variation of water path with beam width for rods for various transducer diameter

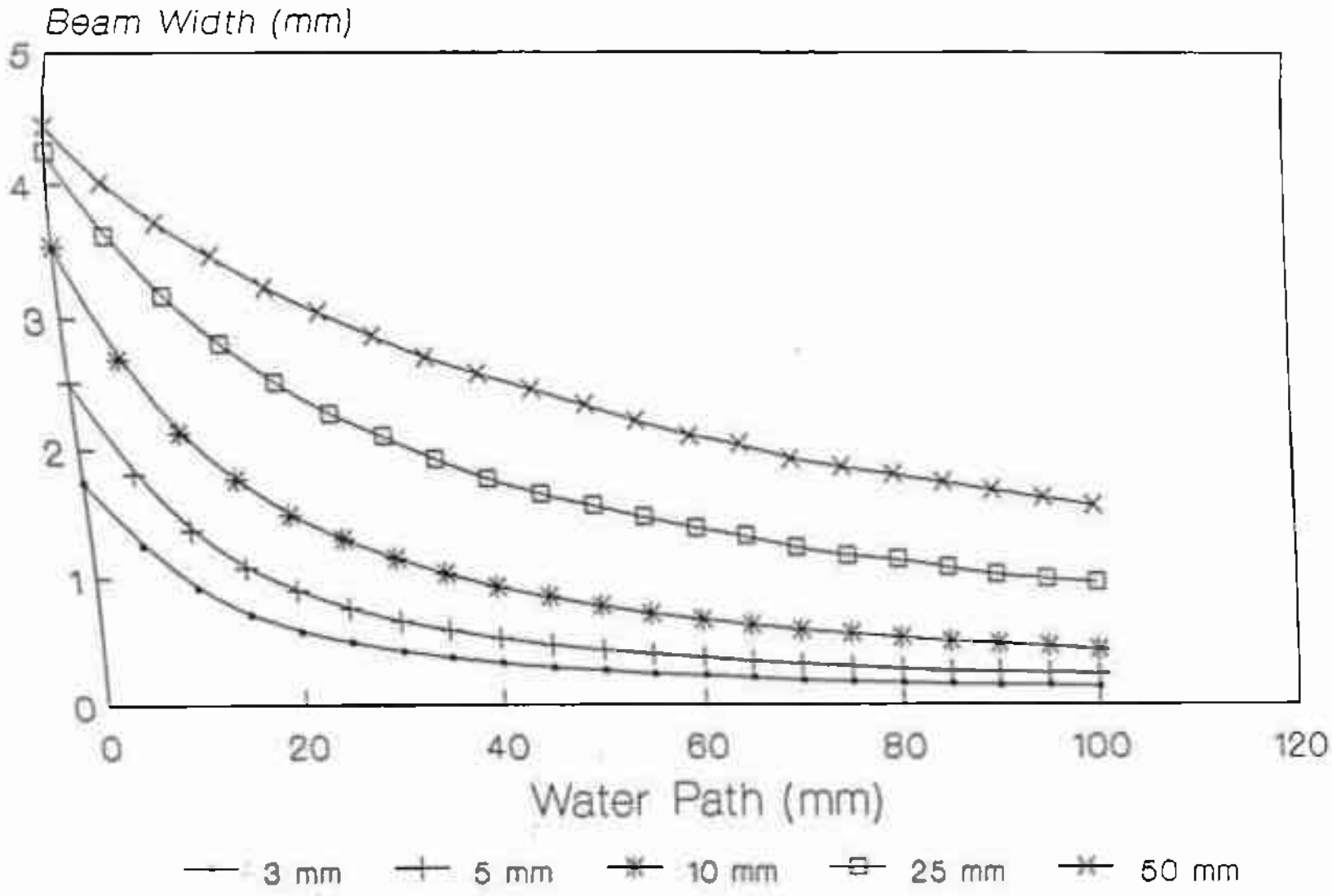

FIG.11. Variation of water path with beam width for rods of varying diameter for 19mm transducer diameter

2.4 EXPERIMENTAL PROCEDURE

An ultrasonic C-scan equipment provides a permanent record of test with high speed automatic scanning. It displays the discontinuities in a planar view. Essentially, a C-scan image provides a two dimensional view of the specimen, in which difference in image contrast is a result of the objects interaction with an impinging acoustic wave.

The block diagram and photographs of the experimental setup are shown in Fig.6 and 7. Following equipment were used for the measurement.

i) Ultrasonic flaw detector - Sonatest masterscan 300 model with dynamic gain 99 dB in 1dB steps, operating range 0.5 to 25 MHz.

ii) Immersion tank - Stainless steel tank with overall dimensions of 1250 mm in length, 400 mm in depth and 500 mm in width along with angular and three dimensional micropositioning system attached to the transducer clamp. The linear movements of the transducer in clamp can be manual or controlled electronically by a built in computer programme (Fig. 7).

iii) Transducers - A number of transducers having different frequency and diameter is used to scan the rod for best possible sizing of the defect in a rod. Among these are :

5 MHz, 25 mm diameter, Krautkramer make

5 MHz, 20 mm diameter, Panametric make

7.5 MHz, 12 mm diameter, Panametric make and

20 MHz, 10 mm diameter, Anglia NDT, backed

iv) Digital storage oscilloscope (DSO) - Tektronix 2440 DSO, sampling rate 500 MS/s.

v) Quantiser - The quantiser unit has two functions. One is that it converts the flaw detector's analog output into digital signal and the other is that it provides an interface between the scanning control system and the IBM-PC. This interface passes on the computer commands to the stepper motors via stepper motor drivers provided under the water tank. It also passes on the transducer position coordinates from the potentiometers (fixed along side the stepper motors) to the computer.

vi) Computers - Two sets of personal computers are used. One IBM (80486) personal computer is connected to the quantiser via GPIB interface card and is loaded with the main C-scan software, RCPNDT, under the Window 3.1 environment. This software helps in the generation and control of the required scan pattern. It can produce a quantized colour display and a hard copy printout of the ultrasonic test results. Second computer is to receive the

waveform from the digital storage oscilloscope (connected to flaw detector) and to perform Fourier transform and other mathematical functions on the wave form.

vii) Test sample - The rods taken for inspection are of diameters in the range of 5 mm to 60 mm with varying lengths and materials given in the Table 1. There are a number of simulated defects in each rod like cuts, notches and holes of different diameters at different positions (Fig.12)

To scan the specimen rod, kept on the leveling plate as described earlier with its axis along the Y-axis, U-frame is brought in contact with the rod. The plate and rod are adjusted with the help of screws such that the interface echo height does not change from one end to another end of the rod. Also, the probe is adjusted with the help of micromanipulators till the back wall echo height is maximised.

The scan area is set up by marking two diagonally opposite points. One of the points is called scan start position with index (0, 0). The index pitches and scan lengths are selected by means of a menu displayed on the colour VDU. To scan 100% of the rod, the transducer is moved along the X-axis a distance equal to or more than πr with steps of suitable increment (where r = radius of rod) and along the Y-axis a little more than the

TABLE 1. Various rods used under study with actual dimensions of the simulated defects. L-denotes defect dimension along rod axis (Y-axis in image), W-denotes along X-axis in image and H is the depth

Rod No.	Material	Diameter of rod (mm)	Length of rod (mm)	Defect No.	Defect dimension (mm) L	W	H
1.	Aluminium	51.0	134.0	1.	22.4	3.5	2.32
				2.	0.9	13.5	0.43
				3.	14.7	1.5	1.5
				4.	15.4	1.5	1.5
				5.	14.2	1.5	1.5
				6.	1.66	6.6	6.6
				7.	19.8	3.0	3.0
				8.	1.33	1.33	31.7
				9.	19.0	4.0	0.2
2.	M. Steel	8.8	146.0	1.	1.26	7.14	2.6
				2.	1.33	1.3	6.26
				3.	1.2	6.2	1.06
				4.	1.33	1.33	6.06
				5.	0.9	5.5	0.88
3.	S. Steel	5.8	107.0	1.	0.62	Circ	0.7
				2.	5.0	5.0	0.49
				3.	0.9	5.0	0.42
4.	S. Steel	5.8	108.8	1.	0.9	Circ	0.55
5.	Brass	9.4	98.8	1.	1.32	1.26	7.06
6.	Steel	9.0	164.0	1.	0.8	3.0	0.5
7.	Steel	38.0	20.5	1.	16.8	6.65	6.65
8.	Aluminium	212.0	50.0	1.	2.3	2.3	10.2
				2.	2.3	2.3	10.2
				3.	9.8	29.6	29.6

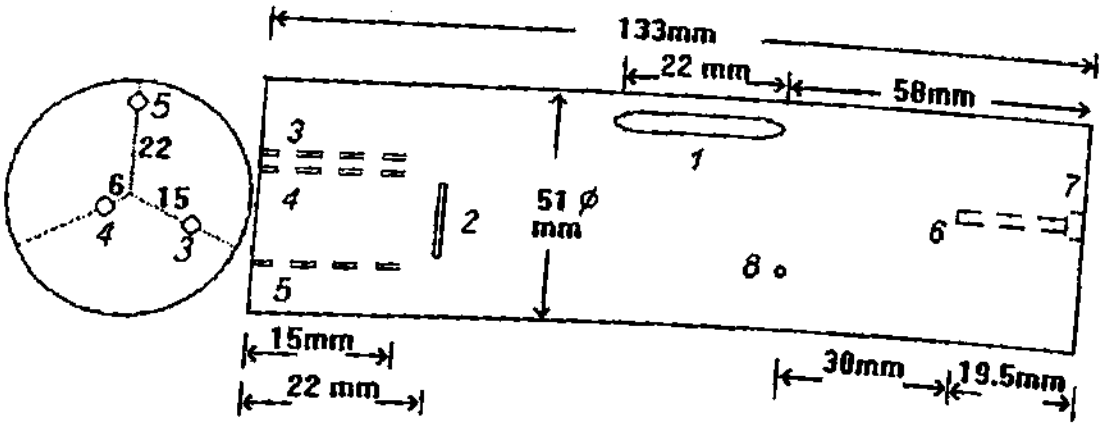

(a) Rod No 1

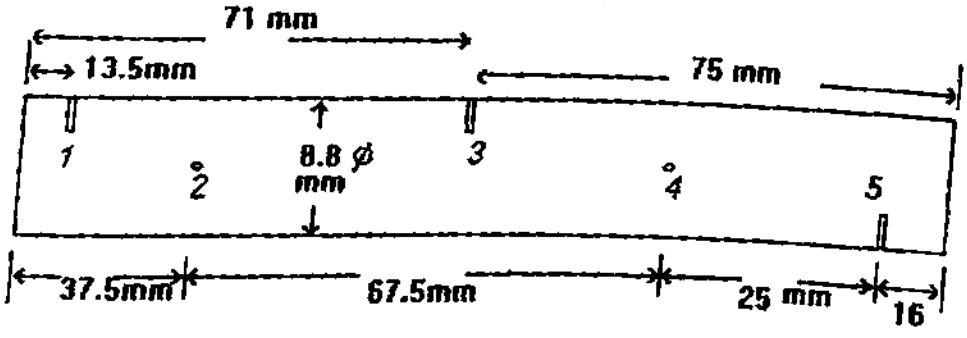

(b) Rod No 2

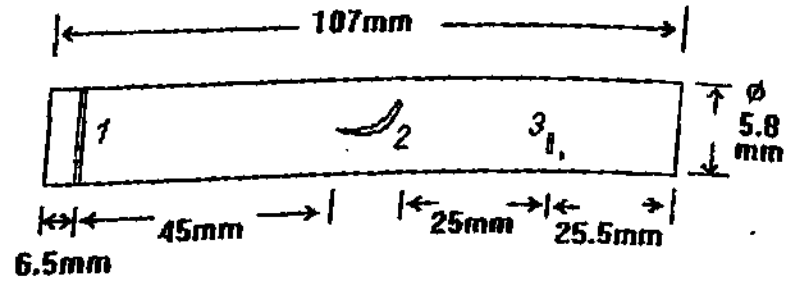

(c) Rod No 3

Fig. 12 Rods taken for detection of simulated defects

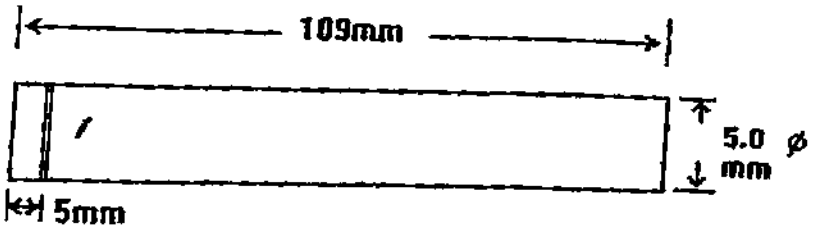

(d) Rod No 4

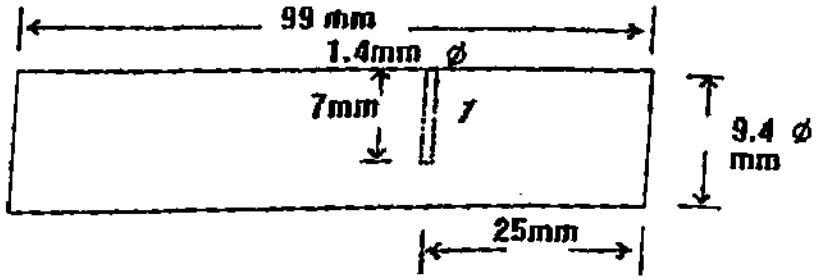

(e) Rod No 5

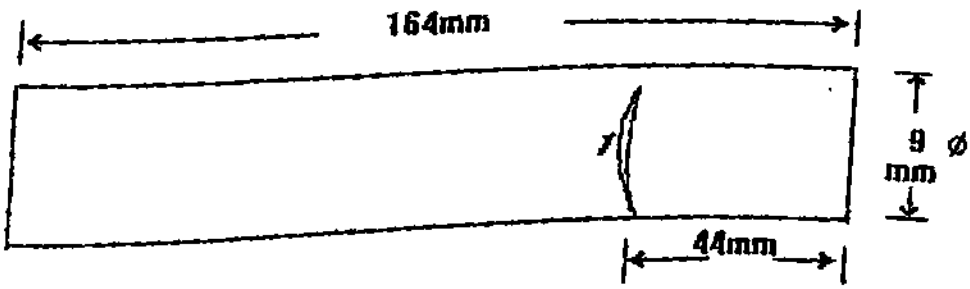

(f) Rod No 6

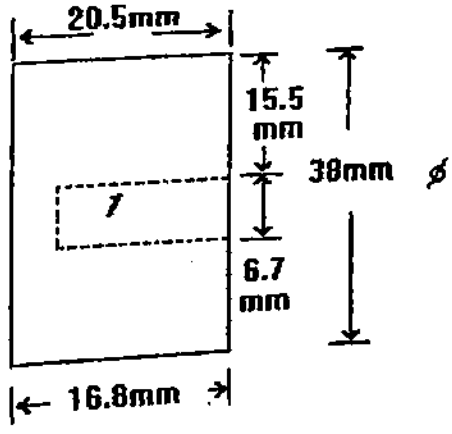

(g) Rod No 7

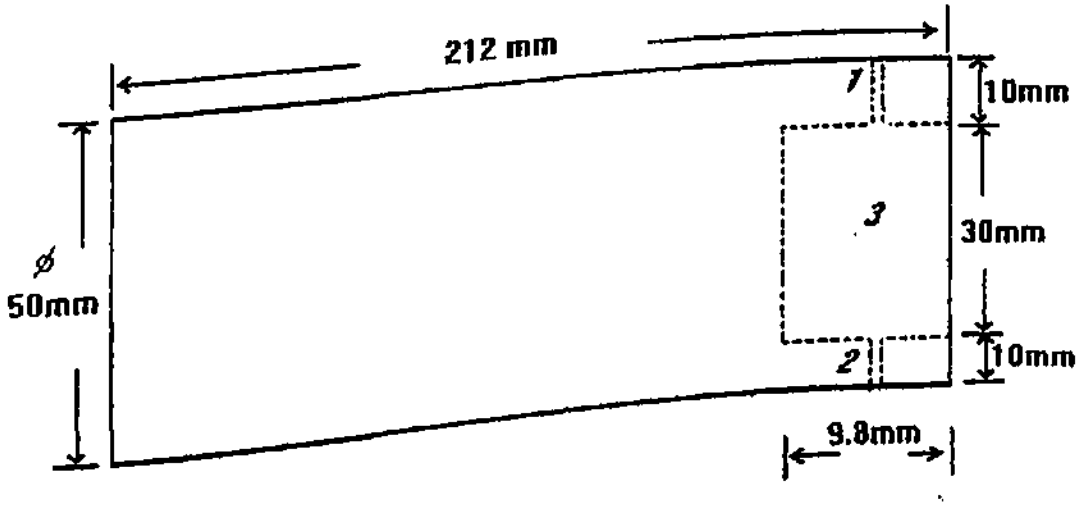

(h) Rod No 8

length of the rod. In this way the C-scan image will represent the rod as two dimensional view of a block of dimensions equal to πr and length of rod. Pulse echo signal of longitudinal wave received from the back wall through the diameter of rod is gated for C-scan image. Scan image shows the number of defects depending on their size compared to the wavelength of sound wave, their orientation, beam width, etc. Though the depth of defect from the surface can not be evaluated from the C-scan image, but the length and width of the defect along with the position from the side of rod can be analysed. If need be there, the depth of the defect can be evaluated by positioning the transducer above the defect position and analysing the A-scan available on the flaw detector.

2.5 RESULTS AND DISCUSSION

As discussed above in Section 2.2.1, the time gate can be set at various positions, namely, at the interface or between the interface and back wall echo or at the back wall echo. An experiment was done to compare the scan image of a 51 mm diameter aluminium rod for different gate positions. These images are shown in Fig. 13(a), (b) and (c) respectively. It is found that the gating at interface and that between interface and back wall gives poor response for detection of all the internal defects. Interface echo perhaps can give some

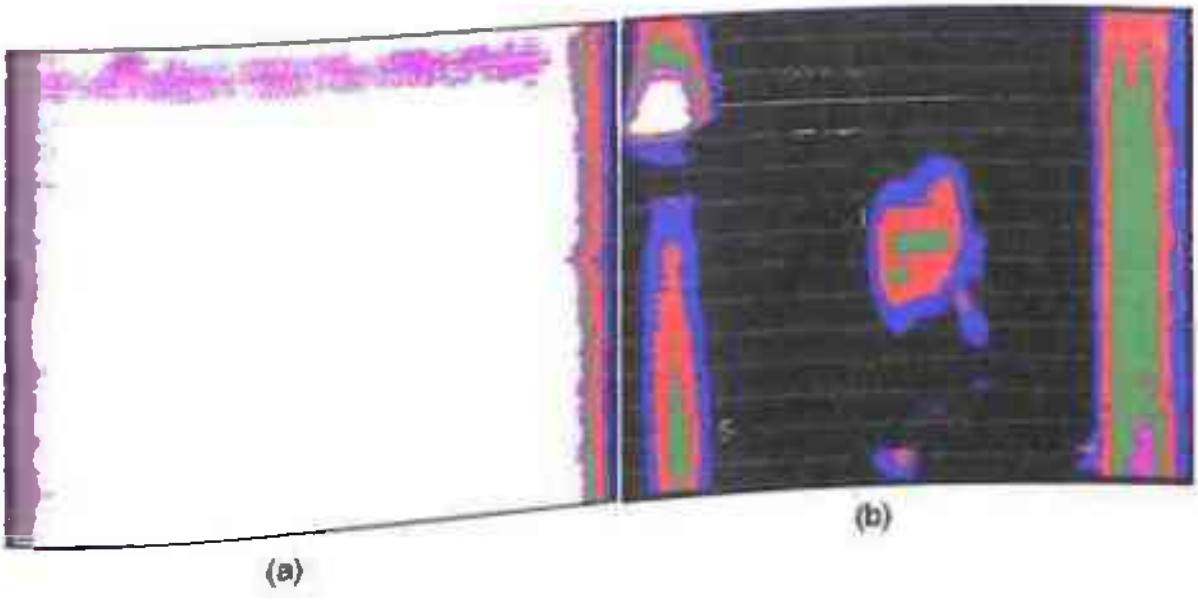

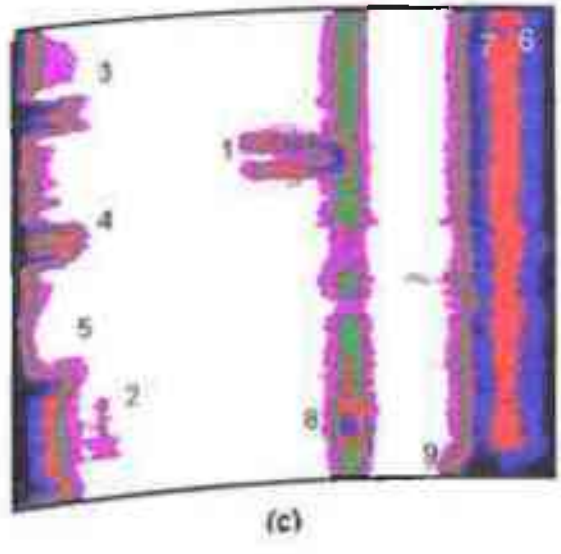

Fig. 13. Comparison of C-scan image for aluminium rod inspection using gating for

(a) Interface echo
(b) Between interface and back wall echoes
(c) Back wall echo

information about the surface defects. The best gating position observed is that of the back wall echo gating.

A comparison of different transducers used was also done by evaluating the Fast Fourier Transform (FFT) of back wall echoes from 51 mm diameter aluminium rod. These are shown in Fig. 14(a,b,c). Though it is expected that the results would be better for higher frequency transducers, but the FFT observed for back wall echo of rod has very few components of higher frequencies. This is due to the attenuation of higher frequencies in rod material and in the water path used. The band width of the flaw detector system is also limited and the signal of higher frequencies may not amplify by the same gain as the lower frequency signal. For this reason the flaw detector was always set at wide band width which is 3 to 18 MHz at 6 dB down with peak at 13 MHz. It is observed from the frequency spectra that 6 dB frequency bandwidth for 5 MHz transducer is 3.3 to 6.3, that for 7.5 MHz it is 4.4 to 7.6 and for 20 MHz it is 4 to 9 MHz. To make this clear an experiment was performed to see the nominal frequency of the transducer. Using 20 MHz transducer FFT of the echoes from water-aluminium (V1-7076T block) interface for a water path of 17 mm (Fig.15a) shows the nominal frequency of the transducer as 20 MHz and 6 dB beam width as 5 to 27 MHz. Whereas FFT of the interface echo for a water path 52 mm (Fig.15b) shows the attenuation of the component of higher frequencies in

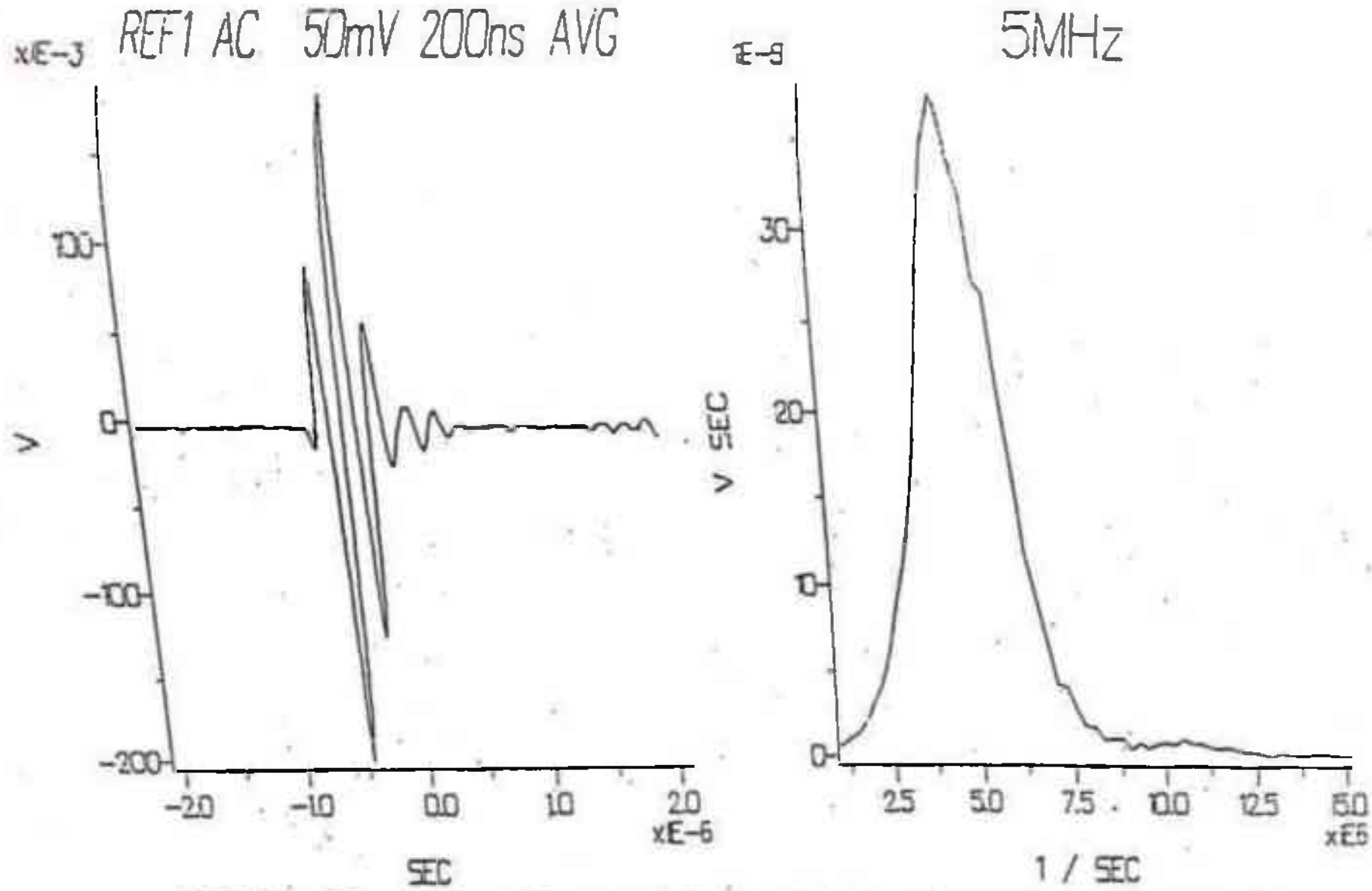

FIG.14. The back wall echo signal and its frequency spectra from aluminium rod for a transducer with nominal frequency

(a) 5.0 MHz/20mm diameter

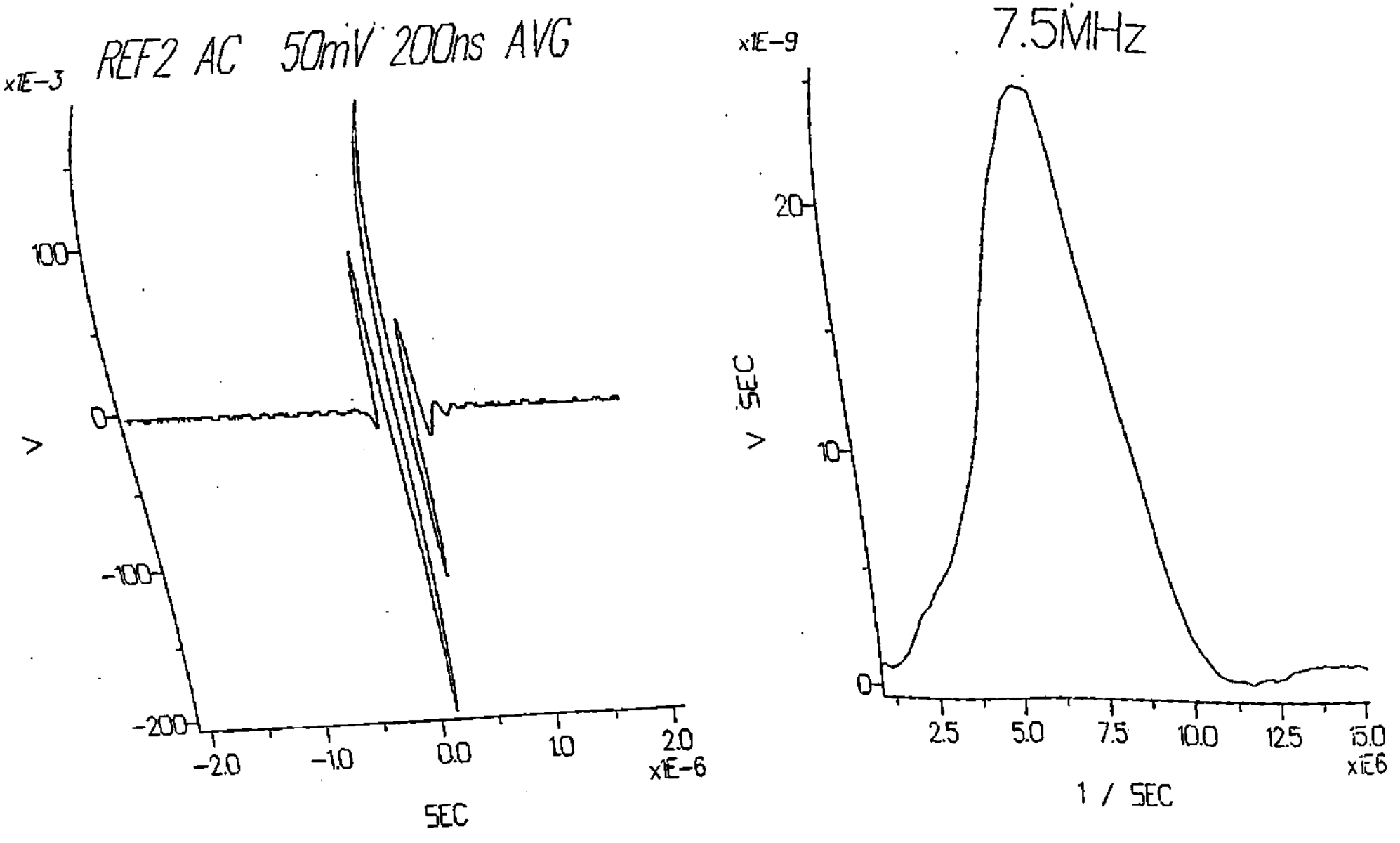

14 (b) 7.5 MHz/12mm diameter

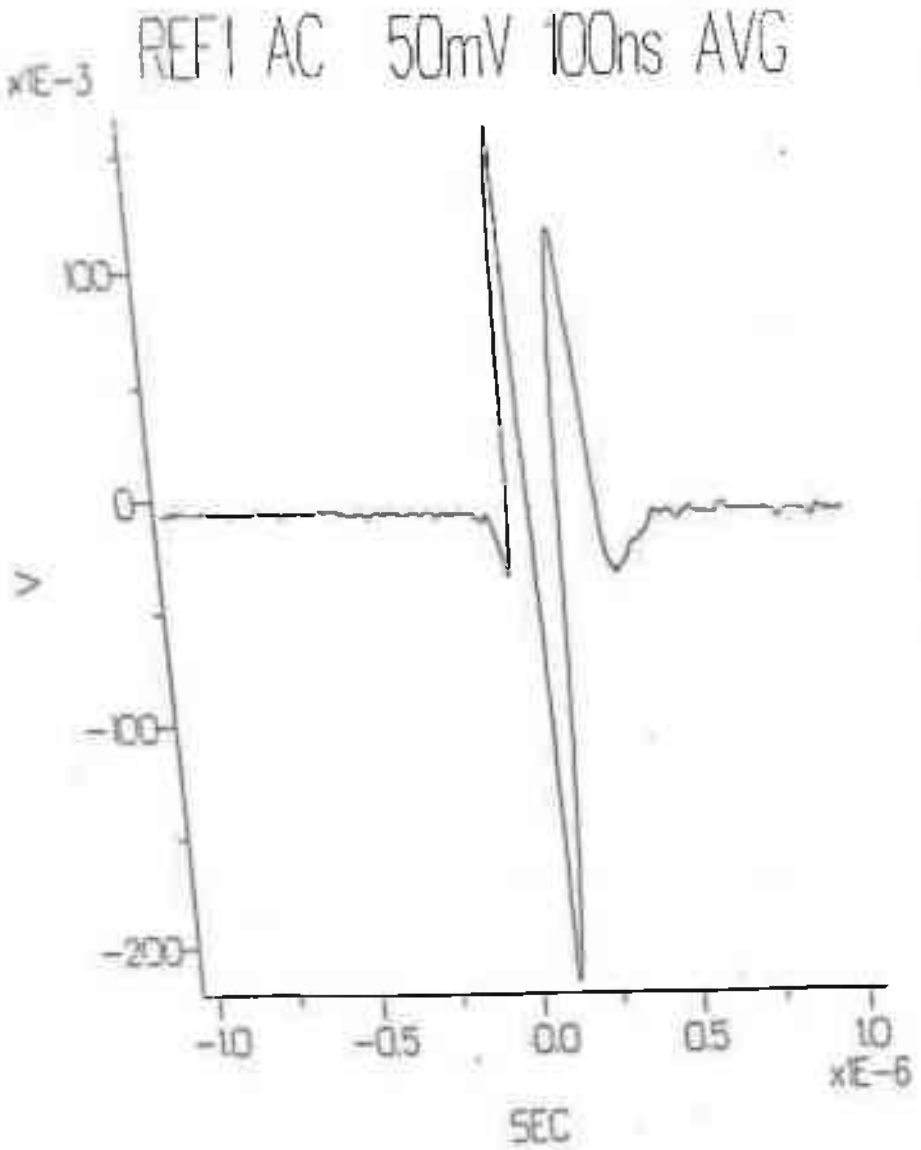

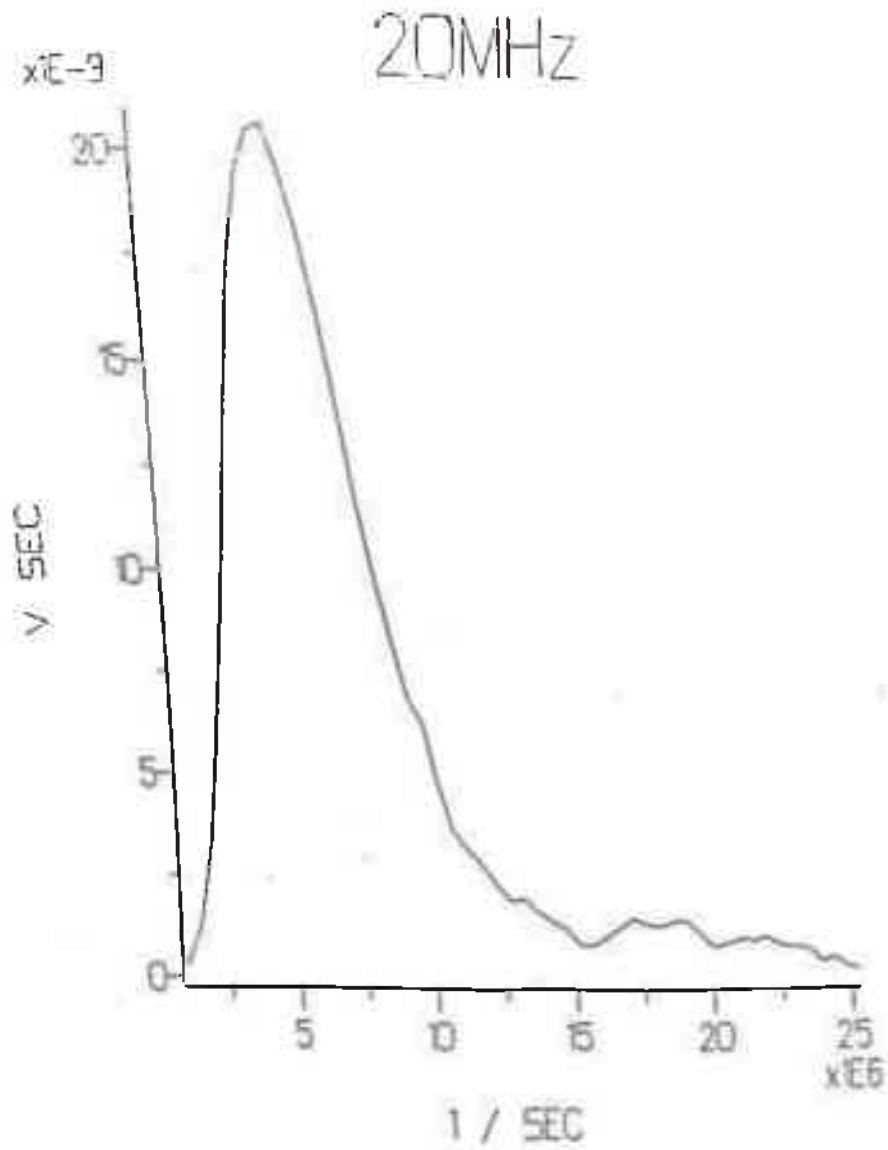

14 (c) 20 MHz/10 mm diameter

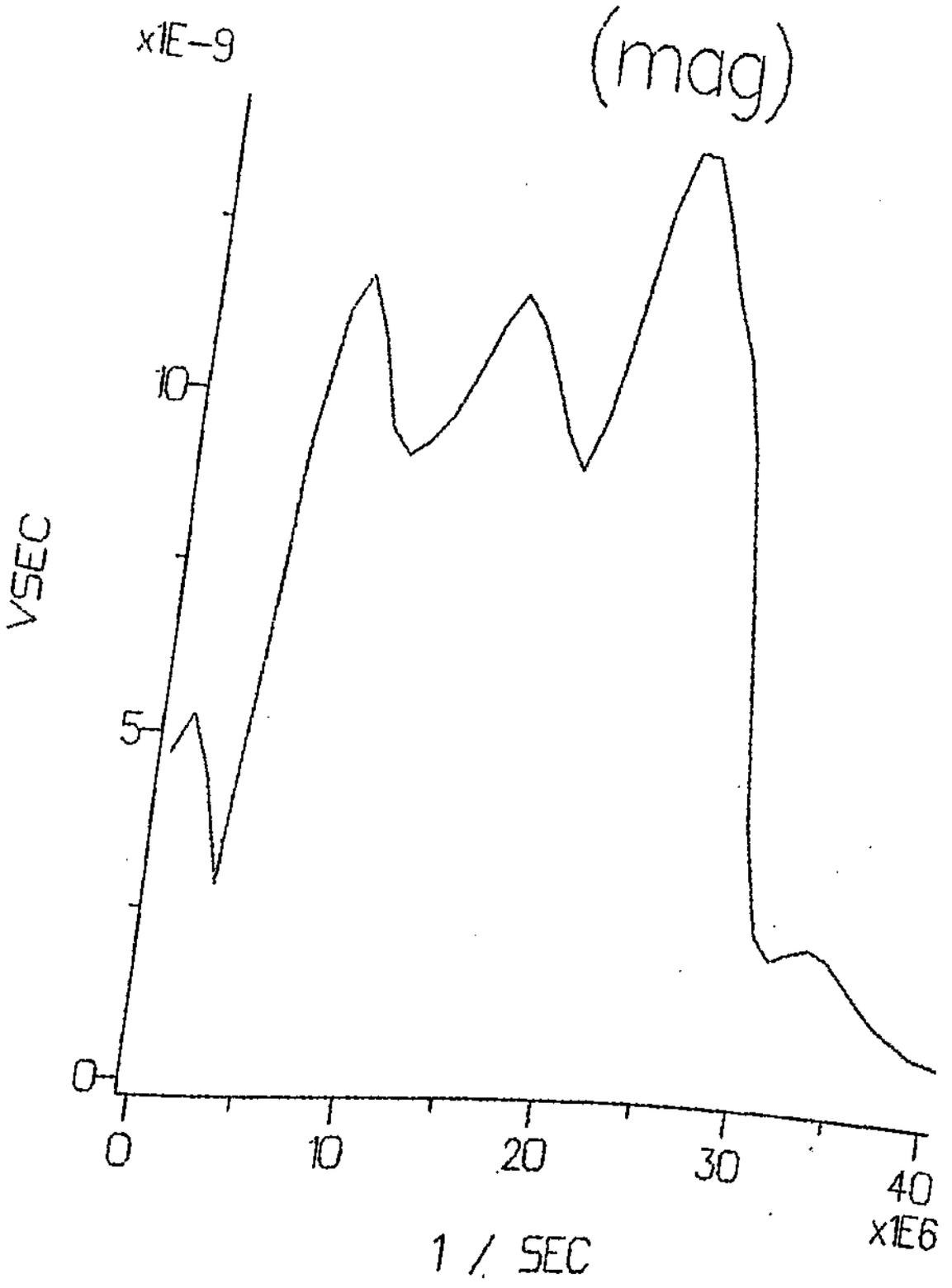

(a) For water path 17 mm

FIG.15. Frequency spectra of the interface echo signal from water-aluminium (V1-7076T block)

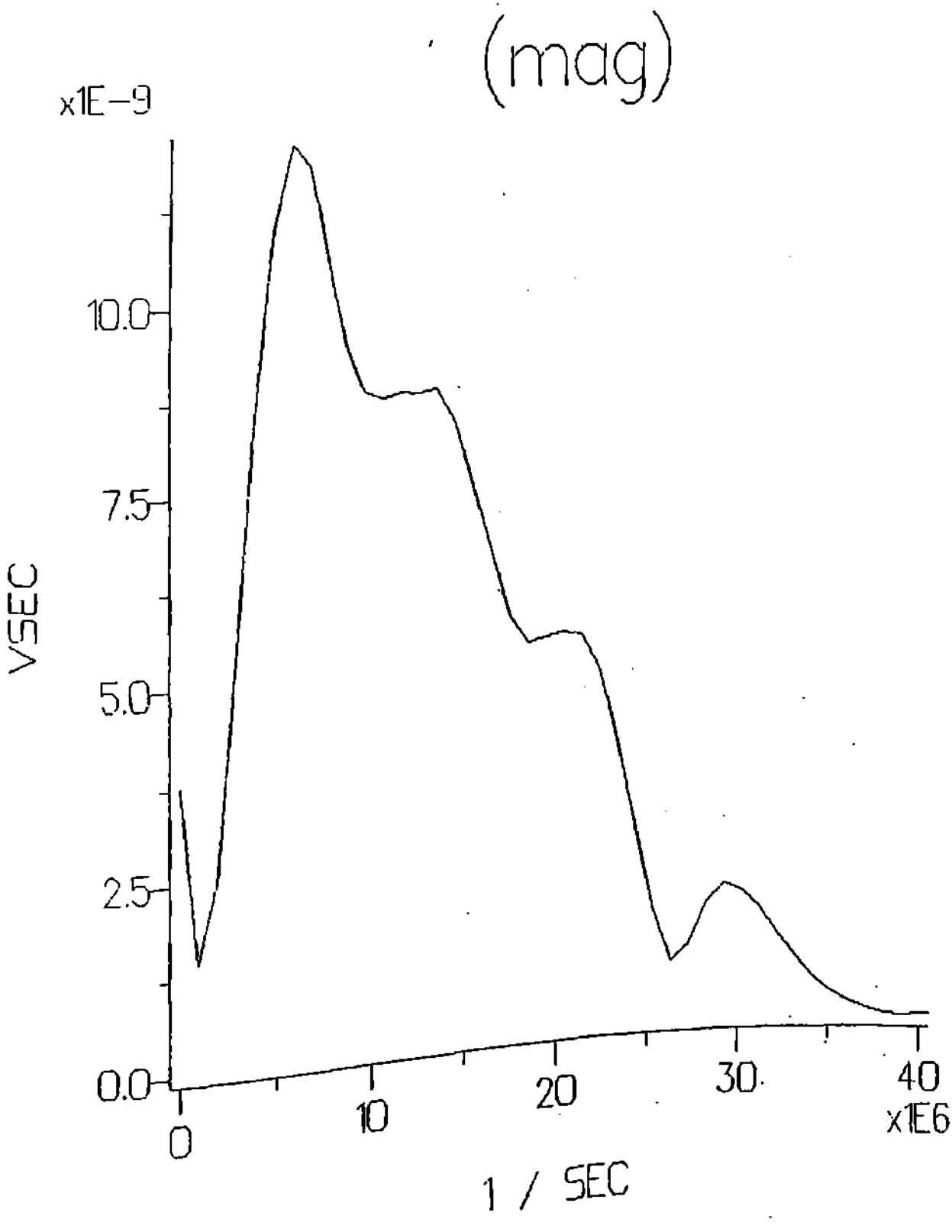

15 (b) For water path 52 mm

water only. Further ultrasound attenuation is more in metals as compared to the water at higher frequencies. It makes clear that the transducer of nominal frequency 20 MHz the higher frequencies are getting attenuated in water path. It was therefore thought appropriate to scan most of the rods either by 5 MHz or by 7.5 MHz transducers. The water path also can not be too much minimised as the effective beam width of the transducer increases by reducing the water path (Fig. 10 and 11) For smaller diameter rods high frequency probe may be better as it would give higher sensitivity. Since the water path can also be reduced up to some extent, the attenuation of higher frequency component may not be very high and useful higher frequency component may still be available.

Experiments were performed on a number of rods (Table 1). The sizes and locations of the artificial defects in the rods were evaluated from the scan images (C-scan) of the rods and compared with the actual sizes of the defects. The parameters of each scan plan selected were stored into a computer file along with the records of the scan (Fig.16, 17).

It is found that all the different shaped defects are observed clearly with the system developed. The effective diameter of the beam along the direction perpendicular to the rod axis becomes very small due to the line contact of ultrasound beam. The defects width

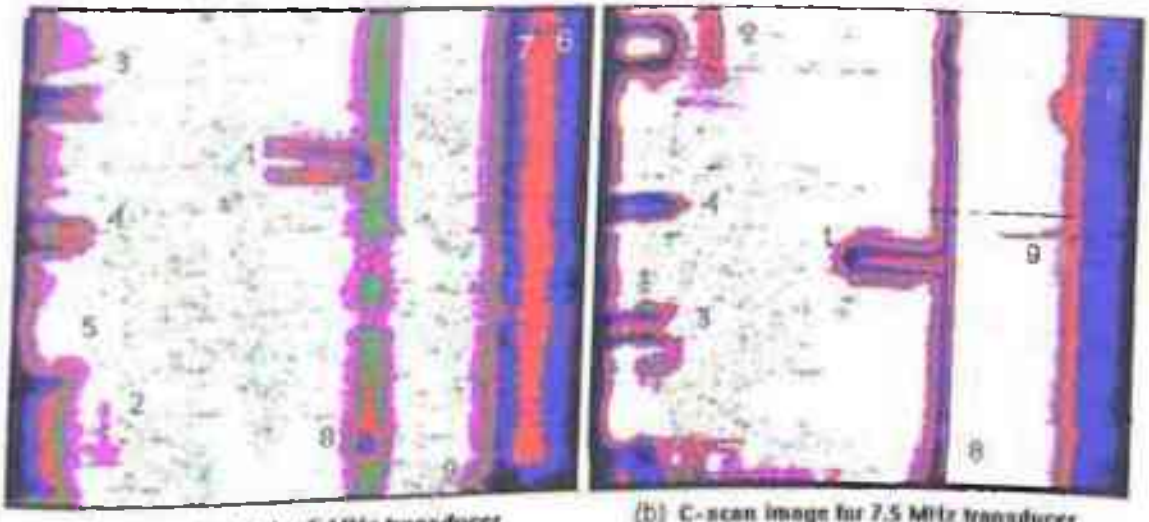

(a) C-scan image for 5 MHz transducer

(b) C-scan image for 7.5 MHz transducer

Fig. 16. Comparison of C-scan image for aluminium rod inspection using transducer with frequency

(a) 5 MHz / 20mm
(b) 7.5 MHz / 12mm
(c) 20 MHz / 10mm

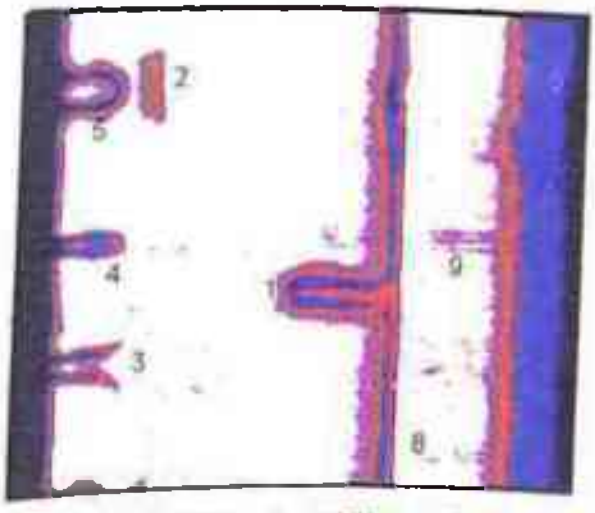

(c) C-scan image for 20 MHz transducer

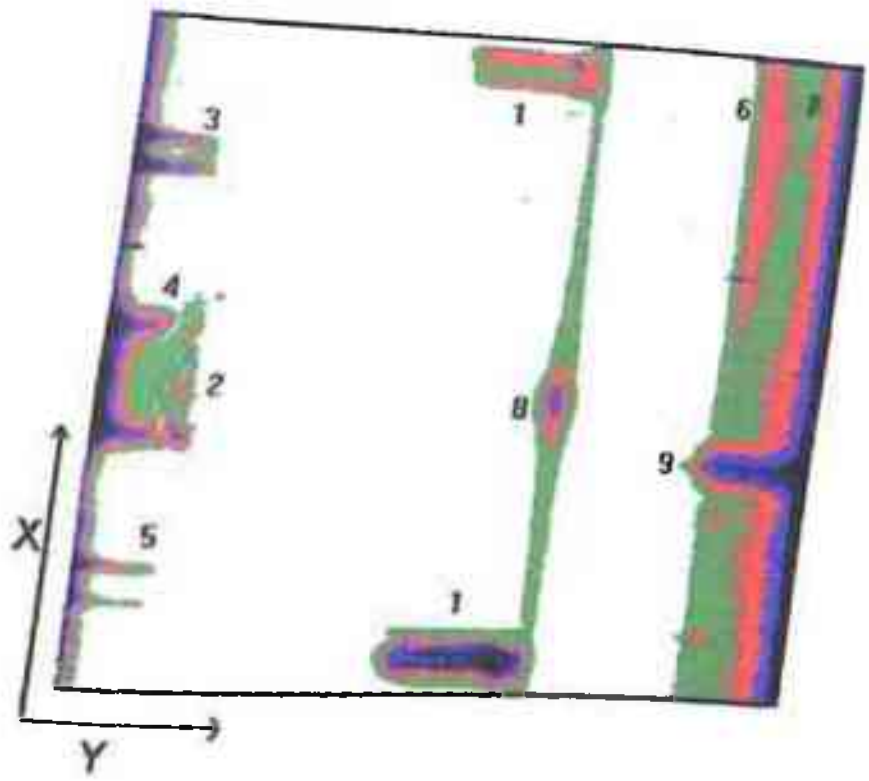

17(a) Rod No. 1. Defect 1 is seen twice due to scanning by more than 27 times

Fig. 17. C-scan image of different rods. X and Y axis represent circumference and rod axis respectively

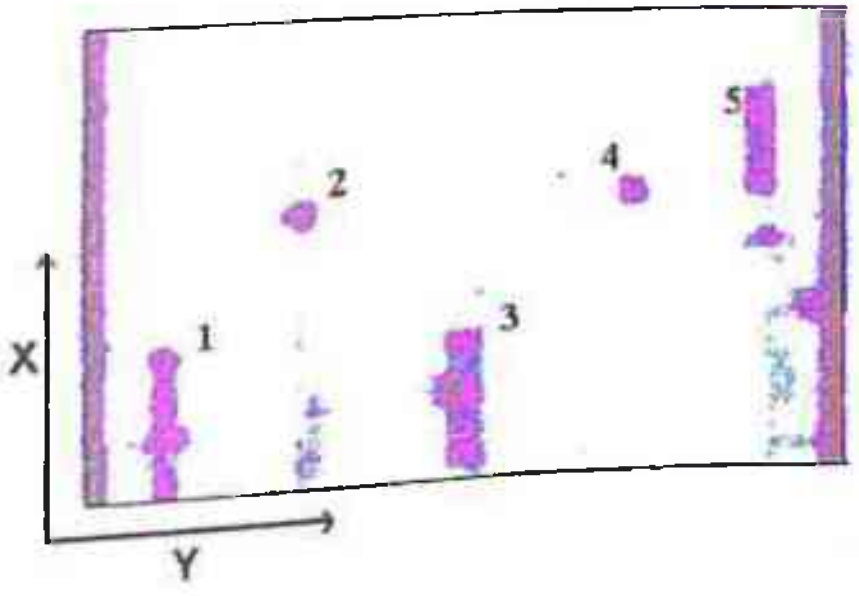

17 (b) Rod No. 2

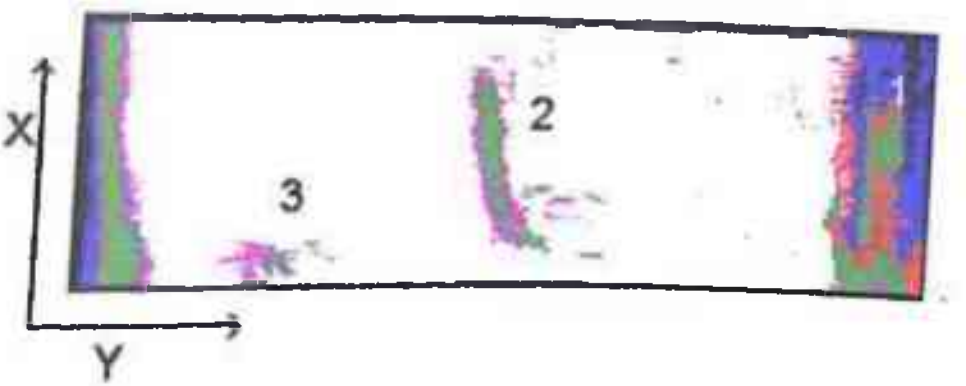

17 (c) Rod No. 3

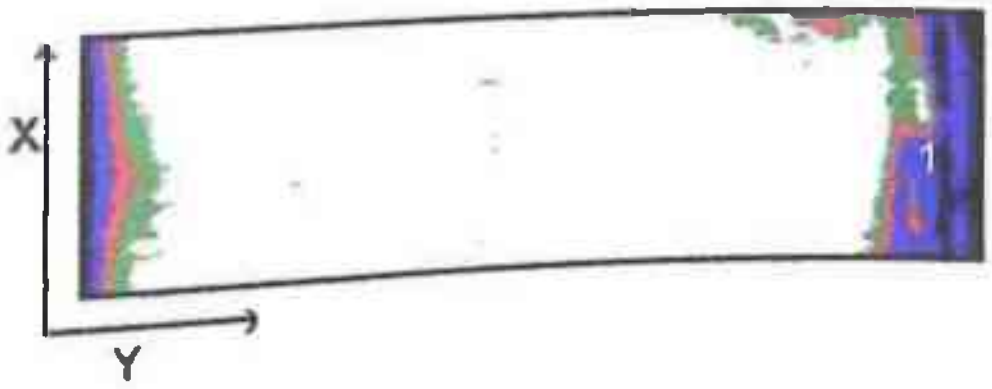

17 (d) Rod No. 4

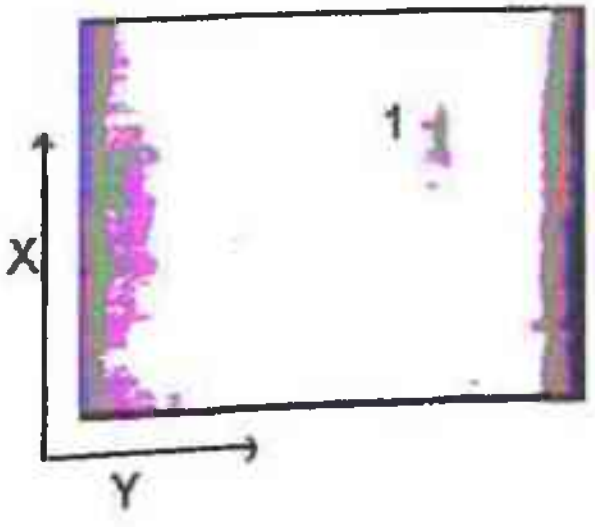

17(e) Rod No. 5

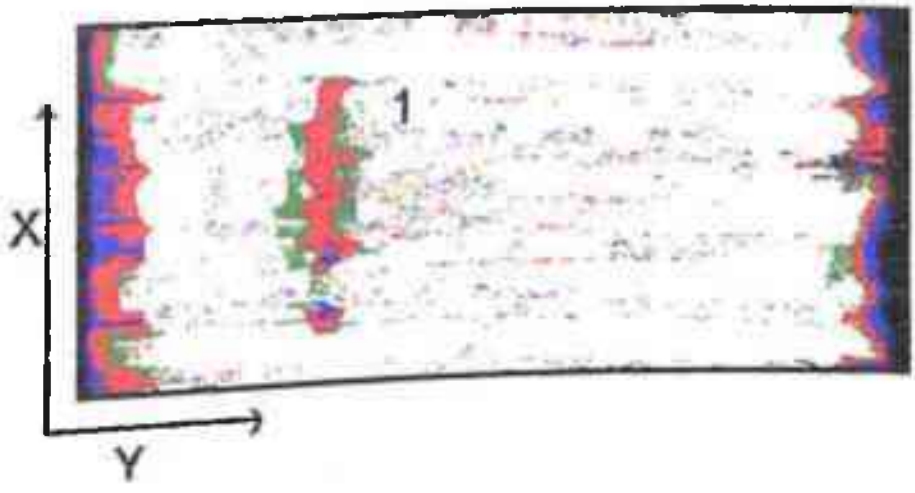

17(f) Rod No. 6

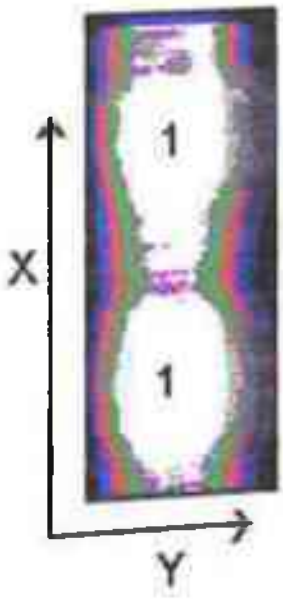

17(g) Rod No. 7. Scanning about $2\pi r$ times along X axis

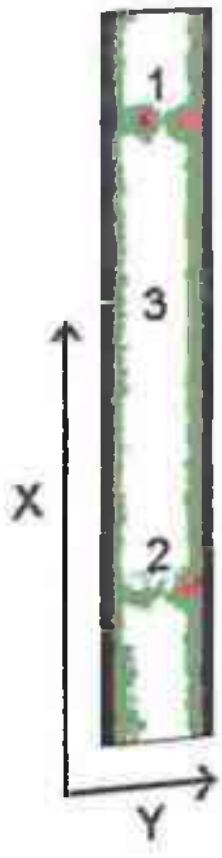

17(h) Rod No. 8. Scanning about $2\pi r$ times along X axis

(W) along the circumference as measured on X-axis of scan image therefore give comparable results. Perhaps to determine the correct size of the defect it is essential that setting up procedures are correctly followed and ultrasonic beam is in a plane and perpendicular to the rod axis. Otherwise defects particularly of the transverse type which are along the beam axis in smaller diameter rods may be missed. As in Fig. 18 compared to 17(b), the transducer emitting the ultrasound beam was slightly off the rod axis for 8.8 mm diameter rod.

Defect number 1 and 2 in aluminium rod No. 1 are in oval shape. The problem is faced when the defect occurs at the bottom or when two or more defects occur simultaneously. In that case the results may vary from actual size due to the shadow effect. It is found that due to lack of knowledge of depth in C-scan image, defect in the shape of a circle on surface, hole or any significant defect lying at the center of rod will show a line on scan image and only the length of hole can be predicted as in case of defect number 6 and 7. In steel rod the dimension of defects along the rod axis is very small and could not be measured correctly and show larger size due to larger beam width.

The number of rods with simulated defects under study are given in Table 1. The defects observed are tried to measure and defect length and width is given in the Table 2. A comparison of the present system,

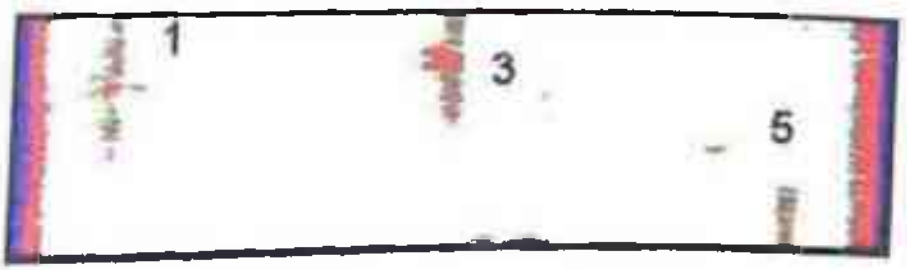

Fig. 18. Ultrasonic C-scan image of rod No. 2 with slightly off axis from rod axis

TABLE 2. A comparison of simulated defects actually measured and evaluated by ultrasonic C-scan image. L, W - denotes defect dimensions along rod axis (Y-axis in image) and along circumference (X-axis in image) respectively

Rod No.	Defect type	Defect No.	Defect Dimension in (mm) (L) Actual	(L) Measured	(W) Actual	(W) Measured
1.	Oval	1.	22.4	22.5	3.5	6.5
	Oval	2.	0.9	3.0	13.5	12.5
	Hole	3.	14.7	14.5	1.5	2.0
	Hole	4.	15.4	16.5	1.5	1.0
	Hole	5.	14.2	13.5	1.5	2.0
	Hole	6.	1.6	2.0	6.6	---
	Hole	7.	19.8	19.5	3.0	---
	Hole	8.	1.33	3.0	1.33	---
	Hole	9.	19.0	19.0	4.0	3.8
2.	Cut	1.	1.26	2.8	7.14	10.4
	Hole	2.	1.33	3.0	1.3	1.4
	Cut	3.	1.2	2.8	6.2	9.0
	Hole	4.	1.33	3.5	1.3	1.4
	Cut	5.	0.9	2.8	5.5	6.9
3.	Circ	1.	0.62	1.6	Circ	---
	Cut	2.	5.0	6.3	5.0	5.7
	Cut	3.	0.9	1.5	5.0	5.6
4.	Circle	1.	0.9	1.8	Circ	---
5.	CDH	1.	1.32	2.5	1.26	1.4
6.	Cut	1.	0.8	2.5	12.0	17.4
7.	SDH	1.	16.8	15.8	6.65	---
8.	Hole	1.	2.3	3.6	2.3	4.4
	Hole	2.	2.3	3.0	2.3	3.4
	SDH	3.	9.8	9.8	29.6	---

TABLE 3. A comparison of the presented system with the Helical scan system and A-scan system

Present system with add-on arrangement (C-scan)	Conventional system (Helical Scan)	A-scan system
Immersion	Immersion	Direct contact
Automatic	Automatic	Manual and time consuming
Coupling uniform	Coupling uniform	Coupling nonuniform
Detection, location and sizing of the defect	Detection and location of the defect	Detection, and location of the defect
No change required for different diameter rods	Major changes are required	No change required for different diameter rods
Faster	Fastest	Slow, individual dependence
Rod length depend on tank size	Any length	Any length
Hard copy print out with mapping	Chart paper printout	Chart paper printout
Very small effective beam diameter, highest sensitivity	Small effective beam diameter, highest sensitivity	Poor sensitivity

Helical scan system and the A-scan system is given in Table 3. In some cases where defect depth is larger or comparable to the radius of rod the width of defect is seem to increase. Also the observed width is found slightly more than the actual. This is due to the fact that we are measuring the curved surface of the defect actually as an arc of circular cross section of the rod. In some cases where dimension of defect along rod axis is less than the beam diameter the measured size is found approximately equal to the beam width. To measure the size more accurately focused transducer also may be tried. These transducer however require several other aspect to be considered for overall effect of the beam into the rod and have not been presented in the work here.

2.6 CONCLUSION

A new technique using longitudinal waves and circumferential scanning through diameter of the rod has been tried for observing the defects and their size evaluation. The technique works well to detect and size the defects. It requires only small and inexpensive add-on arrangement to the existing C-scan system. The technique has been found very useful and has advantage over the other methods as the effective beam width into the rod material becomes comparable to the defects size. It depends on the frequency, transducer diameter, rod diameter, rod material velocity and water path between

transducer and rod surface. Since the transducer parameters and water path can be controlled, the desired beam width can be obtained without much difficulty.

2.7 REFERENCES

1. Zen, C., et al., Acoustic wave guiding rods with graded velocity profiles, Ultrasonics 30 (1992)91-94

2. Rose, J, Neural nets for flaw classification potential with guided waves, Proc. 14WCNDT (1996) 41-46

3. Rose, J. and Barshinger, J., Guided wave application in aging aircraft, Proc. 14WCNDT (1996) 157-60

4. Krautkramer, J. and Krautkramer, H., Ultrasonic Testing of Materials, Third edition, Springer Verlag Berlin, Bonn (1983)

5. Hinsley, J.F., Nondestructive Testing, Macdonald & Evans Ltd., London (1959)

6. Banks, B., Oldfield, G. and H. Rawding, Ultrasonic Flaw Detection in Metals, Prentice Hall Inc. New Zersy (1962)

7. Morris, J.L., Metal Casting, Prentice Hall Inc. (1957)

8. Campbell, J.S. Jr., Casting and Forming Processes in Manufacturing, McGraw Hill Book Co., NY (1950)

9. Bhardwaj, M.C., Fundamental developments in ultrasonics for advanced NDC, Proc. NDT of High Performance Ceramics, Boston (1987) 472-527

10. McGonnagle W. J., Nondestructive Testing, Mc Graw-Hill Book Co., Inc. N.Y. (1961)

11. Nichols, R.W., Development in Pressure Vessel Technology -Insp. and Testing, Appl. Sc. Pub. NY (1979)

12. McMaster R.C., Nondestructive Handbook Vol 1 & 2, The Ronald Press Co. NY (1959)

13. Highmore, P.J. and Rogerson, A., Advances in ultrasonic flaw characterization in NDT (Ed. JM Farley and RW Nichols), 3 (1987) 1553-1563

14. Babikov, O.I., Ultrasonics and Its Industrial Applications, Consultant Bureau, NY (1960)

15. Fitting , D.W. and Adler, L., Ultrasonic Spectral Analysis for Nondestructive Evaluation, Plenum Press, NY & London (1981)

16. Drury, J.C., Ultrasonic flaw Detection for technicians, Unit Inspection Co. Ltd (1983) 163-195

17. Oliver, J., Dispersion of elastic waves in cylindrical rod by a wide band short duration pulse technique, J. Acoust. Soc. Am. 29 (1957) 189-94

18. Ambardar, R., Muthu, M.T., Pathak, S.D., and Parbhakar, O., Effect of porosity, pore diameter and grain size on ultrasonic attenuation in aluminium alloy castings. INSIGHT 37 (1995) 536-543

19. Drury,J., Ultrasonic sizing of defects, a lighthearted look at the problem, British J. NDT, 21 (1979)200-207

20. IS-3664 (1981), Code of practice for ultrasonic pulse echo testing by contact and immersion testing, Bureau of Indian Standards.

21. IS-6394 (1986), Code of practice for ultrasonic testing of seamless metallic tubular products by contact and immersion methods, Bureau of Indian Standards.

22. ASTM E-1001 (1984), Standard practice for detection and evaluation of discontinuities by the immersed pulse echo ultrasonic method using longitudinal waves, American Society of Testing Materials.

23. Pohl, D., Ein beitrag zur ultraschallprufung von rundstahl, Stahl u. Eisen 82 (1962) 97-106

24. Brandt, H.G., Uberschallprufung von rundstahl auf innenfehler, Stahl u. Eisen 73 (1953) 1717-20

25. Krautkramer O.J., Arch. Eisenhuttenwes, 30 (1959) 693-703

26. Arbeit von, Kreits, K. and Ivens, G., Mater. Pruf. 2 (1960) 240-44

27. Kimura, K., Cylindrical surface echoes in the ultrasonic flaw detection of round bars, Trans. Nat. Res. Inst. Met. 7 (1965) 21-28

28. Kimura, K., Cylindrical surface echoes in UFD of round bars, Trans. Nat. Res. Inst. Met. 5 (1963) 43-51

29. Ciorau, P., Contribution of flaw sizing in tubular steels products by ultrasound, British J. NDT 33 (1991) 333-336

30. Krautkramer, J., et. al., The ultrasonic reflection from small surface cracks and the problems associated with reference defects, when examining tubes and bars, Conf. Ind. Ultrason., (1969) 133-144

31. Whittington, K. and Cox, B., Application of phased array to ultrasound flaw detection in tubes, Conf. Ind. Ultrason., Sep.23-25 (1969) 107-32

32. Zheng, K.S., Chen, Y. and Peng, Y., A new ultrasonic testing technique for titanium bars with small diameter, Proc. 14WCNDT (1996) 633-638

33. Peng, Y., Jian. L., et. al., A new ultrasonic testing technique for small bars and inquisition for relevant theory, Proc. 14WCNDT (1996) 667-672

34. Sastry, G., Shankar, K. and Rajeshwar Rao, N., Evaluation of bar for critical applications using ultrasonics, Proc. 14WCNDT (1996) 673-80

35. Brewester, J. and Ashbee, K., Further insight into the potential role of shear wave caustics in NDE of rods and pipes, Ultrasonics 29 (1991) 52-256

36. Moshfeghi, M., NDT of rod and pipes using shear wave caustics, Ultrasonics 24 (1986) 19-24

37. Yudhisther Kumar, Ashok Kumar and B. Kumar, Improvised technique for immersion testing of rods, National Symp. on Advances in NDE, New Delhi, Nov. 8-10 (1995)

38. Yudhisther Kumar, Ashok Kumar and Basant Kumar, Nondestructive evaluation of rods by ultrasonic C-scan system, Proc. 14WCNDT (1996) 647-650

39. Gordan, G.A., Canumalla, S. and Tittman, B.R., Ultrasonic C-scan imaging for material characterization, Ultrasonic 31 (1993) 373-380

40. Tan, K., Hing, P., Wong, B., and Ong, S., Ultrasonic C-scan of embedded foreign inclusions in sintered ceramics, Proc. 14WCNDT (1996) 781-84

41. Ponyakin, V.T., Rybakov, N.K. and Panchenko, Y.N., Ultrasonic defects measurements of fuel welded joints, Proc. 14 WCNDT (1996) 323-26

42. Neubauer, W.G., Observation of acoustic radiation from plane and curved surfaces, in Physical Acoustics By Mason W.P. and Thurston R.N., Vol. 10, Academic Press, NY (1973) 61-125

43. Yan-Rongming and Deng-Jianping, The smallest discontinuity that can be detected by ultrasound, Proc. 14WCNDT (1996) 957-60

CHAPTER - 3

ULTRASONIC VELOCITY MEASUREMENT IN ROD MATERIAL

CHAPTER - 3

ULTRASONIC VELOCITY MEASUREMENT IN ROD MATERIAL

3.1 INTRODUCTION

Ultrasonic velocity has become a valuable tool for the study of various physical and chemical properties of the matter. Ultrasonic velocity measurement offers a rapid and nondestructive tool for the characterisation of materials. Elastic constants of an isotropic solid can be determined ultrasonically when both longitudinal and transverse wave velocities are known [1-3]. The estimation of grain size has been going on for past several years by the measurement of ultrasonic velocity. Attempts to correlate grain size, and hence heat treatment, with velocity has also been studied with reasonable success [4]. Several other features of materials such as porosity, strength, inhomogeinity, anisotropy, density, corrosion, thickness and presence of flaws can be effectively determined by measuring the ultrasonic velocity in these materials [5-8]. Though changes are small, nevertheless modern methods are capable of giving reliable results. The study of variation of ultrasonic velocity with temperature has been done in past by non-contact method using laser generation of ultrasound and interferometer for reception

[9,10]. Theoretical and experimental studies have been made by a number of researchers on elastic wave propagation in cylindrical rods of different homogeneous and anisotropic materials and of different diameters at varying frequencies [11-19].

The basic concept of ultrasonic velocity measurement comes from elementary physics i.e. the velocity of an ultrasonic wave in a medium is simply the distance traveled by the wave in the medium per unit time. To make accurate determination of the velocity, time of flight of the ultrasonic wave and thickness of the sample are required to be measured accurately. Various methods have been proposed in past by several authors for the measurement of ultrasonic velocity, on increasing the speed and accuracy, and on augmenting the scope of application of velocity measurement in different materials. Some of the useful and common techniques of velocity measurement have already been described in Chapter 1.

The present work reports a new and novel technique to determine the ultrasound velocity in a solid material. The material is taken in the form of a rod. Since ultrasonic velocity measurement requires accurate measurement of dimension of sample besides the time of flight, it is imperative to work on sample having precisely machined faces. A parallel plate will require not only the smoothness of the surfaces but also the paral-

lelism between the opposite faces so that the variation in thickness from point to point is within the desired limit of accuracy, usually 0.002 mm [20]. This is often very difficult to achieve and certainly quite expensive and tedious. If however the sample is taken in the form of a rod shape, it is easier to achieve the required accuracy in dimensions, such as circularity and uniformity throughout the length. Consequently, a sample in the form of rod provides a simple and economical technique of accurate velocity determination. However, a number of triangular echoes, various modes of propagation and multireflection make it difficult to analyse the received echo signals in a rod. The measurement of velocity may get further aggravated if the diameter of the rod is smaller particularly for the shear wave.

A simple, accurate and new technique has been developed for the determination of ultrasonic velocity of longitudinal and transverse wave in rod material. In the present work the new technique of ultrasonic velocity measurement has been described and its results presented for a number of cylindrical rod samples. Only a single longitudinal wave normal beam transducer is used for the measurement of both longitudinal as well as transverse wave velocity. The method can be applied to measure the velocity of any isotropic material. The only requirement is that the sample has to be a cylindrical rod and that the diameter should be small enough

such that the transverse wave is not attenuated completely and large enough such that the 2nd and 3rd echoes are resolved with the available equipment. These requirements, as will be seen later, are fairly easy to meet. Study has been made for the velocity determination on rods of different materials for rod diameter ranging from 5 mm to 50 mm and of maximum length about 300 mm.

3.2 THEORETICAL CONSIDERATION

When a longitudinal wave normal beam transducer is put in contact with the curved surface of the rod such that the beam axis is along the diameter of the rod, back wall echoes are observed at equal spacings. As the contact between the transducer and the curved surface of rod is a line contact, the divergence angle is large and a number of echoes besides the back wall echo can be observed. The ultrasonic waves can take any path and some of the waves will be able to reach the transducer after multiple reflections. All the waves which radiate at an angle such that they are reflected back to the point of origin will be observed as echoes. First three echoes only are of interest to us for the measurement of ultrasonic velocity. It may be noted that the length of the "contact line" is equal to the transducer diameter whereas the width depends upon the coupling condition and rod diameter. Thin and highly pressed couplant has negligible thickness and hence very small line contact

width but sufficient enough to transmit and receive the ultrasonic waves.

3.2.1 Importance of First Three Echoes

We consider only first three echoes for our study (Fig.1). These three echoes for an isotropic and flawless rod material are found unique. The uniqueness has been established by the theory and validated by the experiment.

If the rod material under study is flawless and surface is smooth, the first echo results from the signal received after a reflection from the back wall (Fig.2a), that is, diametrically opposite point. This covers a to and fro path into the rod and is denoted by T1. Second echo results when the ray of the transducer refracted into the rod makes an angle of 30° with normal. It will be reflected at incident and reflected angles of 30° at two points on the curved surface of the rod and then received by the transducer. The ray covers an equilateral triangular path and can be denoted by T2 (Fig.2b). Third echo results when another ray, radiated as longitudinal wave undergoes mode conversion into the transverse wave at the first point of reflection and again mode converted to the longitudinal wave to be received by the transducer (Fig.2c). This also covers a triangular path and denoted by T3. The importance of these echoes is that these are unique in the sense that

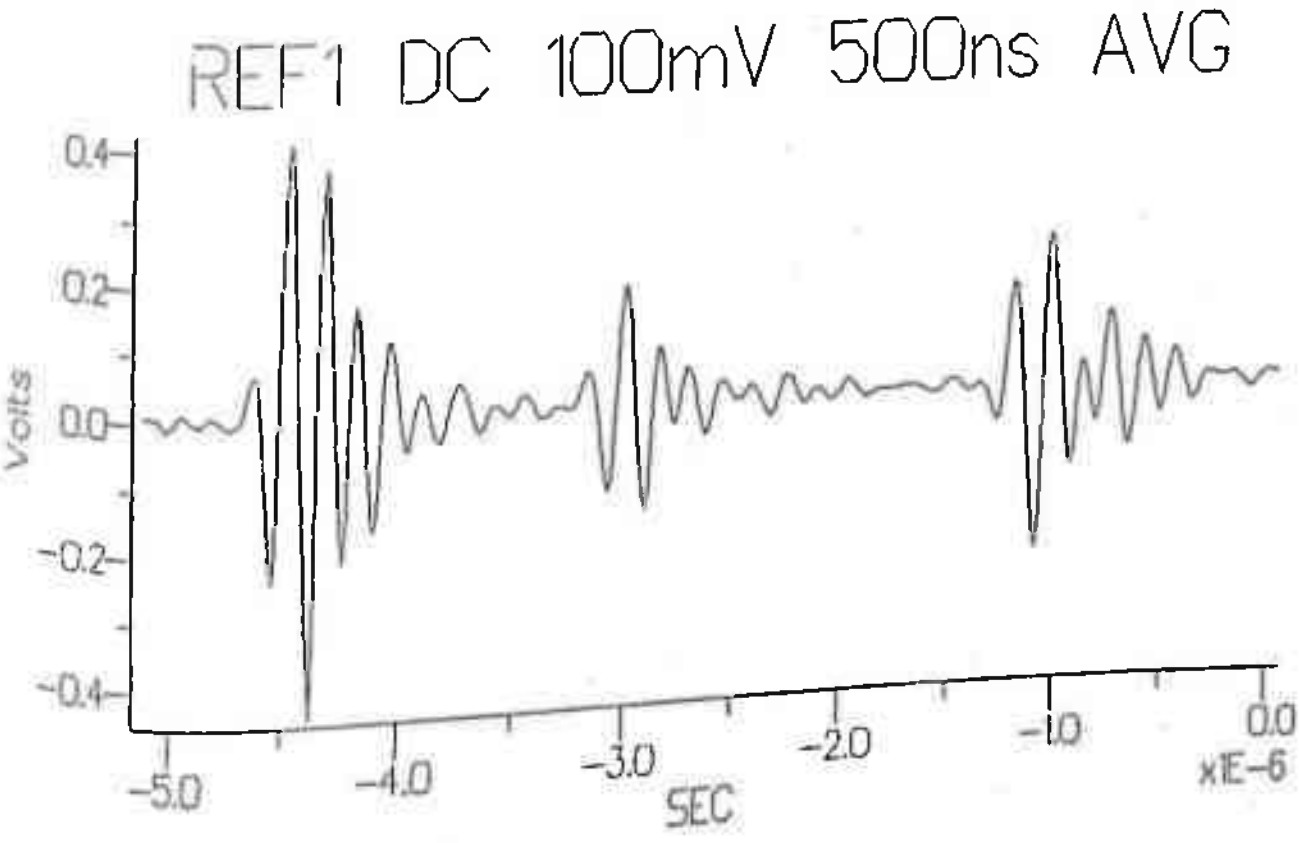

Fig. 1. First three echo signals for path T1, T2 and T3

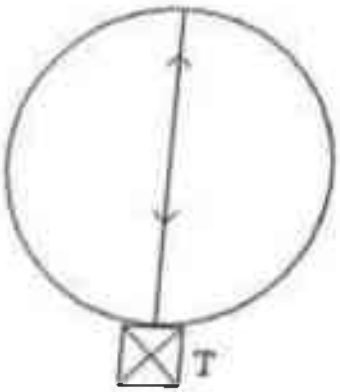

FIRST ECHO PATH (T1)

(a)

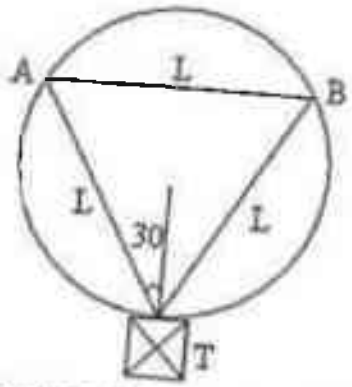

SECOND ECHO PATH (T2)

(b)

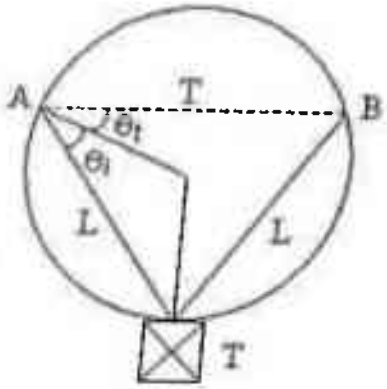

THIRD ECHO PATH (T3)

(c)

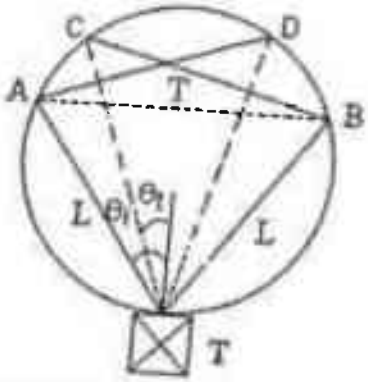

OTHER ECHO PATHS

(d)

Fig.2. (a) Back wall echo reflection in rod

(b) Triangular reflection in rod with out mode conversion

(c) Triangular reflection in rod with mode conversion

(d) Other possible triangular reflections

two and only two triangular paths are such that rays traveling along these path are received by the transducer. All other rays, reflected and mode converted at various points, either miss the transducer's contact line or come at a much later time after the 2nd back wall echo. It is this uniqueness which has been utilised for the measurement of ultrasonic velocity in rods.

One may recall that there is no phase change when the reflected wave is transverse and the incident wave is longitudinal (Eq. A.2 of Ref. 5). However, there is a phase change of π when the reflected wave is longitudinal and the incident wave is either longitudinal or transverse (Eq. A.1 and A.3 of Ref. 5) and when the reflected wave is transverse for incident transverse wave (Eq. A.4). The phase difference between the transmitted and received signals for various paths of T3 can be calculated as follows while keeping an eye on Fig.2d.

Path 1

$$TA(L) \overset{0}{\text{-----}} AB(T) \overset{\pi}{\text{-----}} BT(L) \quad \text{Total phase change } \pi$$

Path 2

$$TA(L) \overset{\pi}{\text{-----}} AD(L) \overset{0}{\text{-----}} DT(T) \quad \text{Total phase change } \pi$$

Path 3

$$TC(T) \overset{\pi}{\text{-----}} CB(L) \overset{\pi}{\text{-----}} BT(L) \quad \text{Total phase change } 2\pi$$

It may be seen that path 2 and 3 are in opposite

phases and should cancel each others contribution. Besides, the longitudinal wave transducer with liquid couplant can neither generate (path TC) nor receive (path DT) transverse wave.

Another path TA-AD-DT-TC-CB-BT is also a possibility from the Fig.2d but this will be exactly double of the TA-AB-BT path and hence this is also ruled out.

It may therefore be concluded that the echo T3 arises due to one and only one path TA-AB-BT.

It may also be seen that there will be a phase difference of 2π at the received signal for T2 while it will be π for T3. Thus T2 and T3 will be in opposite phases, as can be seen in Fig.1. The heights of these three echoes depend on the angle dependent reflectivity, path length and the attenuation.

3.2.2. Ultrasonic Velocity Evaluation

(i) Longitudinal wave velocity (V_l) : The signals obtained from the straight path T1 as well as the triangular path T2, can be used for the evaluation of the ultrasonic velocity of longitudinal wave. The only difference is that signal to noise ratio may be low for some materials for signal T2.

Let d = diameter of the rod

t_1 = round trip time for back wall echo, path T1.

t_2 = time of flight for signal for the path T2

t_3 = time of flight for the signal for the path T3

θ_i = angle of incidence for a longitudinal wave

θ_t = angle of reflection for shear wave

From Fig. 2b. it can be seen that in equilateral triangle with side 's' we have

$$\frac{s}{2} = \frac{d \cos 30}{2} \qquad \ldots(1)$$

or total sound path

3 s = 3 d cos 30 irrespective of material.

The longitudinal wave velocity

$$V_l = \frac{2d}{t_1} \quad \text{(using path T1)} \qquad \ldots(2)$$

$$= \frac{3 d \cos 30}{t_2} \quad \text{(using path T2)} \qquad \ldots(3)$$

(ii) Transverse wave velocity (V_t) : From Fig.2c. and using trigonometry it follows that

$$4 \theta_i + 2 \theta_t = 180$$

$$\text{or} \quad \theta_t = 90 - 2 \theta_i \qquad \ldots(4)$$

If incident and reflected angles (θ_i, θ_t) for the path T3 are known, the transverse wave velocity can be determined using the Snell's law, that is,

$$V_t = \frac{V_l \sin\theta_t}{\sin \theta_i} \quad \text{(using path T3)} \qquad \ldots(5)$$

Eliminating θ_t from the above equations it can be shown that

$$\sin\theta_i = \frac{1}{4}\left[-\frac{V_t}{V_l} + \sqrt{\frac{V_t^2}{V_l^2} + 8}\right] \quad \ldots(6)$$

Negative sign from ± of the above equation is discarded since it will result in such a value of θ_i which will not satisfy equation (4). The travel time t_3 for the signal T3 can be given by considering the Fig.2c.

$$t_3 = \frac{2d\cos\theta_i}{V_l} + \frac{d\cos\theta_t}{V_t} \quad \ldots(7)$$

Using equation (4) and (5)

$$t_3 = \frac{2d\cos\theta_i}{V_l} + \frac{d\cos(90-2\theta_i)\sin\theta_i}{V_l\sin(90-2\theta_i)}$$

or

$$V_l\frac{t_3}{2d} = \cos\theta_i + \frac{\sin2\theta_i\cos\theta_i}{2\cos2\theta_i}$$

The above equation can be rewritten in the cubic form as

$$\cos^3\theta_i - 2K\cos^2\theta_i + K = 0 \quad \ldots(8)$$

where $K = V_l t_3 / 2d$

θ_i can be determined by solving the root of the cubic equation (8). θ_t can be determined from the equation (4).

Thus longitudinal and transverse wave velocity of

the material can be evaluated by using the equation (2),(3) and (5). Since solution of the cubic equation is not straight forward, a computer program in BASIC language is used and given in Table 1 for determination of the values of θ_i which is then used to calculate θ_t, V_l and V_t.

3.3 EXPERIMENTAL PROCEDURE

The block diagram and photograph of the experimental setup for contact testing is shown in Fig. 3 and 4. Both, the direct contact technique and the immersion technique have been used. In contact technique the sample, a flawless cylindrical rod is kept on a V-shaped stand. The broad band transducer with frequency range in a few MHz was put on the cylindrical surface of the rod sample with fixed pressure on the transducer. Ultrasonic flaw detector (Sonatest, Master Scan - 300) is used to excite the transducer and to receive the echoes. First three echoes were successively sampled and the delay time for each echo was measured by the digital storage oscilloscope (Tektronix - 2440). The echoes can be stored and transferred to an IBM-PC via GPIB interface to have a printout of the wave form. Measurements were taken only when all the three echoes were quite steady i.e. pressure between rod and transducer was equal or slightly more than a certain pressure. In immersion technique, the rod sample is put into the water tank and transducer is adjusted for the maximum back wall echo

Table 1. Computer program for determining the velocity of longitudinal and transverse waves, incident angle for longitudinal wave, reflected angle for transverse wave (V_l, V_t, θ_i, θ_t)

```
 10 REM TO DETERMINE LONGITUDINAL AND TRANSVERS WAVE
 20 REM VELOCITY IN ROD MATERIAL, D = DIA OF THE
 30 REM TRANSDUCER, T1, T2, T3 ARE TIME OF FLIGHT
 40 REM FOR CORRESPONDING ECHO PATH THETAI, THETAT
 50 REM ARE ANGLE OF INCIDENCE AND REFLECTION,
 60 REM VL1,VL2,VT ARE VELOCITIES BY  TIME T1,T2,T3
 70 INPUT D,T1,T2,T3
 80 VL1 = 2*D/T1
 90 RAD = 3.1415/180
100 VL2 = (3*D*COS(30*RAD))/T2
110 LET A = VL2 * T3 / (2*D)
120 FOR X = .1 TO .9 STEP .001
130 Y = X^3/(2*X^2 - 1)
140 IF Y > A + .01 GO TO 210
150 IF Y < A -  .01 GO TO 210
160 THETAI = (ATN (((1 - X^2)/X^2)^.5))/RAD
170 THETAT = 90 - 2 * THETAI
180 VT = (VL2*SIN (THETAT*RAD)) /SIN(THETAI * RAD)
190 LPRINT VL1,VL2,VT,THETAI,THETAT
200 GO TO 210
210 NEXT X
220 END
```

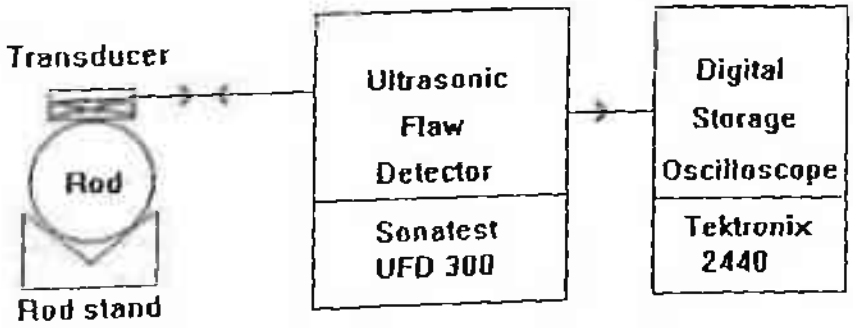

Fig. 3. Block diagram of the experimental set up

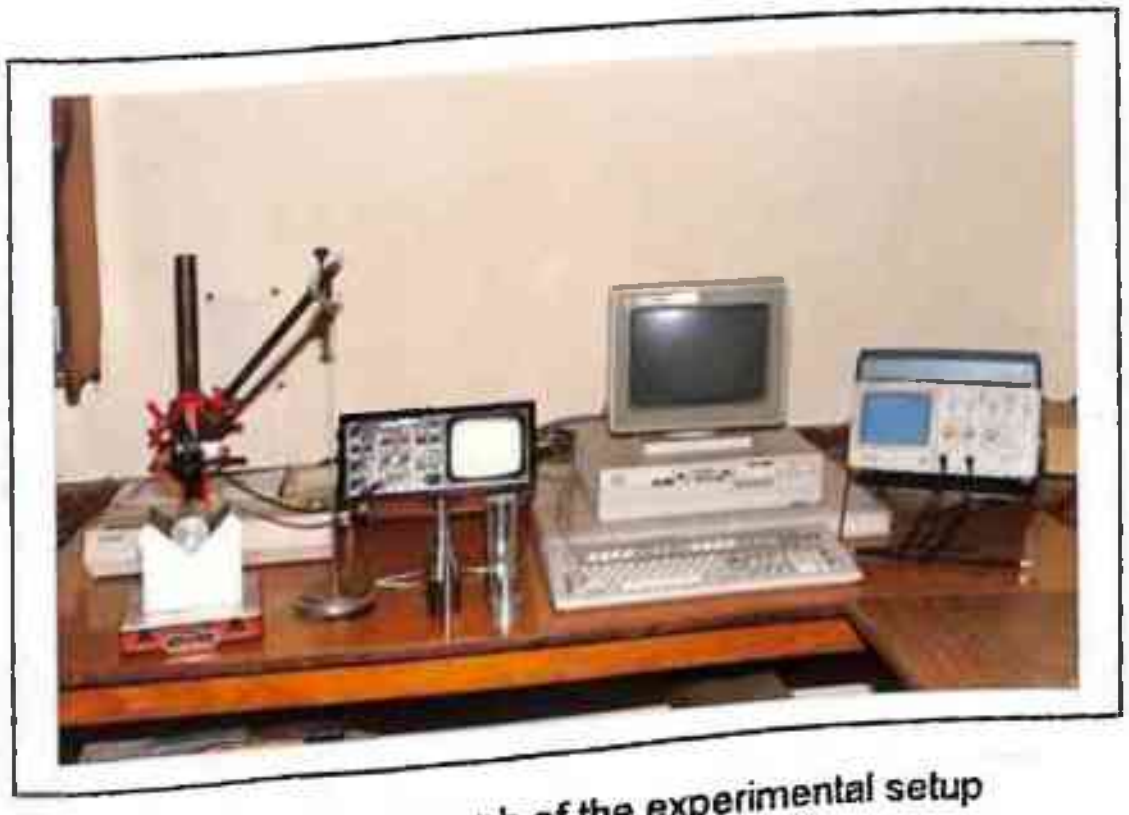

Fig.4. Photograph of the experimental setup

height.

A number of rods of different materials and varying diameters are taken and marked differently. The dimensions of the rod taken are in the range of 12 mm to 60 mm in diameter given in the Table 2. Study was made by using the three transducers of nominal frequencies 5 MHz (contact type), 5MHz (immersion type) and 7.5MHz (immersion type). Both the contact method and the immersion method are used to see the relative performance of the technique and also to establish the uniqueness of the paths followed by the first three echoes.

3.4 RESULTS AND DISCUSSION

The evaluated ultrasonic velocities for longitudinal and transverse waves in rod material has been given in Table 3 and 4. It is observed that the values observed by the echoes T2 and T3 are of the same order of magnitude as the values given in literature for the same material [5,21]. The values of longitudinal wave velocities as evaluated by the back wall echo T1 and by echo T2 are in excellent agreement.

The immersion technique is found more suitable and provided better reproducibility and relatively easy manipulation of transducer to maximise the echo height.

The ultrasonic velocity values can be used to characterise the rod material by determining the various

Table 2. Number of rods used with their diameter and length for measurement of ultrasound velocity.

Sr. No.	Rod marked	Metal	Diameter (mm)	Length (mm)
1	1V	Al alloy	50.78	152.60
2	2V	Steel	50.01	59.95
3	3VS	Al alloy	19.98	70.80
4	3VB	Al Alloy	37.64	70.80
5	4VS	Al Alloy	24.97	70.80
6	4VB	Al Alloy	49.00	70.80
7	5V1	Al Alloy	12.06	164.00
8	5V2	Al Alloy	20.06	164.00
9	5V3	Al Alloy	30.08	164.00
10	5V4	Al Alloy	45.00	164.00
11	5V5	Al Alloy	60.02	164.00
12	6V1	M. Steel	12.70	164.00
13	6V2	M. Steel	20.02	164.00
14	6V3	M. Steel	29.99	164.00
15	6V4	M. Steel	45.00	164.00
16	6V5	M. Steel	60.00	164.00

Table 3. Longitudinal and transverse wave velocities evaluated in different rods with time of flight for different triangular echoes by immersion method.

Rod No.	Time (μs)			Velocity (mm/μs)			Angles (°)	
	t_1	t_2	t_3	V_l By t_1	V_l By t_2	V_t	θ_i	θ_t
1V	16.28	20.88	28.40	6.238	6.318	3.111	36.5	17.0
2V	16.98	21.79	28.13	5.890	5.962	3.255	35.7	18.6
3VS	6.32	8.06	11.08	6.322	6.439	3.128	36.6	16.8
3VB	11.87	15.15	20.88	6.343	6.456	3.136	36.6	16.8
4VS	7.84	10.00	14.08	6.369	6.487	3.109	36.7	16.6
4VB	15.43	19.82	27.14	6.353	6.424	3.121	36.6	16.8
5V1	3.87	4.94	6.72	6.232	6.343	3.123	36.5	17.0
5V2	6.46	8.25	11.21	6.211	6.317	3.110	36.5	17.0
5V3	9.64	12.32	16.5	6.241	6.343	3.123	36.5	17.0
5V4	14.44	18.44	25.16	6.233	6.340	3.121	36.5	17.0
5V5	19.24	24.67	33.52	6.239	6.321	3.112	36.5	17.0
6V1	4.35	5.53	7.13	5.773	5.966	3.257	35.7	18.6
6V2	6.78	8.67	11.23	5.905	5.999	3.234	35.8	18.4
6V3	10.16	13.10	16.17	5.904	5.947	3.288	35.8	18.7
6V4	15.28	19.56	25.28	5.890	5.977	3.263	35.7	18.6
6V5	20.36	26.05	33.84	5.895	5.985	3.228	35.8	18.4

Table 4. Longitudinal and transverse wave velocities evaluated in different rods with time of flight for different triangular echoes by contact method

Rod No.	Time (μs)			Velocity (mm/μs)			Angles (°)	
	t_1	t_2	t_3	V_l By t_1	V_l By t_2	V_t	θ_i	θ_t
1V	16.320	20.976	28.528	6.223	6.290	3.097	36.5	17.0
2V	17.024	22.088	28.360	5.875	5.882	3.252	35.6	18.8
3VS	6.392	8.224	11.328	6.252	6.312	3.067	36.6	16.8
3VB	11.936	15.400	21.240	6.307	6.350	3.044	36.7	16.8
4VS	7.936	10.240	14.120	6.293	6.335	3.037	36.7	16.6
5V1	3.984	5.120	7.000	6.055	6.119	3.013	36.5	17.0
5V2	6.520	8.400	11.280	6.153	6.204	3.136	36.4	17.2
5V3	9.760	12.520	16.920	6.163	6.242	3.114	36.4	17.2
5V4	14.528	18.400	25.520	6.194	6.354	3.046	36.6	16.6
5V5	19.360	24.160	33.680	6.200	6.454	3.053	36.7	16.5
6V1	4.416	5.760	7.280	5.752	5.728	3.246	35.4	19.1
6V2	6.896	8.944	11.184	5.806	5.816	3.377	35.2	19.5
6V3	10.288	13.344	17.168	5.830	5.839	3.188	35.7	18.6
6V4	15.360	19.920	25.760	5.859	5.869	3.204	35.7	18.6
6V5	20.440	26.520	33.560	5.871	5.878	3.331	35.4	19.2

elastic constants using the equations (1) to (6) given in Chapter 1.

3.5 CONCLUSION

A method employing the single longitudinal wave normal beam transducer has been used to measure both longitudinal and transverse wave velocity in materials of rod shape. The results can be used to determine various mechanical characteristics of a material by evaluating the elastic constants.

3.6 REFERENCES

1. Schreiber, E., Anderson, O.L. and Soga, N., Elastic Constants and Their Measurement , McGraw Hill Book Co., NY (1973)

2. Nagy, P.B. and Renee, M.K., Ultrasonic assessment of poission ratio in thin rods, J. Acoust. Soc. Am. 98 (1995) 2694-701

3. Wu, T.T., and Fang, J.S., and Liu, G., Kuo, M., Determination of elastic constants of a concrete specimen using transient elastic waves, J. Acoust. Soc. Am. 98 (1995) 2142-48

4. Mossalamy, M.E., Bahay, M. and Abd El, N., Ultrasonic studies on brass (70/30), J. Pure Appl. Ultrason. 19 (1997) 1-8

5. Krautkramer, J. and Krautkramer, H., Ultrasonic Testing of Materials, Third edition, Springer Verlag Berlin, Bonn (1983)

6. Panakkal, J.P., Longitudinal ultrasonic velocity a predictor of material properties of porous materials, Proc. 14WCNDT (1996) 2279-82

7. Chen, Y.F. and Zhang, J., A research on testing elastic module of workpiece materials, Proc. 14WCNDT (1996) 2267-70

8. Naik, T.R. and Malhotra, V., The ultrasonic pulse velocity method, Chapter 7 in Handbook on Nondestructive Testing of Concrete, V.M. Malhotra and N.J. Carino Eds. CRC Pres Inc. Boston (1991)

9. Chatterjee, A.K., Panda, B. and Mishra, C., Condition monitoring of oxygen making vessel by laser technique, Proc. 14 WCNDT (1996) 1073-78

10. Balasubramaniam, K., Shah, V.V. and Costley, D.R., Laser generated guided ultrasonic waves applications in nondestructive evaluations, Proc. 14 WCNDT (1996) 2311-14

11. Oliver, J,. Dispersion of elastic waves in cylindrical rod by wide band short duration pulse technique, J. Acoust. Soc. Am. 29 (1957) 189-94

12. McSkiman, H.J., Propagating of longitudinal and shear waves in cylindrical rods at high frequencies, J. Acoust. Soc. Am. 28 (1956) 484-494

13. Hughes, D.S., Pandrom, W.L. Mims, R.L., Propagation of elastic pulses in metal rods, Phys. Rev., 75 (1949) 1552-1556

14. Joseph, Z. Jr., An experimental and theoretical investigation of elastic waves propagation in cylinder, J. Acoust. Soc. India 51 (1972) 265-283

15. Papedakis, E.P., Traveling wave reflection method for measuring ultrasonic attenuation and velocity in thin rods and wires, J. Appl. Phys. 42 (1971) 2990-95

16. Nagy, P., Longitudinal guided waves propagation in transversely isotropic rod immersed in fluid, J. Acoust. Soc. Am. 98 (1995) 2694-2701

17. Dayal, V., Longitudinal waves in homogeneous anisotropic cylindrical bars, J. Acoust. Soc. Am. 93 (1993) 1249-55

18. Ashok Kumar, Yudhisther Kumar and Basant Kumar, On the measurement of longitudinal and shear ultrasonic velocities, Nondestr. Test. Eval. 13 (1997) 121-26

19. Sviridov Yu. and Vesemeenko S., Study of the acoustic channel for velocity and attenuation measurement of ultrasound in thin rods, Defektoskopia No.6 (1986) 60-68

20. Ashok Kumar, Correction factor due to couplant in ultrasonic thickness measurement, INSIGHT 38 (1996) 336-337

21. Kinsler, L.E. and Frey, A.R., Fundamentals of Acoustics, Wiley Eastern Ltd., (1990)

CHAPTER - 4

ULTRASONIC ATTENUATION MEASUREMENT IN ROD MATERIAL

CHAPTER - 4

ULTRASONIC ATTENUATION MEASUREMENT IN ROD MATERIAL

4.1 INTRODUCTION

Ultrasonic attenuation is a difficult quantity to measure accurately, particularly in solid material, such as common structural metals, at the test frequencies usually applied in nondestructive testing i.e. 1 to 10 MHz. The overall result usually observed includes other losses such as beam spread, field effects, couplant mismatch, transducer bonding or sample geometry. These factors are difficult to isolate perfectly. Use of special technique and equipment can reduce the contribution due to these factors.

Ultrasonic attenuation values are helpful in estimating the grain size, tensile strength, yield strength, crystalline damage, fatigue damage, impact strength or hardness of a material [1-6]. Also, attenuation has an important role in ultrasonic nondestructive evaluation (NDE) such as in defining the limit of frequencies over which a material may be tested [7,8]. Higher frequency is preferred for getting better resolution, but it attenuates much faster. To detect small

flaws and to avoid attenuation low frequencies can be used. But optimum frequency has to be selected keeping in view the attenuation and resolution. According to Malecki [6-9], if dependence of the attenuation coefficient on the frequency can be expressed by formula

$$\alpha = p + q^{m}$$

then for a given flaw distance a the optimal frequency is

$$f_{opt} = \frac{1}{\sqrt[m]{mqa}}$$

where p,q and m are constants. Also attenuation in the material must be known for defect sizing using DGS diagrams for better estimation of equivalent flat bottom hole (FBH) diameter. Higher accuracy in the measurement of attenuation will result in better estimation of these parameters.

The loss of acoustic energy of a sound beam propagating through the material arises from

(a) Deviation of energy from the parallel beam by regular reflection, refraction, diffraction

(b) Scattering and

(c) Absorption.

The combined effect of absorption and scattering is known as attenuation. Absorption losses for which

mechanical energy is converted into heat by internal friction are characteristics of material through which the wave travel and their evaluation can yield information about physical properties of the medium like viscosity and thermal conduction. The absorption can be due to either hysteresis or relaxation [9].

4.1.1 Hysteresis Type of Absorption

When adiabatic stress is applied to a medium, the resultant strain does not vary linearly with the applied stress. The stress strain curve then takes the form of a hysteresis loop. The area of the loop gives the amount of energy absorbed per half cycle for unit volume of the material. Loss per cycle is independent of frequency with the result that absorption increases with frequency in a linear manner.

4.1.2 Relaxation Type of Absorption

The relaxation type of absorption is observed at megahertz frequencies. During the positive half of stress cycle energy is absorbed and during the negative half cycle energy is released. A finite period of time is required for this exchange of energy to take place. When frequency of wave is increased from a low value, absorption at first increases, rises to peak at frequency, called the relaxation frequency and then diminishes to zero at frequency so high that there is insufficient time for any energy exchanges.

4.1.3 Attenuation Due to Scattering

Ultrasonic energy is reflected or scattered from the elastic discontinuities at grain boundaries. The amount of scattered energy depends on relative magnitude of wavelength and average grain diameter. Attenuation is known to increase with increasing grain diameter (D_g). For a ratio of $\lambda/D_g > 30$, the attenuation is essentially constant and for a ratio of $\lambda/D_g < 6$ it increases rapidly. At higher frequencies attenuation appears to vary as 4th power of frequency. This is because the scattering increases (approximately D_g^3) for an average grain size $D_g > \lambda/10$.

4.1.4 Attenuation Coefficient

Where attenuation is uniform through out the ultrasonic field, it can be characterized as attenuation coefficient, α. Considering a thin layer of medium of thickness 'dx' normal to the direction of propagation, at a distance x from an origin. For uniform attenuation the fractional loss of amplitude α, per unit path length, from the layer should be constant. Thus

$$dp/p = - \alpha.dx$$

Integrating and for x = 0, pressure = p_0 and for x = d, pressure = p.

$$p = p_0 \exp(-\alpha d) \qquad \ldots(1)$$

The natural log of the equation gives

$$\alpha d = \ln (p_0/p)$$

which is the total attenuation over the distance d, a dimensionless number which is expressed in nepers (Np). The attenuation coefficient is given in Np/cm. Another unit is decibel per meter or abbreviated dB/m. Alternate form some time used and their conversions are :

$$\alpha d = 20 \log (p_0/p) \text{ dB} \quad \text{and}$$

$$1 \text{ Np/cm} = 8.686 \text{ dB/cm}$$

Various methods are being used for measurements of ultrasonic attenuation [10-13] and techniques have been refined by several workers to relax various approximations [14-16]. Diffraction correction was introduced which deeply affects the attenuation measurements, particularly at low frequencies, as diffraction losses become comparable with true attenuation. Most methods measuring attenuation depend initially on measuring the coefficient of reflection. Reflection coefficient is frequency dependent and is influenced by surface roughness [17], a factor that can dominate mechanical test results. Some of the common technique for evaluation of ultrasonic attenuation are also referred to in Chapter 1

The attenuation measurement for ultrasonic longi-

tudinal and transverse wave in rod shaped material becomes difficult due to its curved geometry . Comparatively a few studies have been made earlier in measuring attenuation in rods [18-21]. Present work reports a new technique for the evaluation of true ultrasonic attenuation in rods utilising two sections of different diameters. The rod has a line contact with a broad band transducer used in pulse echo mode. It is assumed that due to line contact, emission of ultrasound into the rod is equal in different directions. Fast fourier transform (FFT) algorithm has been used for frequency spectrum analysis of the echoes received. First three echoes, those used for velocity in the preceding chapter, are taken into account for evaluation of attenuation in such a way that use of diffraction correction and reflection coefficient parameters is eliminated. Technique is also useful to evaluate attenuation values at varying frequencies within the 6dB frequency bandwidth of the broad band transducer. The results obtained by this technique are presented for rods of different materials and varying diameters.

4.2 THEORETICAL CONSIDERATION

When a normal beam longitudinal wave transducer is placed on the curved surface of a cylindrical rod, it makes a line contact between transducer and surface of the rod. Due to very small width of the contact line, the divergence angle is also very large and a number of

echoes is observed. First three echoes for a flawless and isotropic metal rod sample are taken for the determination of ultrasonic attenuation values similar to velocity evaluation. The first echo is from back wall that is from diametrically opposite side. Second echo results when a ray from the transducer makes an angle of 30° with the diameter and covers a triangular distance (Fig.2c, Chapter 3). This equilateral triangular path is traversed by longitudinal waves. The third echo observed is from the longitudinal wave, L, mode converted into Transverse wave, T, and then mode converted back to longitudinal wave which is then received by the transducer.

Let the path of first, second and third echo be denoted as T1, T2 and T3 as in the preceding chapter. It may be noted that the path of echoes T1, T2 and T3 are unique. For a rod of diameter d, the path for echo T2 can be given as

$$T2 = 3d \cos\theta_i \qquad \ldots(2)$$

and path for echo T3 can be given as (Fig.2c, Chapter 3)

$$T3 = 2\,d \cos\theta_i + d \cos\theta_t \qquad \ldots(3)$$

The law of reflection governing the angle of incidence θ_i for a longitudinal wave and angle of reflection θ_t for shear wave is

$$\frac{V_s}{V_l} = \frac{\sin\theta_t}{\sin\theta_i} \qquad \ldots(4)$$

$$4\theta_i + 2\theta_t = 180 \qquad \ldots(5)$$

Eliminating θ_t from equation (4) and (5) it can be shown that

$$\sin\theta_i = \frac{1}{4}\left[-U + (U^2+8)^{1/2}\right] \qquad \ldots(8)$$

where $U = V_t / V_l$ ...(7)

In the present work pressure amplitude of the first three echoes have been utilised for the ultrasonic attenuation measurement. It is therefore important to consider the dependence of the pressure amplitude of these echoes on various factors in addition to the dependence on the path for individual echoes. The problem is discussed in light of reflectivity, beam spread, phase change and attenuation.

4.2.1 Reflectivity

Considering the angular dependence of reflectivity, the echo by path T3 can have larger amplitude as compared to echo by path T2. Referring to path T2 (Fig.2b, Chapter 3) and taking the example of steel/air, the pressure in reflected longitudinal wave AB will be 68.34% of incident longitudinal wave TA at A (Fig. 1) [22,23], the angle of incidence being 30° (equation A.1 to A.4 of Reference 7). The pressure will be further

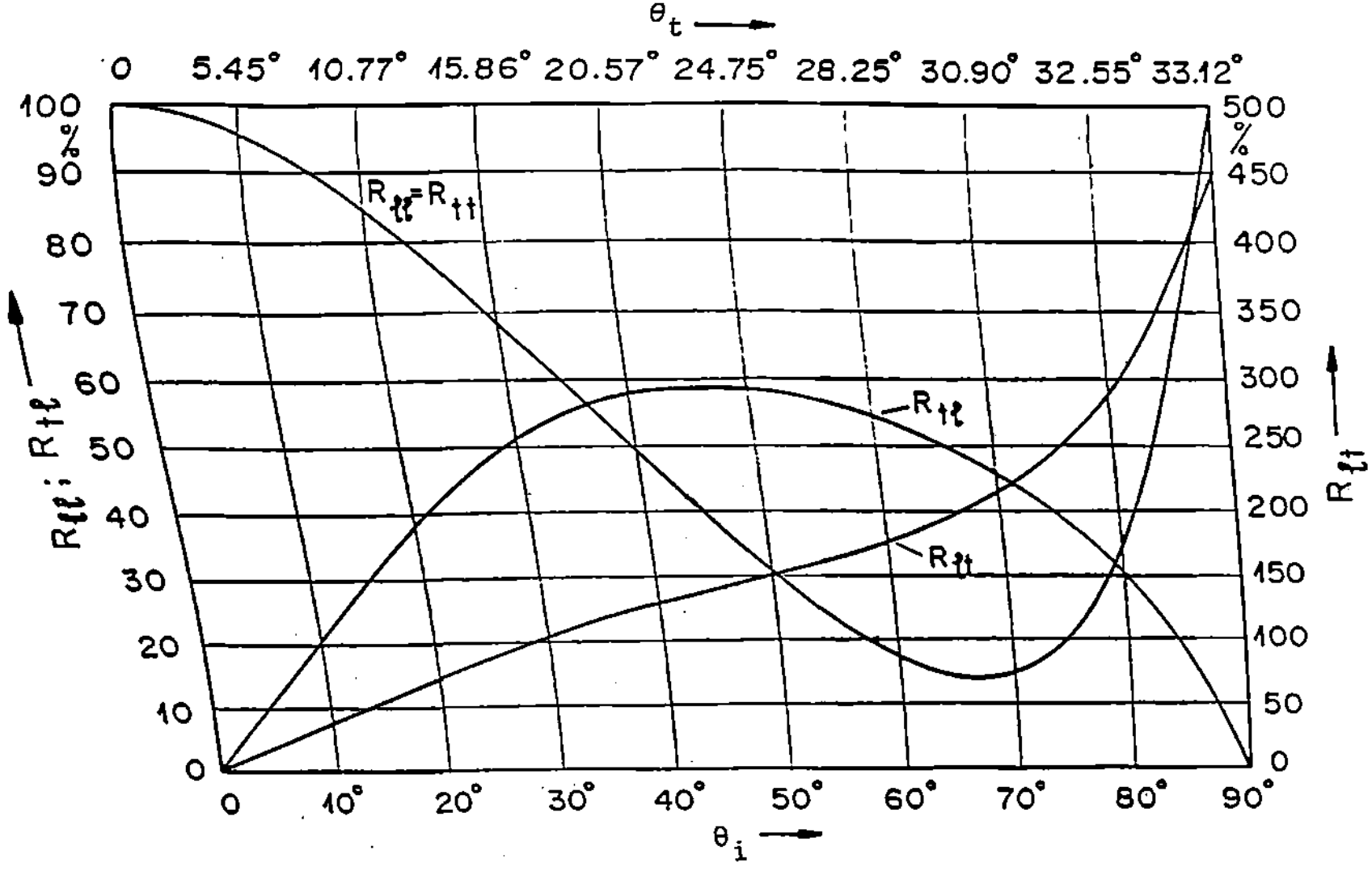

Fig.1. Reflection coefficient at free boundary of steel. First subscript refers to reflected wave and second refers to incident wave, l refers to longitudinal and t refers to transverse wave

reduced to 68.34% on reflection at B. The pressure received by the transducer will thus be 48.70 % of the transmitted pressure if loss due to reflection alone is taken into consideration.

For paths T3 (Fig.2c, Chapter 3) the angle θ_i will be 35.7° and angle θ_t will be 18.6° for steel having V_l 5900 m/s and V_t = 3230 m/s. The pressure in reflected transverse wave AB will be 55.99% of incident longitudinal wave. However, this will be increased by 119.58% on reflection at B. The pressure received at the transducer will thus be 67% of the transmitted pressure which is higher than the pressure 46.7% for the path T2. Similarly for aluminium alloy for V_l = 6420 m/s and V_t = 3114 m/s the angle θ_i will be 38.6° and θ_t will be 16.8°. The pressure received at the transducer for echo path T2 will be 60.93 % and for T3 it will be 78.35 %. Similar calculations can be done for the different aluminium alloy and other metals.

A point worth mentioning here is that in Ref.7 the curve of R_{tl} in diagram 1 does not directly correspond to the equation (A.2) of this reference. The exact values have been calculated using the equation A.1 to A.4 and corrected diagram is given here in Fig. 1.

4.2.2 Phase Change

Discussed in the previous chapter on velocity the

path is unique on the basis of phase consideration. and other paths are ruled out. Since we are currently interested only in the relative heights of T2 and T3, we need to consider only one of the two directions.

4.2.3 Beam Spread

The effect of the beam divergence on the relative heights of the echoes is not being considered significant since in the present work it is the comparison of two echoes which arise out of the paths covering almost equal distances. The distance corresponds to much more than three times the near field in the far field region where change in amplitude is not significant. The distance covered by the echo T3 is 2.56 times the rod diameter and that by the echo T2 is 2.60 times the rod diameter for an aluminium alloy. For a rod of 25 mm diameter, these distances are 64.07 mm and 64.95 mm, respectively. The near field, given by $W^2/4\lambda$ where W is the width of contact line, will be 0.5 mm for W = 2 mm and V_l = 6000 m/s at 3 MHz.

Another important reason for not taking into consideration the diffraction effects is that the echoes considered are due to a single ray and not the beam. It is the beam which experiences the divergence and not the ray.

4.2.4 Attenuation Versus Reflectivity

In measuring the attenuation the effect of reflectivity and that of beam divergence have to be reduced. Since the attenuation of transverse wave is more than that of the longitudinal wave, the attenuation will reduce echo height due to path T3 more than path T2. This will try to reduce the contribution due to reflectivity which may make T3 higher than T2. The relative heights of T3 and T2 will therefore depend upon the combined effect of reflectivity and attenuation. For a rod of higher diameter, the path traveled by the transverse wave will become higher as compared to that in lower diameter rod. The attenuation effect will consequently dominate the reflectivity in larger diameter rods, for the contribution due to reflectivity will remain the same for all diameters of the rod of a given material. It may, therefore, be concluded that echo height for T3 will be higher than that for T2 for small diameter rods. For larger diameter rods the echo height for T2 will be higher than that for T3. This has been shown by an experiment also for a stainless steel rod of 38 mm and 14 mm diameter (Fig. 2)

It may now be concluded that the amplitude of the echo height of the three echoes depend mainly on the reflectivity and attenuation and for evaluating the true value of ultrasonic attenuation one has to consider the

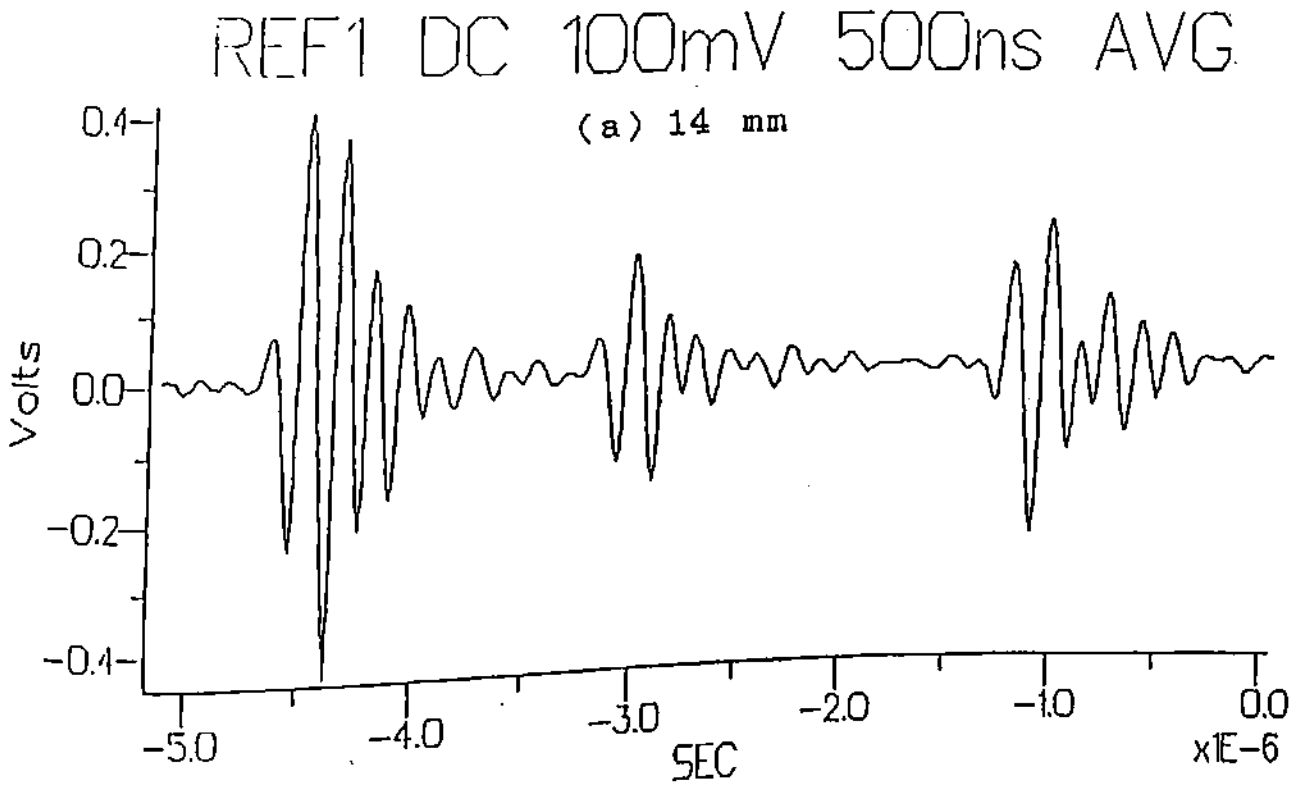

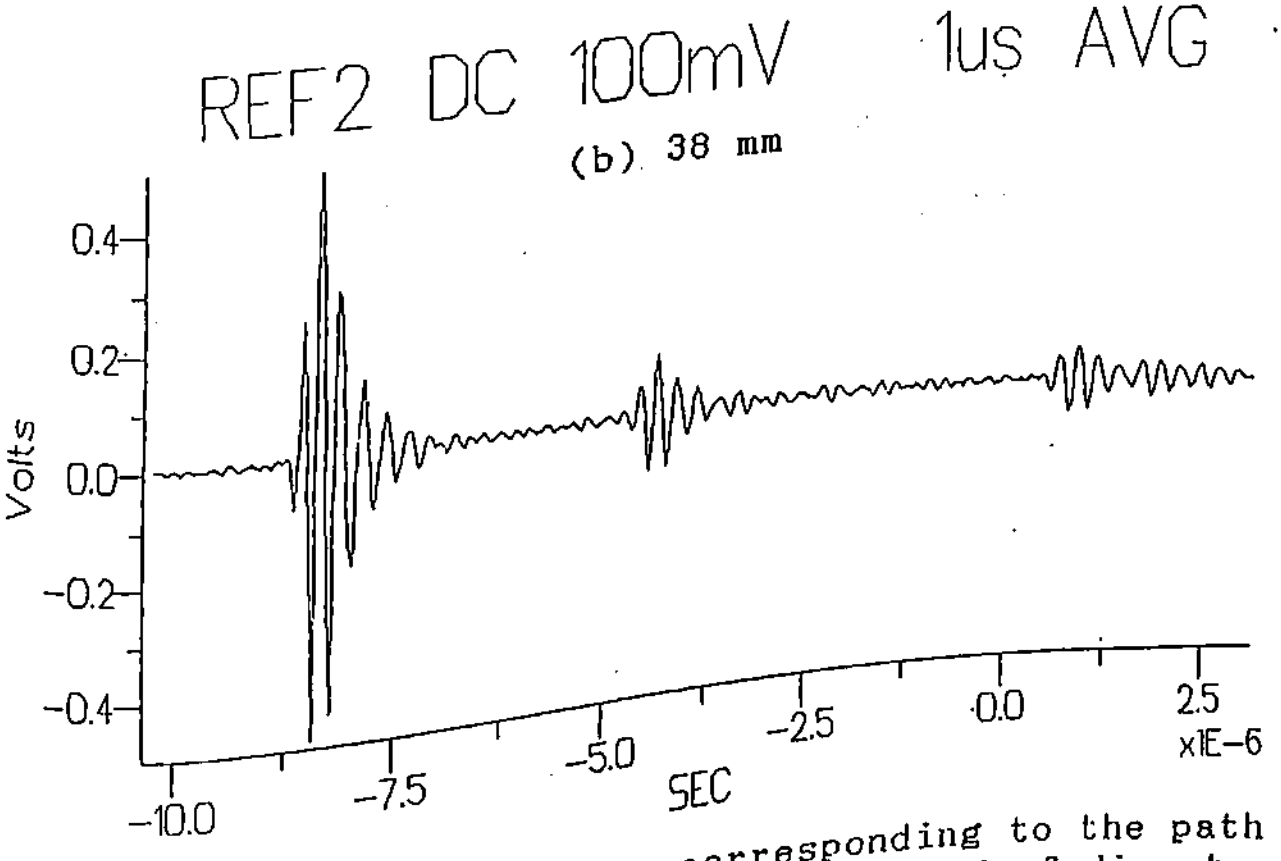

Fig. 2. First three echoes corresponding to the path T1, T2, T3 for stainless steel rod of diameter (a) 14 mm (b) 38 mm

4.2.5 Determination of Attenuation

The material, in which attenuation is to be evaluated, is taken in the form of a single rod of two different end diameters or two rod samples of different diameter and of the same material. The single rod can be machined to have two different diameters for measuring pressures from echoes corresponding to paths T1, T2 and T3. The diameter of the rod is selected such that the three echoes are resolved clearly and their amplitudes are well above the noise level.

Let,

d_1 = diameter of rod at one end

d_2 = diameter of rod at another end

P_{11}, P_{12}, P_{13} = pressures of echoes by T1, T2 and T3, respectively from rod end of diameter d_1

P_{21}, P_{22}, P_{23} = pressure of echoes by T1, T2 and T3, respectively from rod end of diameter d_2

R_1 = Reflection coefficient for incident longitudinal ray at normal incidence for rod metal-air or metal-liquid interface.

R_2 = Reflection coefficient for incident longitudinal ray at an angle 30° and reflected longitudinal ray

R_3 = Reflection coefficient for incident longitudinal ray at an angle θ_i and reflected transverse ray at angle θ_t

R_4 = Reflection coefficient for incident transverse ray at an angle θ_t and reflected longitudinal ray at angle θ_i

α_l, α_t = Attenuation of longitudinal and transverse wave, respectively

Various pressure equations can be written as follows.

$$P_{11} = A_1 \exp(-2\alpha_1 d_1) R_1 \quad \ldots(8)$$

where A_1 is the acoustic pressure of ray immediately after its entrance in rod of diameter d_1. The reflection coefficient can be taken as 1 for normal incidence at metal/air interface.

$$P_{12} = A_1 \exp(-\alpha_1 3d_1 \cos 30).R_2^2 \quad \ldots(9)$$

$$P_{13} = A_1 \exp(-\alpha_1 2d_1 \cos\theta_i - \alpha_t d_1 \sin 2\theta_i) R_3 R_4 \quad \ldots(10)$$

Similar equations can be written for rod of diameter d_2.

$$P_{21} = A_2 \exp(-2\alpha_1 d_2).R_1 \quad \ldots(11)$$

$$P_{22} = A_2 \exp(-\alpha_1 3d_2 \cos 30).R_2^2 \quad \ldots(12)$$

$$P_{23} = A_2 \exp(-\alpha_1 2d_2 \cos\theta_i - \alpha_t d_2 \sin 2\theta_i) R_3 R_4 \quad \ldots(13)$$

It may be noted that reflection coefficients do not change with change in diameter. The initial pressures, of course, may be different due to different contact line width but is found to cancel out. Using the equations (8),(9), (11) and (12),

$$\frac{(P_{11}/P_{12})}{(P_{21}/P_{22})} = \exp[-\alpha_1 (d_2 - d_1)(3\cos 30 - 2)]$$

or,

$$\alpha_1 = - \frac{1}{0.598(d_2 - d_1)} \log_e \frac{P_{11}/P_{12}}{P_{21}/P_{22}} \quad \ldots(14)$$

Using equations (9), (10), (12) and (13),

$$\frac{P_{12}}{P_{22}} = \frac{A_1}{A_2} \exp [-2.598\ \alpha_1(d_1-d_2)] \quad \ldots(15)$$

$$\frac{P_{13}}{P_{23}} = \frac{A_1}{A_2} \exp [-2\alpha_1(d_1-d_2)\cos\theta_i - \alpha_t(d_1-d_2)\sin 2\theta_i] \quad \ldots(16)$$

Dividing equations (15) and (16)

$$\frac{P_{12}/P_{22}}{P_{13}/P_{23}} = \exp[(d_1-d_2)(-2.598\alpha_1 + 2\alpha_1 \cos\theta_i + \alpha_t \sin 2\theta_i)]$$

or

$$\alpha_t = \frac{1}{\sin 2\theta_i} \left[\frac{1}{d_1-d_2} \log_e \frac{P_{12}/P_{22}}{P_{13}/P_{23}} + \alpha_1(2.598 - 2\cos\theta_i) \right] \quad \ldots(17)$$

Equations (14) and (17) give attenuations α_1 and α_t in terms of known angle θ_i, diameters d_1 and d_2 and measured ratio of echo heights (P_{11}/P_{12}), (P_{12}/P_{13}), (P_{21}/P_{22}) and (P_{22}/P_{23}).

4.3 EXPERIMENTAL PROCEDURE

The block diagram of the experimental setup is given in Fig.3. Various rod samples were taken and their ultrasonic velocity measured as in the previous Chapter and the attenuation values were measured as per this Chapter. The measurement method requires a flawless isotropic cylindrical rod sample having two different end diameters. The two rods of different diameters and same material can also be used. A broad band transducer was put onto the curved surface of the sample with a fixed pressure with the help of a mechanical arrangement. The rod sample is put on a V-shaped stand and the transducer is coupled to rod as in direct contact technique. The fixed pressure required is to make the echo signal steady and to give repetitive results. The couplant thickness has been kept minimum possible such that the echo height obtained is constant after a certain pressure. This was done because the line width of contact is minimised up to 1.5 mm. Ultrasonic flaw detector (Sonatest, Master scan-300) is used to excite the transducer and to receive the echoes. First three echoes for each end of the rod in UFD were separately sampled, averaged for 128 samples, stored in the digital storage oscilloscope (Tektronix 2440) and later transferred to IBM-PC via GPIB interface. FFT of the signal stored is performed to analyse the data by magnitude spectrum using the standard software SPD-GURU from Tektronix.

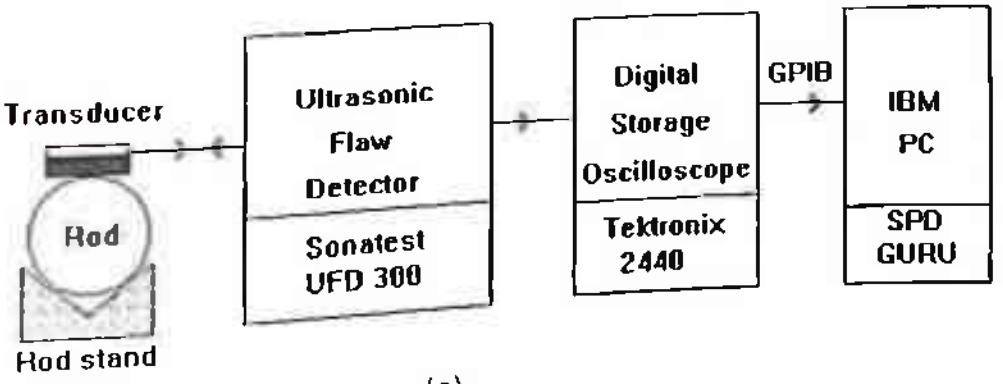

(a)

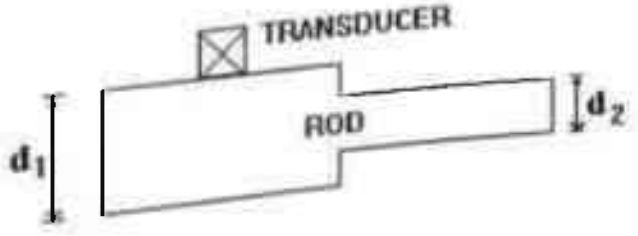

(b)

Fig.3. Block diagram of the experimental setup and sample of the rod

The echoes observed after third echo were not considered in our experiment. Measurements were taken only when all the three echoes were quite steady i.e. pressure between rod and transducer was equal or more than a certain pressure keeping minimum couplant layer. Measurements can also be made using the immersion technique. In this technique transducer has to be kept at a distance approximately equal or more than the near field to minimise the effective contact line width. This technique appears to be better at least to maximise the amplitude of the echoes as transducer can be manipulated as desired. But it may give lesser amplitude for higher frequencies due to attenuation of high frequency sound waves into water path. The immersion method needs to be further explored and has not been discussed further in this work.

Attenuation for longitudinal and transverse wave was determined according to the equations (14) and (17) respectively. Rod sample with steps of different diameters was also taken and attenuation values were measured using the combination of two different step diameters to achieve the validity of the method developed.

4.4 RESULTS AND DISCUSSION

The evaluated attenuation values for longitudinal and transverse waves are shown in Fig.4(a to e) It is observed that the values for longitudinal attenuation

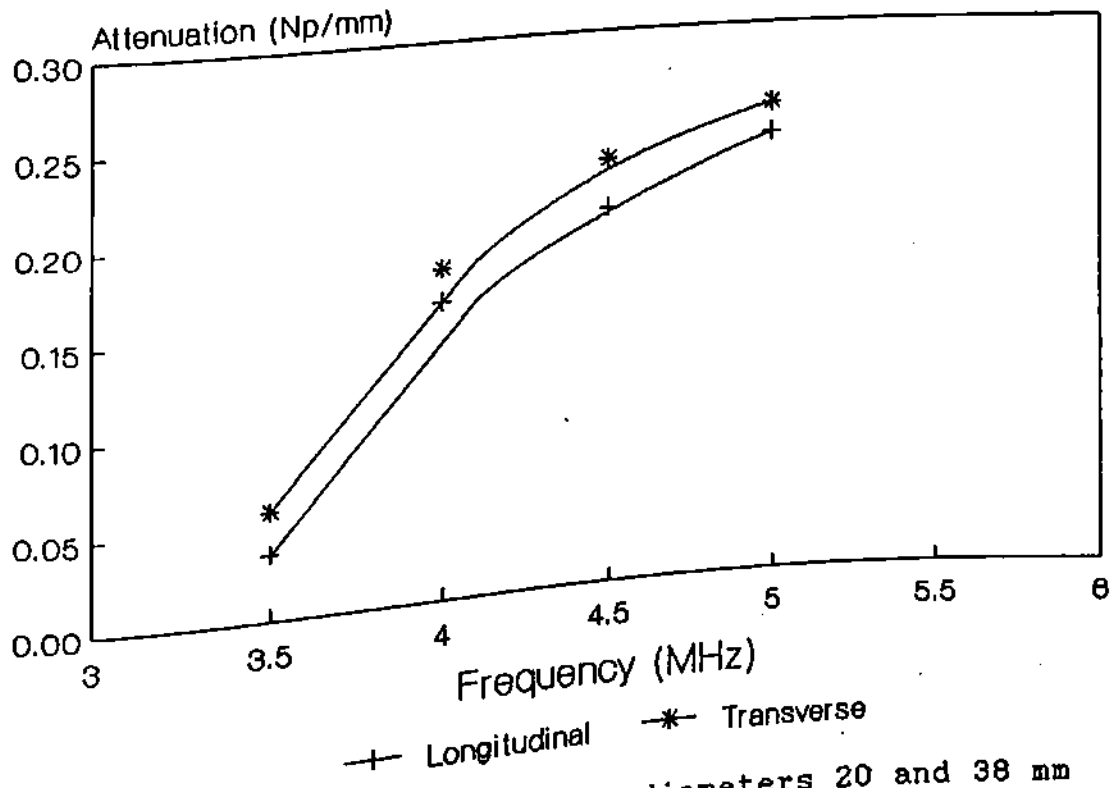

(a) Al alloy rod with end diameters 20 and 38 mm

Fig.4. Ultrasonic attenuation for longitudinal and transverse waves in different rod samples at varying frequencies

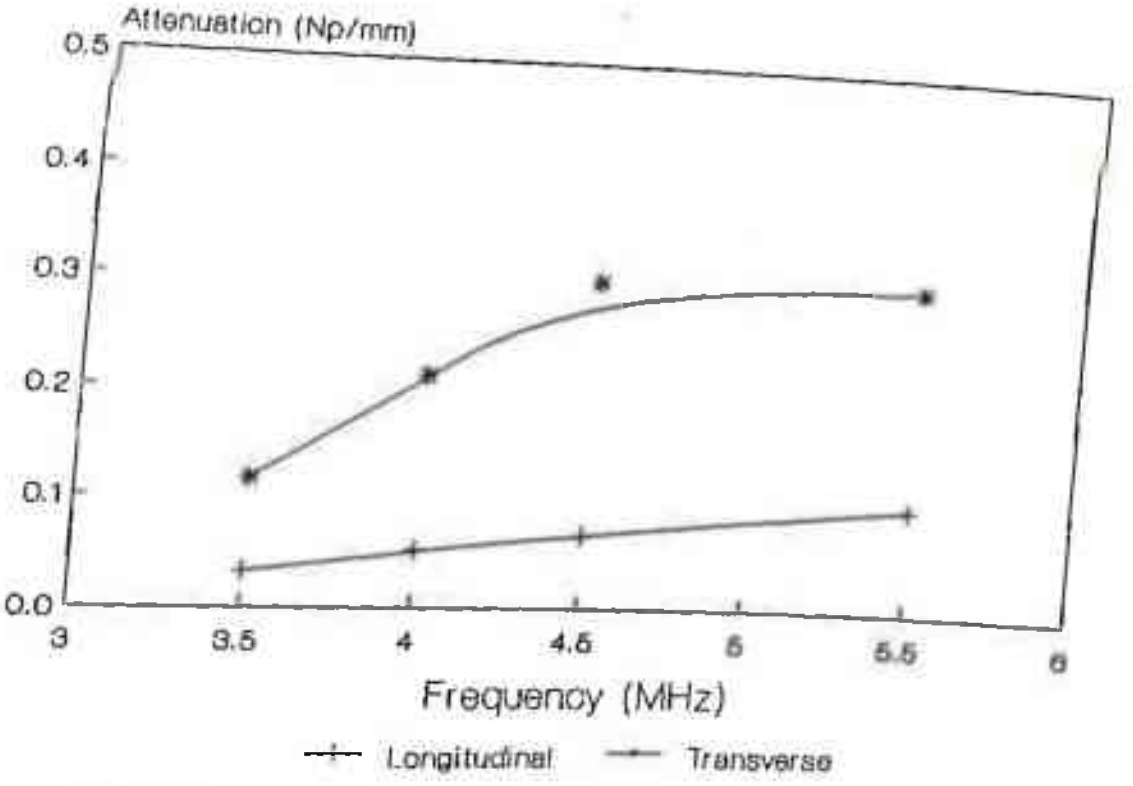

(b) Mild steel rod with end diameters 20 mm and 30 mm

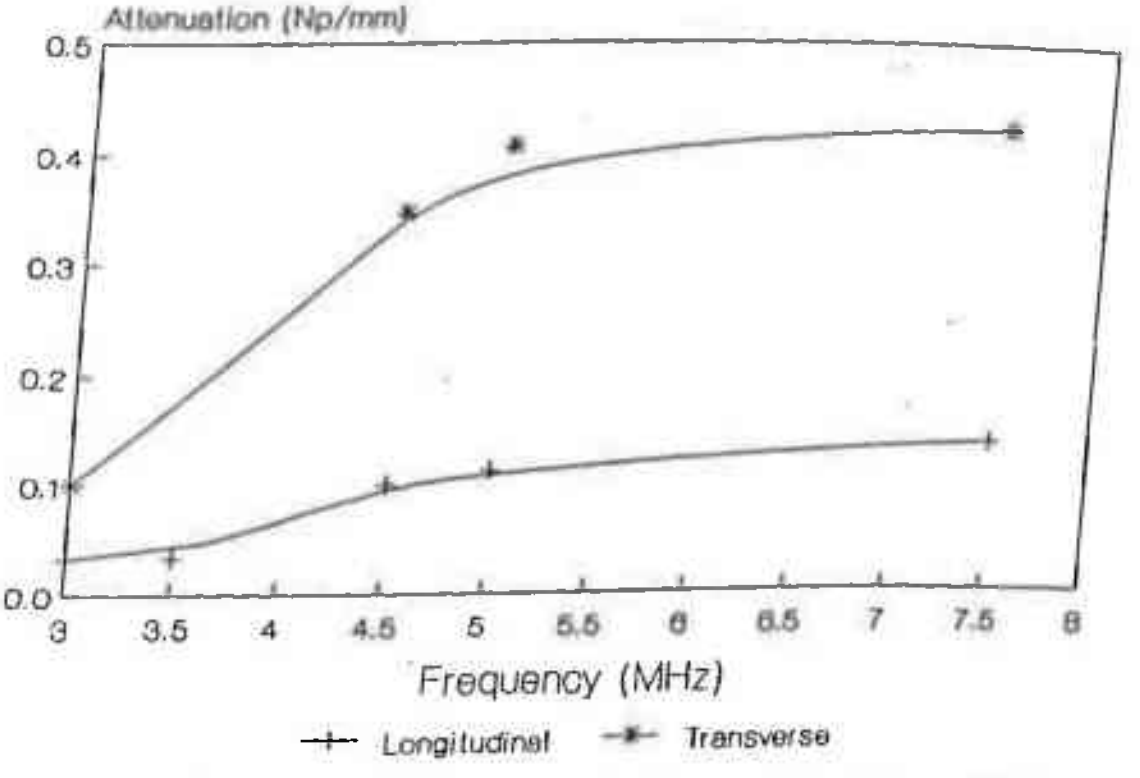

(c) Mild steel rod with end diameters 45 mm and 60 mm

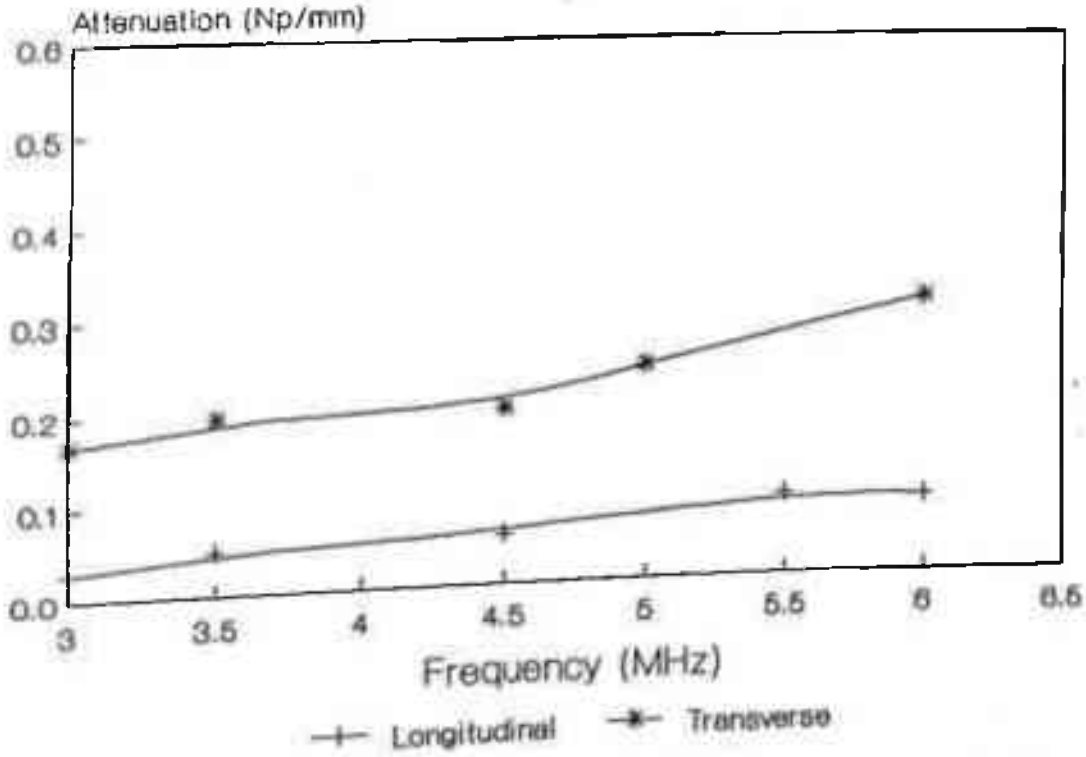

(d) Al alloy rod with end diameters 30 and 45 mm

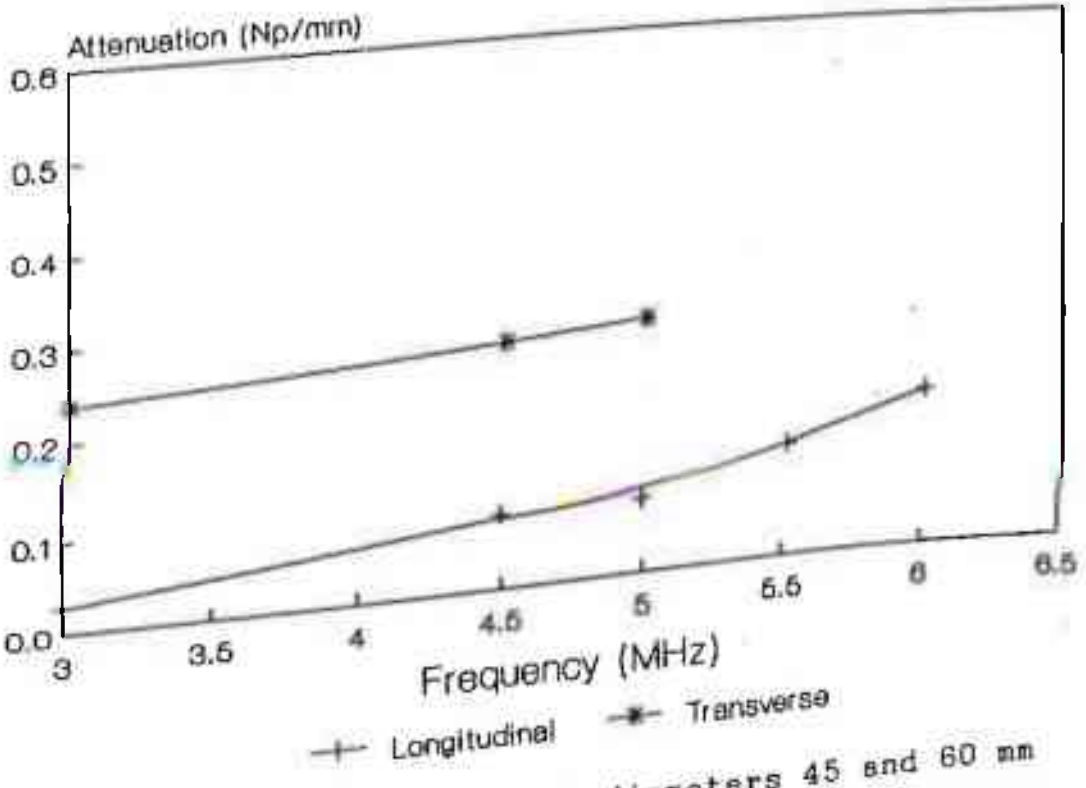

(e) Al alloy rod with end diameters 45 and 60 mm

obtained, at varying frequencies in megahertz range, are of the same order of magnitude as the values given in literature for the similar material. The values for shear wave attenuation are slightly higher than the longitudinal wave attenuation values, as expected. The values for attenuation measured for the rods (Fig. 4 b to e) containing the different steps of varying diameter shows comparative results. This shows the validity of the technique.

4.5 CONCLUSION

A method employing single longitudinal wave normal beam transducer has been used to measure both longitudinal and transverse wave attenuation in isotropic rod shaped material at different frequencies. The method requires neither the beam diffraction correction nor the reflection or transmission coefficient correction. The method may be applied to measure the ultrasonic attenuation values of any material by making the sample in rod shape.

4.6 REFERENCES

1. Ambardar, R., Muthu, M.T., Pathak, S. and Prabhakar, O., Effect of porosity, pore diameter and grain size on ultrasonic attenuation in aluminium alloy castings, INSIGHT 37 (1995) 536-43

2. Mak D., Determination of grain size , hysteresis constant and scattering factor of polycrystalline material using ultrasonic attenuation, Canadian Metallurgical Qrly. 25 (1986) 253-255

3. Serabian S., Frequency and grain size dependency of ultrasonic attenuation in polycrystalline materials, British J. NDT 22 (1980) 69-77

4. Klinman R., Webster G.R., Marsh F.J. and Stephenson E.T., Ultrasonic prediction of grain size, strength and toughness in plain carbon steel, Mat. Eval. 38 (1980) 26-32

5. Adler L, Rose J.H. and Mobley C., Ultrasonic method to determine gas porosity in aluminium alloy castings : Theory and experiment, J. Appl. Phys. 59 (1986) 336-347

6. Koltonski, W. and Malecki, I., Ultrasonic method for the exploration of the properties and structure of mineral layers, Acustica 8 (1958) 307-314

7. Krautkramer, J. and Krautkramer, H., Ultrasonic Testing of Materials : Third Edition, Springer Verlag (1983)

8. Smith, R.L. and Scudder, L., Characterising the microstructure of industrial steel by ultrasonic attenuation spectral analysis, Proc. Ultrasonic International-87 (1987) 832-37

9. Herzfeld, K.F., and Litovitz, T.A., Absorption and Dispersion of Ultrasonic Waves, Academic Press, London (1959)

10. Mak, D.K., Comparison of various methods for the measurement of reflection and ultrasonic attenuation, British J. NDT 33 (1991) 441-449

11. Yudhisther Kumar Yadav, Ultrasonic attenuation measurement in aluminium alloy, BITS ZG629T, MS Dissertation, 30th Nov. (1993)

12. Nagy, P.B. and Nayfeh, A.H., Viscosity-induced attenuation of longitudinal guided waves in fluid-loaded rods, J. Acoust. Soc. Am. 100 (1996) 1501-08

13. Samson, S.L., Williams, J.H. Jr., Stress-wave attenuation in thin structures by ultrasonic through-transmission, J. ND. Eval. 1 (1980) 277-85

14. Basant Kumar and Ashok Kumar, Direct evaluation of ultrasonic attenuation, Ultrasonics 34 (1996)847-53

15. Seki, H., Granto, A. and Truell, R., Diffraction in the ultrasonic field of a piston source and their importance in accurate measurement of attenuation, J. Acoust. Soc. Am. 28 (1956) 230-238

16. Papadakis, E.P., Correction for diffraction losses in the field of a piston source, J. Acoust. Soc. Am. 31 (1959) 150

17. Generazio E.R., The role of reflection coefficient in precision measurement of ultrasonic attenuation, Mat. Eval. 43 (1985) 995-1004

18. Papadakis, E.P., Fowler, K., and Lynnworth, L.C., Ultrasonic attenuation by spectrum analysis of pulses in buffer rods, J. Acoust. Soc. Am. 53 (1973) 1336-1343

19. Sviridov, Y. and Verenenko, S.V., Study of acoustic channel for velocity and attenuation measurement of ultrasound in a thin rod, translated from Defektoscopia, Sov. J. NDT 22 (1986) 411

20. Ashok Kumar, Yudhisther Kumar and Basant Kumar, Ultrasonic attenuation measurements in rod material, J. Acoust. Soc. India 23 (1995) 51-57

21. Ashok Kumar, Yudhisther Kumar and Basant Kumar, A new approach on ultrasonic attenuation measurement for NDE and material characterisation, Proc. 14th WCNDT (1996) 2263-66

22. Ashok Kumar, Yudhisther Kumar and Basant Kumar, On the measurement of longitudinal and shear ultrasonic velocities, Nondestr. Test. Eval. 13 (1997) 121-26

23. Bindal, V.N., Ashok Kumar, Yudhisther Kumar and Jagdish Lal, Intensity of ultrasonic beam reflected from solid-solid interface as a function of incident angle, Acoustics Letters 10 (1987) 167-172

CHAPTER - 5

EFFECT ON ULTRASOUND PROPAGATION IN METAL RODS DUE TO CONTACT WITH LIQUID

5.1 INTRODUCTION

The ultrasonic wave propagation in rods is a complex phenomenon. While the excitation along the rod axis at megahertz frequency range gives rise to predominantly longitudinal waves, the off-centre excitation gives rise to flexural and torsional wave modes [1]. If the rod diameter is small, the reflections and the mode conversion due to side walls complicate the wave propagation further. In any case, the first signal to arrive through the rod will always correspond to a longitudinal wave, traveling parallel to the axis along its length. After the first signal, a few signals will correspond to the longitudinal wave plus the shear wave traveled normal to the axis for distances equal to integer multiple of rod diameter [2]. Since the vibrations in these shear waves are not perpendicular to the curved surface, the signal due to them is not affected by the presence of a damping medium on the surface.

Though the ultrasonic wave propagation in rods has been extensively studied [1-8], the studies are either

with a view to looking at first few signals (echoes) or to use the rods as wave guides and long delay lines such as the cladded rods [9-12]. However, little work seems to have been done to study the signal coming at much later in time. These signals appear to get affected by the damping medium on the surface. The present study [13] looks experimentally at these signals with a view to characterise the rod material and putting them for some applications such as study of solid-liquid interface, liquid level monitoring in hostile environment [14], etc.

5.2 EXPERIMENTAL PROCEDURE

The block diagram and photograph of the experimental setup is given in Fig. 1(a,b,c). It consists of a water tank, probe holder stand, dead weights, a number of different diameter (9.0 mm to 38 mm) rods, ultrasonic flaw detector and probes of nominal frequency 0.5 MHz, 1.0 MHz and 2.25 MHz with crystal diameter 25 mm, 12.5 mm and 25 mm, respectively. The probe holder has a novel arrangement so that the probe face is kept at one end of the rod with uniform pressure throughout the experiment. The ultrasonic flaw detector is used in its pulse echo mode, with its range control set at 5 meters. The tank is first filled with water and then subsequently drained while taking measurements at various steps.

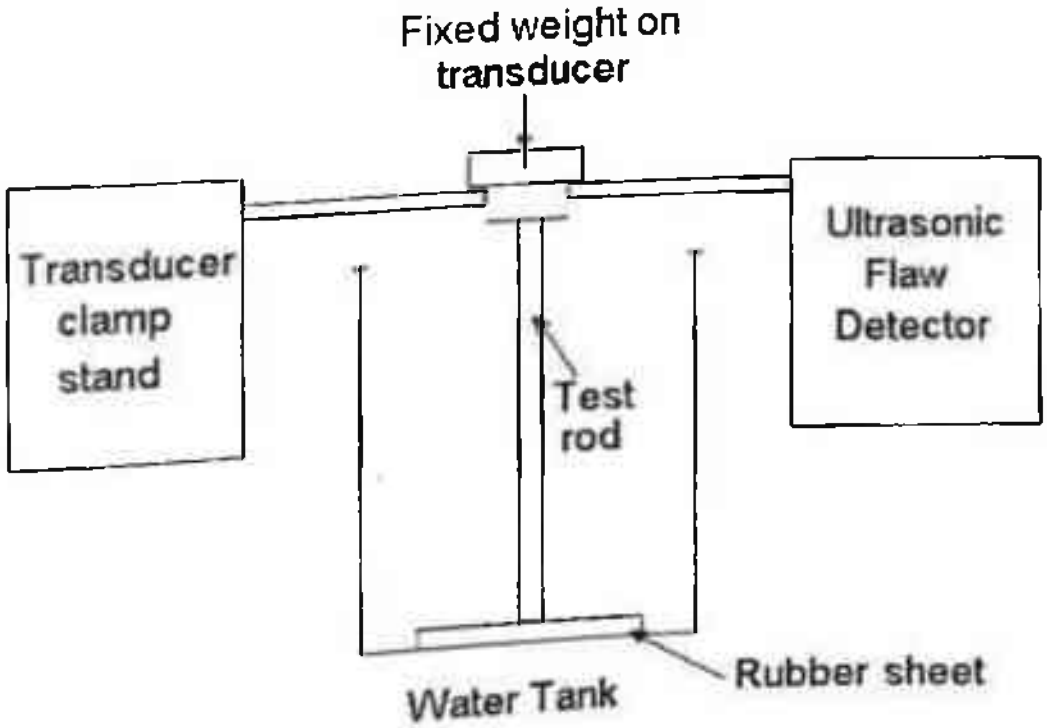

Fig. 1(a) Block diagram of the experimental setup

Fig. 1(b) Photograph of the experimental setup
(Air filled tank)

Fig.1(c) Photograph of the experimental setup
(Water filled tank)

5.3 MEASUREMENTS

Measurements were taken using the pulse echo mode on six different diameter rods. Various rods used were of diameters 9 mm (material SS), 18 mm (material MS), 29 mm (material MS), 38 mm (material MS), 10 mm (material brass) and 12.5 mm (material brass). Table 1 shows the number of rods used with their diameter, length and experimentally measured ultrasound velocity and wave length for longitudinal waves.

The ultrasonic transducer is so coupled to the rods that the beam axis of the transmitted ultrasound is along the axes of the rods. Time waveforms for SS-9 and that of MS-18 rods at 0 and 200 mm water levels are shown in Fig.2(a-d) as examples. This shows the kind of envelop pattern obtained by using 0.5 MHz transducer at UFD screen. Instead of measuring the heights of the reflected signal, as is conventionally done in pulse echo experiments, the area of the envelope of all the echoes arrived at the transducer has been determined. The envelope may be taken as a right angle triangle to the best approximation.

For the calculation of the area of the envelope, the number of divisions on the time scale is measured up to a point where the echoes are just above the noise level. All the observations on time scale are recorded at a fixed gain for various levels of water. The height

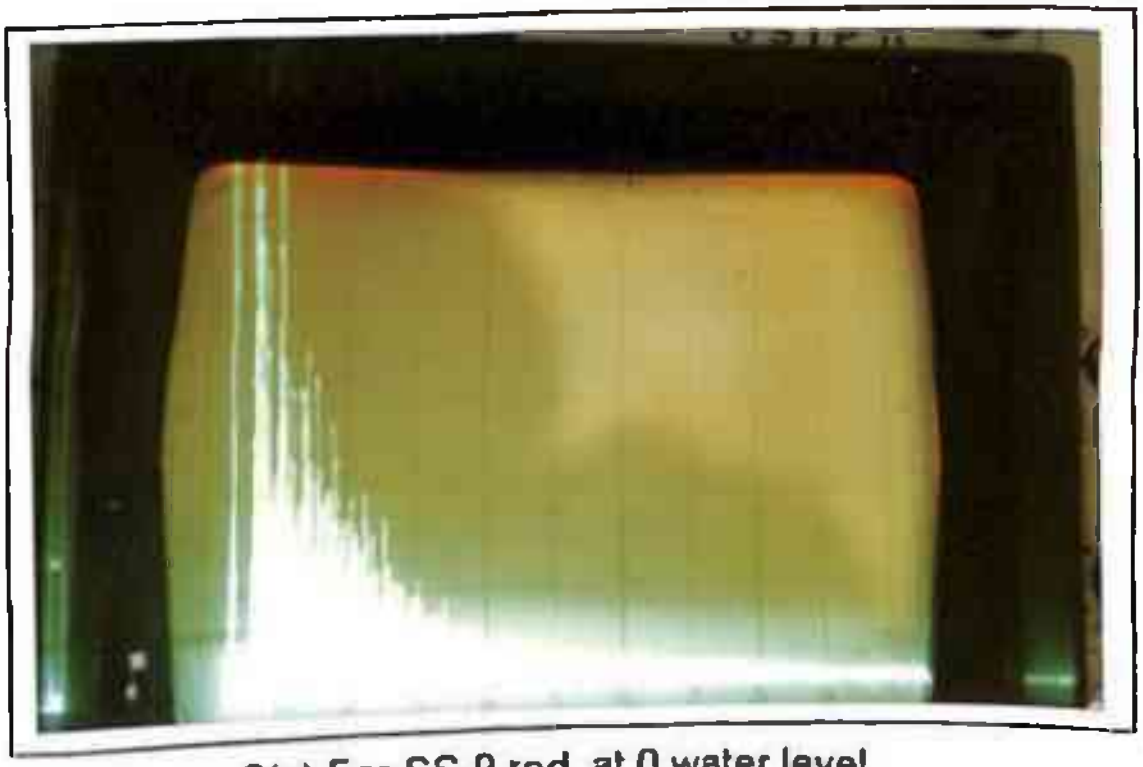

2(a) For SS-9 rod at 0 water level

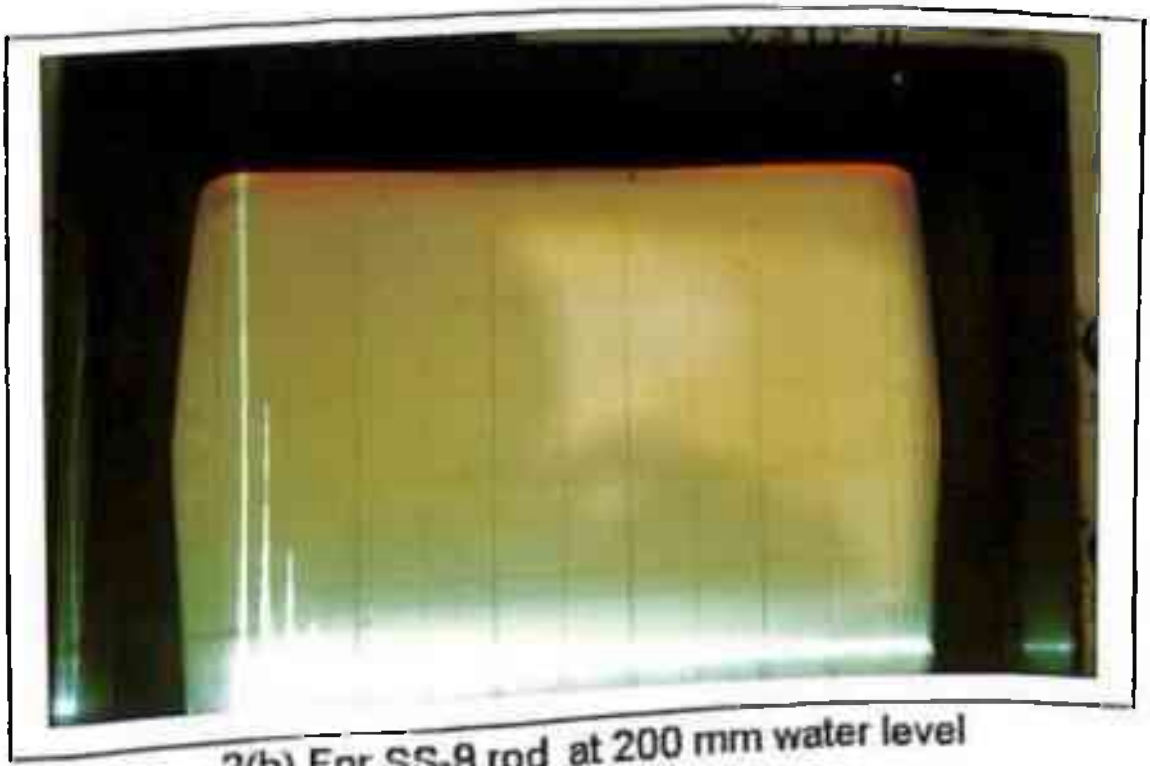

2(b) For SS-9 rod at 200 mm water level

Fig. 2. Photograph of the time waveform

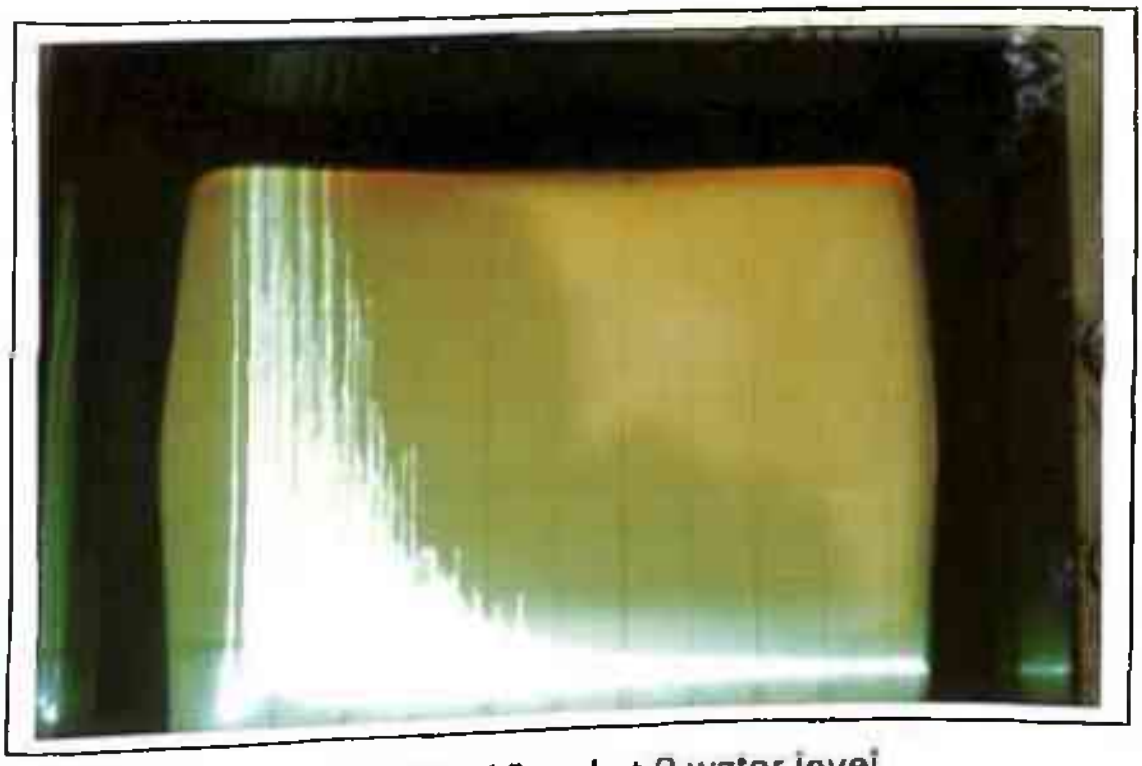

2(c) For MS-18 rod at 0 water level

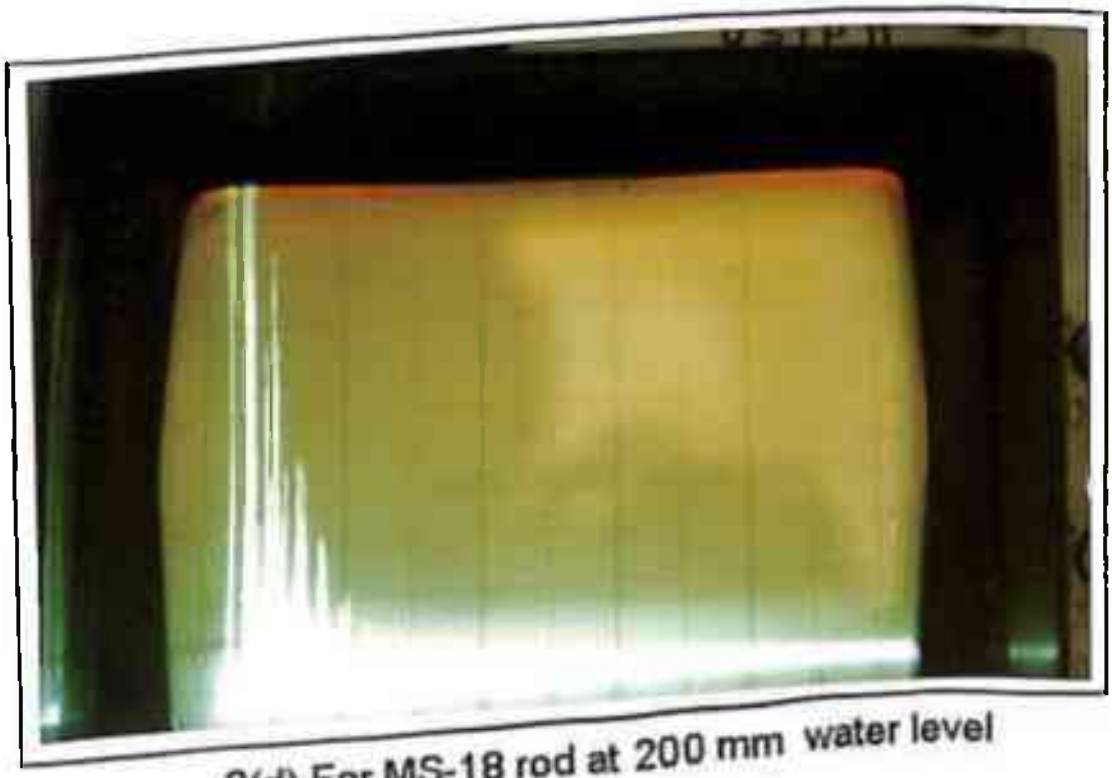

2(d) For MS-18 rod at 200 mm water level

of first echo can not be measured at this gain as it overshoots the vertical scale. To make a measurement of this, the amplifier gain is reduced till the height (h) of the first echo is 80% FSH. The reduction in gain in dB is noted as X for air and Y for water. If P and Q are the divisions on time scale for echoes in air and water, respectively, then :

Area of envelope in air $= 0.5\ P\ (h\ .\ 10^{X/20})$ ...(1)

Area of envelope in water $= 0.5\ Q\ (h\ .\ 10^{Y/20})$ ...(2)

Relative change in envelope area from equations (1) and (2)

$$R = (Q/P)\ .\ 10^{(Y-X)/20} \qquad ...(3)$$

and in dB

$$R = 20\ \log[(Q/P)\ .\ 10^{(Y-X)/20}]$$

$$= (Y-X) + 20\ \log(Q/P) \qquad ...(4)$$

5.4 RESULTS AND DISCUSSION

The variation of relative change in envelope area (R) with water level for SS-9, MS-29, MS-38 is shown in Fig. 3(a) and for SS-9, Brass-10, Brass-12.5 rods in Fig. 3(b) at the same frequency of 0.5 MHz. Figures 4 and 5 show the plots for brass and SS rods at frequencies 1.0 MHz and 2.25 MHz, respectively. It can be seen that the value of R is affected more for lesser diameter of rod for the same material.

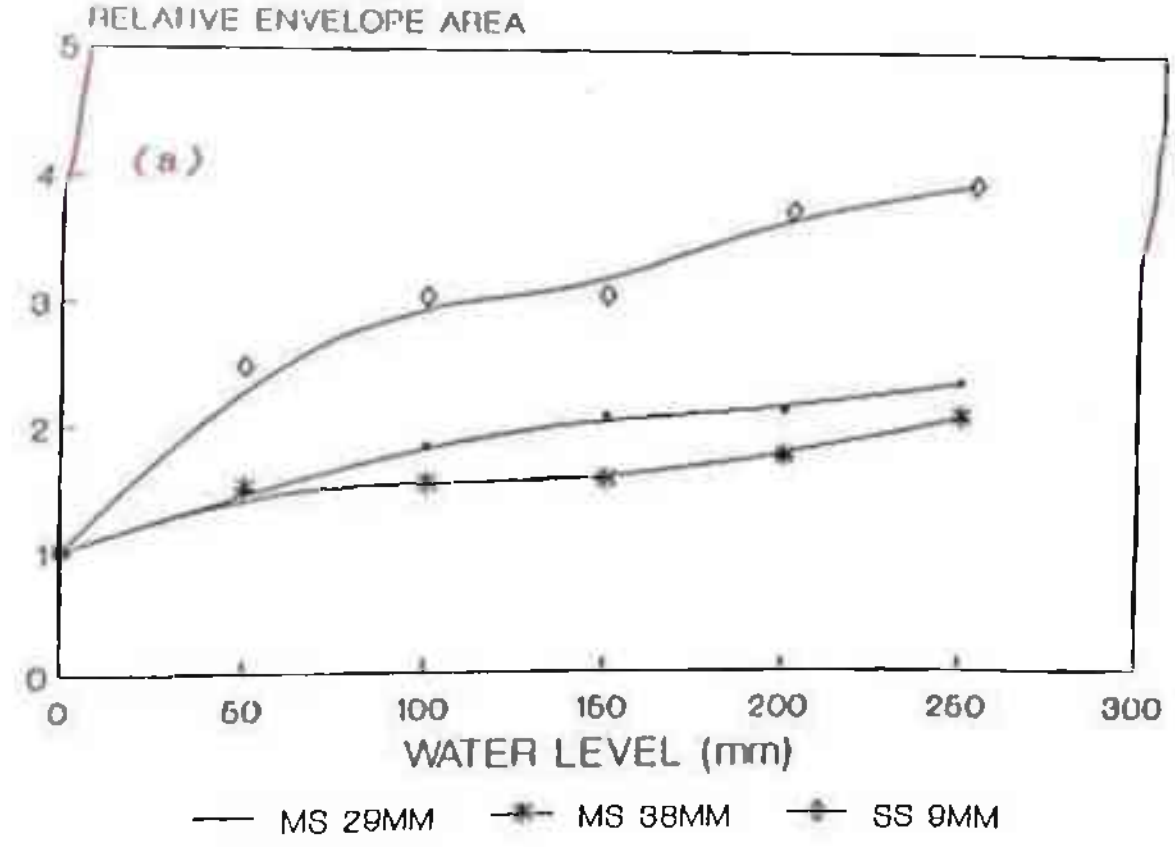

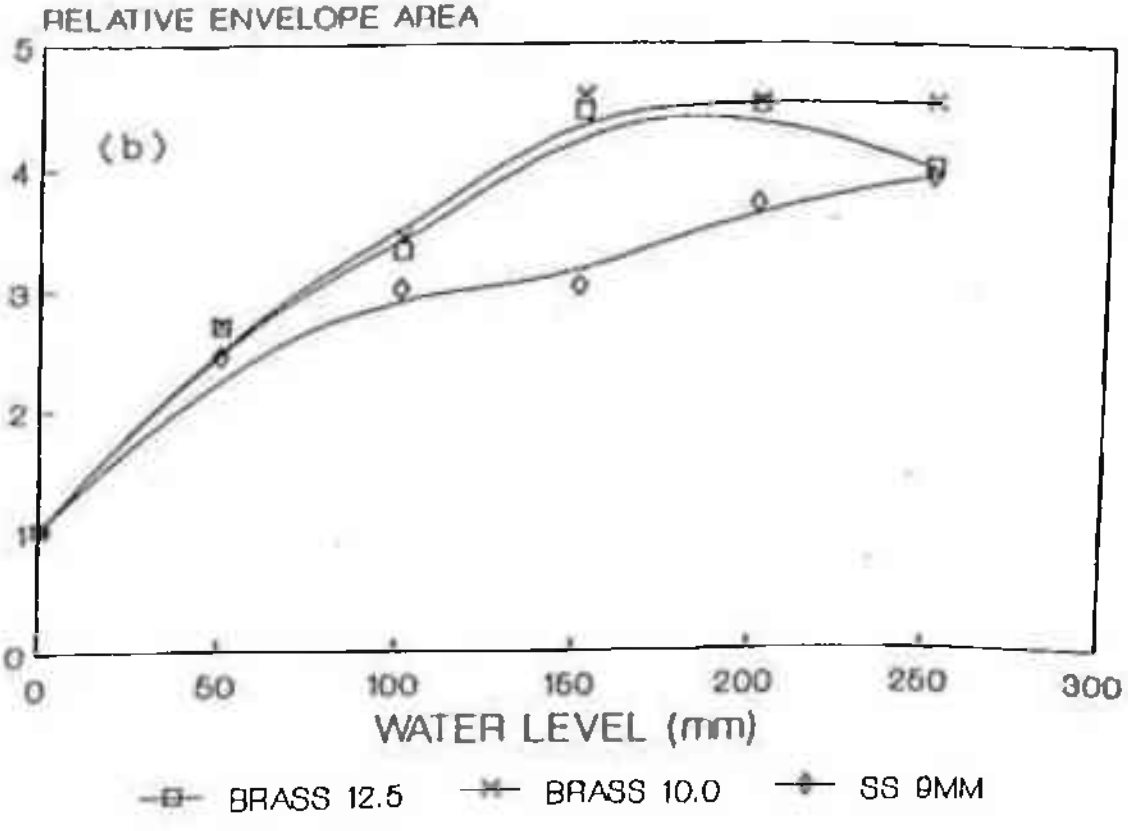

Fig.3. Variation of relative envelope area (R) with water level at 0.5 MHz

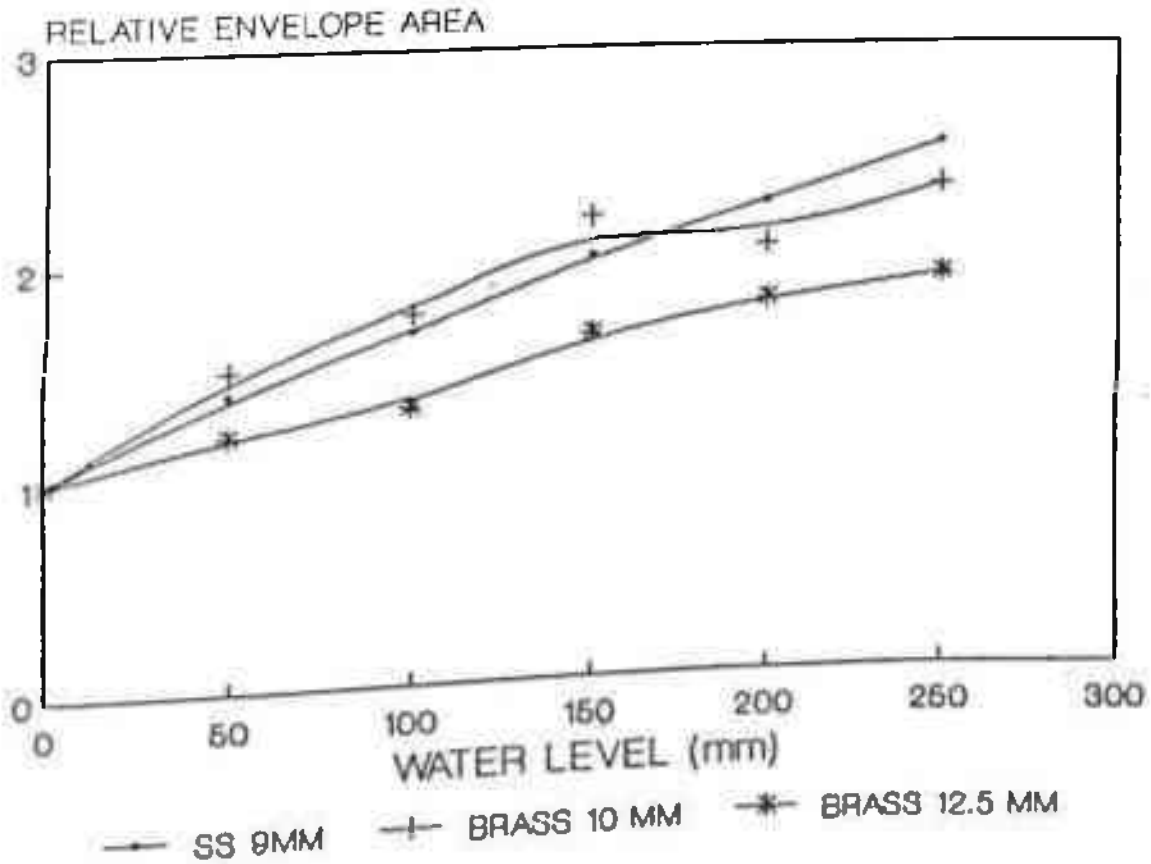

Fig.5. Variation of relative envelope area (R) with water level at 2.25 MHz.

Comparing the results of SS-9 with MS-29 and MS-38 at 0.5 MHz (Fig. 3a), it may be seen that the change in R is more pronounced in SS in which ultrasonic beam scatters more rather than in MS. This may also be seen if we compare SS rods with brass rods (Fig.3b). The brass scatters ultrasonic waves even more and hence the change in R is more pronounced. However, at higher frequencies, 2.25 MHz (Fig. 5), the change in R in SS and brass is not appreciably different. This may be due to the fact that the increase in scattering with frequency in SS is much more than in brass. This is possible if the grain size in SS is smaller than that in brass. The variation in R at 1 MHz further corroborates this view.

Fig. 6 gives the variation of R in dB with frequency at different water levels for various rods. From these figures, it may be seen that for all the rods, except MS-18, the change in R is maximum for 0.5 MHz and then reduces with increase in frequency. This is due to the fact that at lower frequencies beam divergence is higher which causes the ultrasound to strike the side walls of the rod much earlier and also at smaller angles of incidence. The case of MS-18 rod is different because of its exceptionally greater length (Table 1). After traveling larger distances, the divergence effect of 0.5 MHz ultrasound and 1 MHz ultrasound might have become of the same order. The scattering effect will

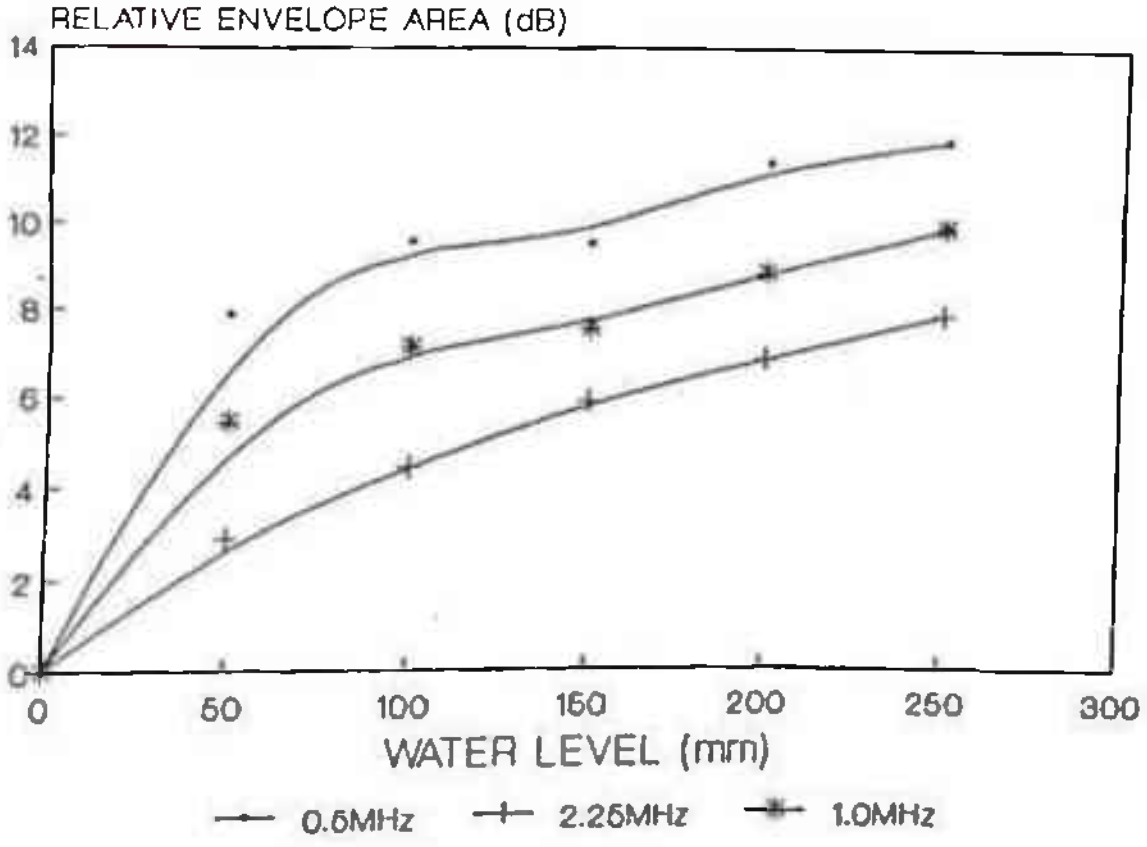

6(a) For SS-9

Fig.6. Change of relative envelope area (R) with frequency for different type of rods

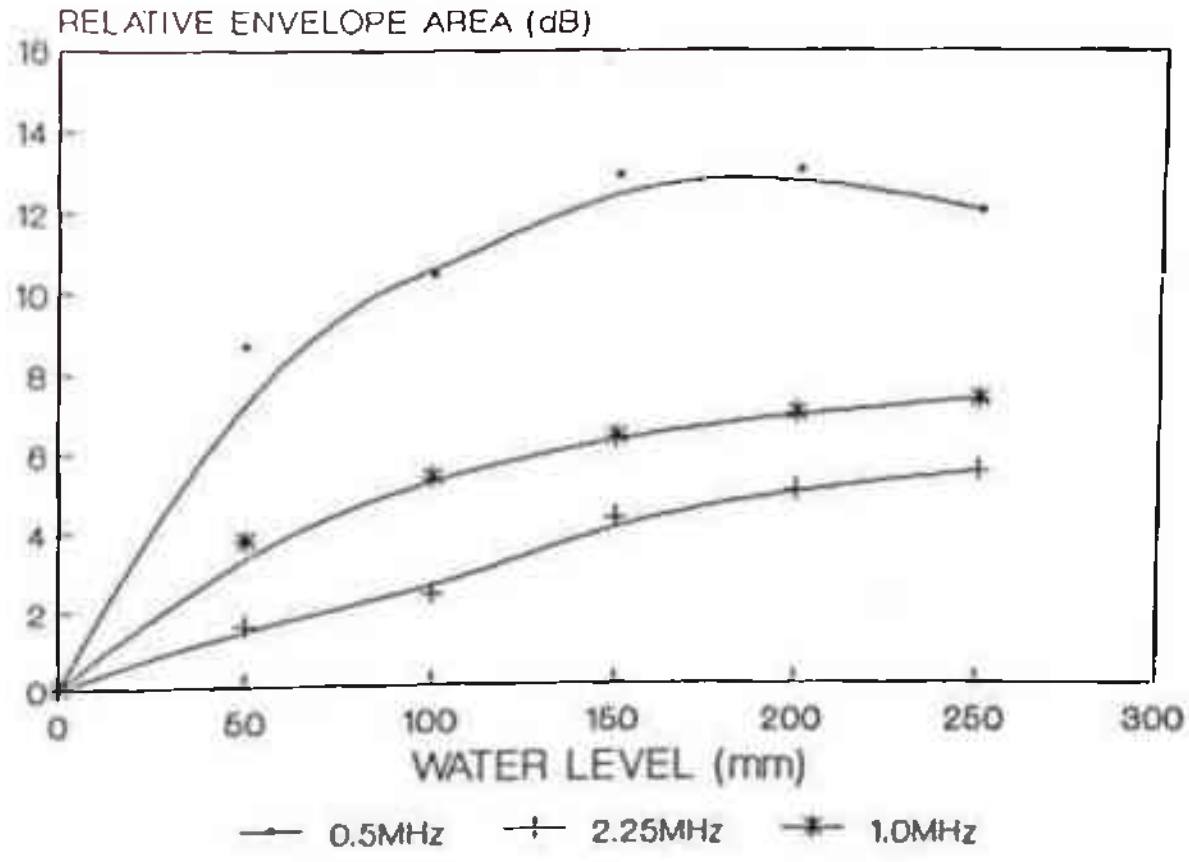

6(b) For Brass 12.5

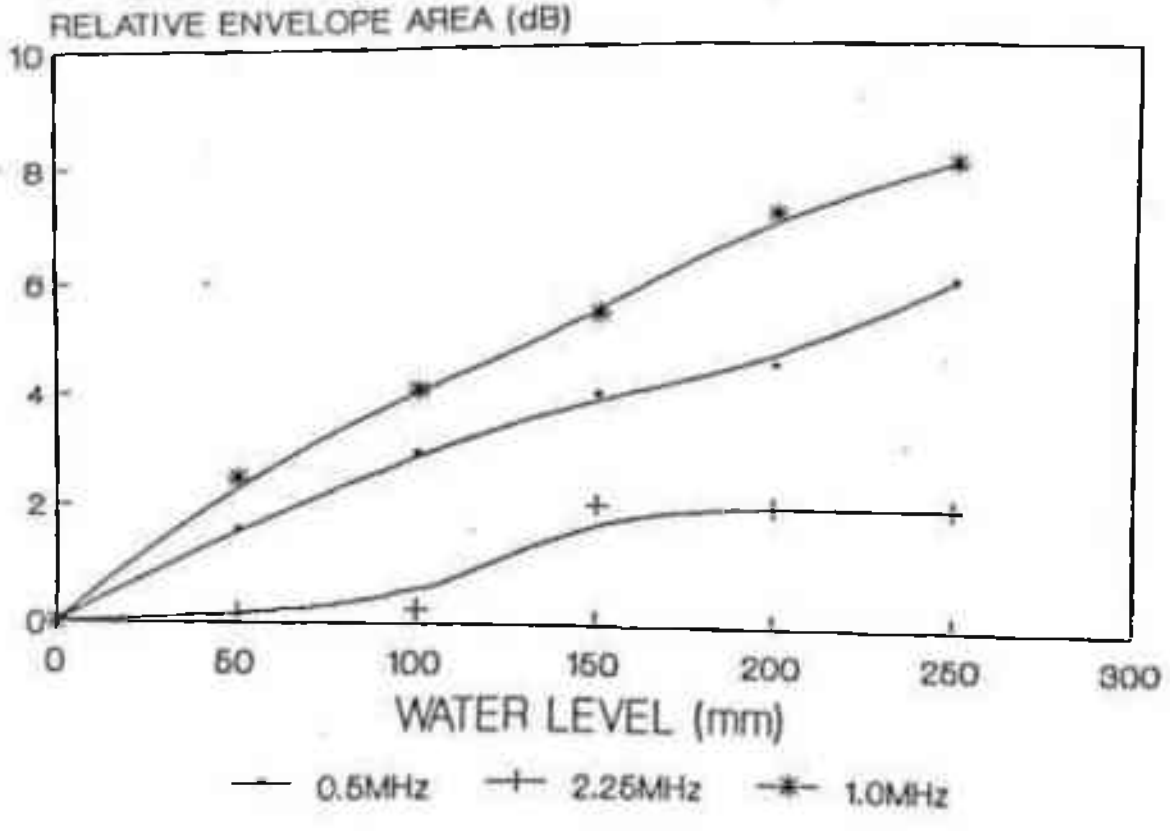

6(c) For MS-18

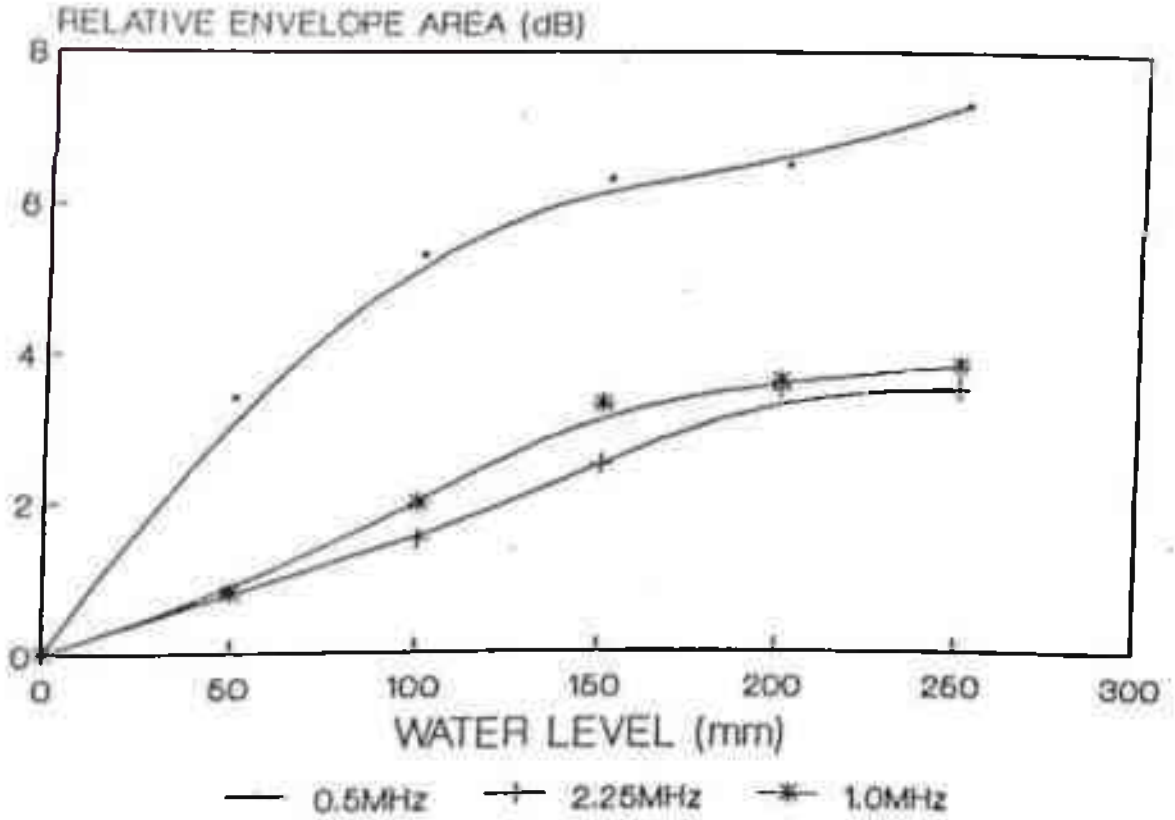

6(d) For MS-29

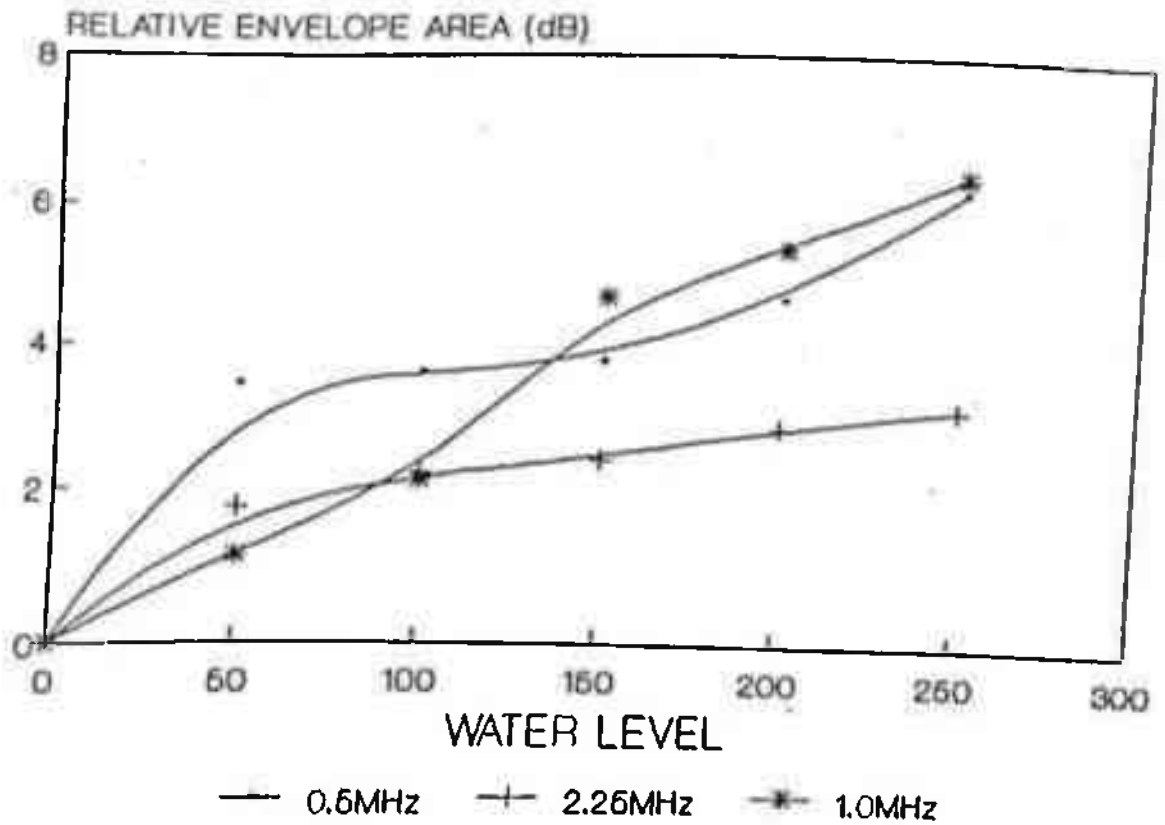

6(e) For MS-38

then take over which will be more for higher frequencies.

At larger diameters of rod such as for MS-38, the behaviour becomes more complex. The beam divergence effect will occur at a farther distance from transducer but the scattering effect may not occur as farther as divergence effect.

5.5 CONCLUSION

Experiments were performed to study the effect of damping due to water on the signals received much later in time when the ultrasound is directed along the axis of a rod. It is observed that the effect of damping increases

(i) sharply towards the far end of the rod,
(ii) for smaller diameter probe
(iii) for smaller diameter rods for a particular material
(iv) with lowering of frequency
(v) for the rod material having more scattering.

The study has several potential applications such as non-destructive testing of bonding at the interface of an embedded cylinder, geophysical studies, characterisation of liquid during process control, liquid level detector, etc. In liquid level detector, for example,

one could use a SS rod of diameter 9 mm or less. This should give a resolution better than 0.1 mm. In liquid level controller, it would be better to keep this rod just dipped in liquid. This should give a resolution better than 1 mm.

5.6 REFERENCES

1. Abramson, H. N., Plass, H. J., Advances in Applied Mechanics, Vol. V, Academic Press, N Y (1958)

2. Abramson, H N, Plass, H J., Rippergear, Stress wave propagation in rods and beams, in Advances in Appl. Mech., Vol. V, Academic Press, N Y (1958) 136

3. Hughes, D.S., Pandrom, W.L., Mims, R.L., Propagation of elastic pulses in metal rods, Phys. Rev. 75 (1949) 1552-1556

4. Filipczynski, L., Ultrasonic wave propagation along the surface of a rod immersed in liquid, Arch. of Acoustics (1979) 272-285

5. Bjorno, L. and Ram Kumar, Fluid influenced stress waves dispersion in submerged rods, Acustica 27 (1972) 329-34

6. Joseph, Z. Jr., An experimental and theoretical investigation of elastic waves propagation in cylinder, J. Acoust. Soc. Am. 51 (1972) 265-283

7. Vinay Dayal, Longitudinal wave in homogeneous anisotropic cylindrical bars immersed in fluid, J. Acoust. Soc. Am. 93 (1993) 1249-55

8. Nagy, P.B., Longitudinal guided wave propagation in a transversely isotropic rod immersed in fluid, J. Acoust. Soc. Am. 98 (1995) 454-57

9. Jen., C.K.,Wang, Z., Miri, A., Nicolle, A., Neron, C., Adler, E.L., Newly developed cladded acoustics rods, IEEE Ultrasonics Symposium (1991) 885-890

10. Jen, C.K., Wang, Z., et. al., Acoustic Waveguiding rods with graded velocity profiles, Ultrasonics 30 (1992) 91-94

11. Redwood, M., Mechanical Wave guides, Pergamon Press, NY (1960)

12. Thurston, R.N., Elastic waves in rods and clad rods, J. Acoust. Soc. Am. 64 (1978) 1-37

13. Yudhisther Kumar, Ashok Kumar and B. Kumar, Effect of ultrasonic propagation in metal rods due to contact with liquid, Acustica 83 (1997) 78-81

14. Seki Soramoto, Michio Sato, et. al., New ultrasonic level gauge using standing waves of bending modes, Jpn. J. Appl. Phys. 35 (1996) 3059-61

CHAPTER - 6

CONCLUSION

CHAPTER - 8

CONCLUSION

The characterisation in its simplest form may be said as the evaluation of various parameters or features of a material including the defects, study of properties or use and suffice for the reproduction of a material. The growing requirement in engineering plants to demonstrate the safety and reliability of the metallic components has encouraged wider use of the nondestructive evaluation and characterisation of materials. Amongst the various NDT techniques, ultrasonic nondestructive testing and evaluation technique has been found most capable of revealing more and significant information. Unlike other products having plane surfaces, the evaluation of defects in rolled, cylindrical or circular rod products is a bit difficult even by ultrasonic techniques. Present work deals in with the characterisation of materials in the form of rods by ultrasonics. The work may contribute significantly towards the solution for several problems faced in the characterisation of rod shaped materials.

Rods or rod shaped components are widely used in engineering plants, building structures and may be subjected to heavy stress and fatigue during their

subsequent use in individual system. There may occur manufacturing defects even in the semifinished products of round bar or rod shaped material. The knowledge of the defects, either created during the manufacturing or by subsequent use, in components is very useful in quality assurances and to prevent hazardous effect.

A new technique for the detection, location and sizing of the defects in rods has been developed. A small and inexpensive add-on arrangement has been made to the existing C-scan system. The technique uses longitudinal beam in the pulse echo mode that scans circumferentially through the diameter of the rod. The technique is found useful and has advantage over the other NDT methods of rod inspection. The dependence of effective beam width into the rod on frequency, transducer diameter, rod diameter, material velocity and water path between the transducer and rod surface has been computed theoretically.

Nondestructive inspection by the new technique has been performed on a number of rods in a diameter ranging from 6 mm to 50 mm with the transducers of nominal frequencies 5 MHz, 7.5 MHz and 20 MHz. Various artificial defects in varying shape and sizes were made in these rods and evaluated. It is found that 7.5 MHz transducer is most suitable for inspection of various rods in the present range of rod diameters. Based on the logic developed and experiments carried out, it has

been found that the gating of the back wall signal gives most useful information about the defect and size of the internal defect.

The present technique is capable of detecting all of the defects clearly as can be seen in the scanning image. The setting up procedure requires the positioning of the transducer correctly so that the ultrasonic beam is in a plane perpendicular to the rod axis. This can be perfected after a few experiments on various rods. Width of the defect along the axis or on circumference could be observed accurately. This may be attributed to the very small effective beam width emitted in the rod due to the curved surface. The depth of the defect, though not being measured by circumferential scanning, can be measured by end scanning in the bigger diameter and smaller length rods samples. An inherent limitation of the ultrasonic technique is that if the size of the defect is smaller than the beam diameter, then the actual size measured is found approximately equal to the beam width. This limitation exists in the present technique also and therefore the sizing of the defects is to be done only for defects having size larger than the beam width although the detection can be carried out reliably.

The characterisation of materials by ultrasonic velocity is a well established technique. The velocity

values, for example, can be utilised to determine various mechanical characteristics of the rod materials by determining elastic constants like shear modulus (G), longitudinal modulus (L), Young's modulus (E) and Poisson's ratio (σ) using given relations in the text.

For the measurement of the ultrasonic velocity of the longitudinal and transverse waves in isotropic flawless rod material, a new technique has been presented. The technique employs a single longitudinal wave normal beam transducer either in direct contact or in immersion technique. The first three echoes observed are unique and verified experimentally. Time of flight for the first three echoes, namely, back wall echo (T1), triangular echo without mode conversion (T2) and triangular echo after mode conversion (T3) have been measured experimentally. Diameter of the rod and time of flight are used to determine the ultrasonic velocity in the expression. A computer program in BASIC language is used for determining the various parameters like incident angle, reflected angle for longitudinal and transverse waves and for determination of the ultrasonic velocities.

The validity of the technique has been verified experimentally by determining the longitudinal wave velocity with back wall echo T1 as well as the triangular echo T2 which have been found similar and comparable to the values available in literature. The

values obtained by the different diameters of the same material also proves that the technique is independent of rod diameter. The evaluation of shear wave velocity is however difficult in higher diameter rods due to the higher attenuation of shear waves.

Another important parameter that can be used to characterise the materials is the ultrasonic attenuation. The attenuation values are helpful in predicting the grain size, hardness, yield strength et. of the material and also in determining the limit of the frequency over which material may be inspected for possible defects. It is a difficult quantity to determine accurately at test frequencies ranging 1 to 10 MHz. The overall result includes other losses such as beam spread, field effect, couplant mismatch, transducer bonding or sample geometry. These factors are difficult to isolate perfectly.

A new technique for the measurement of ultrasonic attenuation of longitudinal and transverse waves in rod materials has been developed. Results have been presented for rods of different diameters for ultrasonic longitudinal and transverse waves at varying frequencies. The technique employs only a single longitudinal wave normal beam transducer and can measure both longitudinal and transverse wave attenuation in the flawless isotropic rod materials. The sample is taken either in the form of

a single cylindrical rod with steps of different end diameter or as two rods of different diameters and same material. Amplitude of first three echoes corresponding to the path T1, T2 and T3 for both of the two diameters are used for the determination of the attenuation of ultrasonic longitudinal and transverse waves. Frequency domain waveform provides the attenuation values at varying frequencies within the 6 dB frequency beam width of the used broad band transducer. The method has been validated experimentally by determining the attenuation values for the same material but for different diameters which give comparable or similar values. Significantly this method requires neither the beam diffraction correction nor the reflection or transmission coefficient correction. The method can be applied to determine the ultrasonic attenuation values with highest accuracy by making the sample in rod shape which is much more convenient and economic than making a parallel plate.

Effect of the ultrasound propagation in metal rods due to the contact with liquid for rods of different material and varying diameter has been studied. The study has several potential applications such as non-destructive testing of bonding at the interface of an embedded cylinder, geophysical studies, characterisation of liquid during process control, liquid level detector, etc. It will help in selecting the rod of particular material and diameter suitable for above applications.

Experiments were performed to study the effect of damping due to water on the signals received much later in time when the ultrasound is directed along the axis of a rod. It is observed that the effect of damping is different for different metal compositions and increases sharply towards the far end of the rod. It also increases with probes of smaller diameters, with rods of smaller diameter, with lowering of frequency and for the rod material having more scattering.

In brief, new techniques have been developed and applied successfully for the detection and location of defects in rods by ultrasonics C-scan system, for ultrasonic longitudinal and transverse wave velocity measurements and for ultrasonic attenuation measurements in rods. The effect on ultrasound propagation in rods in contact with liquid has also been studied. It is expected that the new work done will result in significant advances in scientific research in the area of ultrasonics and in material characterisation.

APPENDIX

LIST OF PUBLICATIONS

(During Jan. 1993 to April 1997)

Papers Published in Journals/Proc.

1. Ashok Kumar, **Yudhisther Kumar** and Basant Kumar, Ultrasonic attenuation measurements in rod material, J. Acoust. Soc. India 23(1995) 51-57

2. R. Mitra, **Yudhisther Kumar**, Ashok Kumar and T.K. Saksena, Absolute calibration of a PVDF membrane hydrophone using phase locked laser interferometry, J. Pure Appl. Ultrason., 17 (1995) 102-106

3. Ashok Kumar, Jagdish Lal and **Yudhisther Kumar**, Calibration of ultrasonic thickness gauges, Advances in Metrology and its Role in Quality Improvement and Global Trade, (Ed. B.S.Mathur etal), Narosa Publishing House (1996) 210-213

4. Ashok Kumar, **Yudhisther Kumar** and Basant Kumar, Ultrasonic study of tissue mimicking materials, Proc. Seventh National Symposium on Ultrasonics, (Ed. G. Shanmugam and V. Rajendran) Allied Publishers (1996) 89-94

5. **Yudhisther Kumar**, Ashok Kumar and Basant Kumar Performance characteristics of ultrasonic transducers used in NDT, Proc. Seventh National Symposium on Ultrasonics, (Ed. G. Shanmugam and V. Rajendran) Allied Publishers (1996) 209-213

6. **Yudhisther Kumar**, Ashok Kumar and Basant Kumar, Non-destructive evaluation of rods by ultrasonic C-scan system, 14 WC Nondestructive Testing, Vol. 2 (Ed. C.G. Krishnadas Nair, et al), Oxford & IBH (1996) 647-650

7. Ashok Kumar, **Yudhisther Kumar** and Basant Kumar, A new approach of ultrasonic attenuation measurement for NDE and Material characterization, 14 WC Nondestructive Testing, Vol. 4 (Ed. C.G. Krishnadas Nair, et al), Oxford & IBH (1996) 2263-2266

8. **Yudhisther Kumar**, Ashok Kumar and Basant Kumar, Effect on the propagation in metal rods due to contact with liquid, Acustica . acta acustica 83 (1997) 78-81

9. Ashok Kumar, **Yudhisther Kumar** and Basant Kumar, On the measurement of longitudinal and shear ultrasonic velocities, Nondestr. Test. Eval. 13 (1997) 121-126

10. Ashok Kumar, Basant Kumar and **Yudhisther Kumar**, On the acoustic impedance of salol, Acustica - acta acustica 83 (1997) 82-87

11. Ashok Kumar, Basant Kumar and **Yudhisther Kumar**, A novel method to determine the acoustic impedance of membrane material, Ultrasonics (Accepted for publication on 17-10-1996)

12. Ashok Kumar, Basant Kumar and **Yudhisther Kumar**, Quality evaluation of ultrasonic calibration blocks, Materials Evaluation (USA) (Revised manuscript sent on 31-10-96)

Paper presented in Conf.

13. **Yudhisther Kumar**, Ashok Kumar and Basant Kumar, Improvised technique for immersion testing of rods, National Symposium on Advances in NDE, November 8-10 (1995)

Dissertation

14. **Yudhisther Kumar** , Ultrasonic attenuation measurement in aluminium alloy, M S Dissertation, BITS Report ZG629T, Nov. 30 (1993)